Supporting Information

Stable, Concentrated, Biocompatible, and Defect-free Graphene Dispersions with Positive Charge

Yuyoung Shin[1,†], Sandra Vranic[2,3,†], Xavier Just-Baringo[1,†], Sai Manoj Gali[4], Thomas Kisby[2,3], Yingxian Chen[2,3], Alexandra Gkoutzidou[5], Eric Prestat[5,6], David Beljonne[4], Igor Larrosa[1], Kostas Kostarelos[2,3,*], Cinzia Casiraghi[1*]*

[1]Department of Chemistry, University of Manchester, Oxford Road, Manchester, UK
[2]Nanomedicine Lab, Faculty of Biology, Medicine and Health, AV Hill Building, University of Manchester, Manchester, UK
[3]National Graphene Institute, University of Manchester, Booth Street East, Manchester M13 9PL, UK
[4]Laboratory for Chemistry of Novel Materials, University of Mons, Mons, Belgium
[5] Department of Materials, University of Manchester, Oxford Road, Manchester, UK
[6]SuperSTEM Laboratory, SciTech Daresbury Campus, Daresbury, UK

[†] shared first authorship
[*]corresponding authors

Table of Contents

S1. Synthesis and Characterization of Pyrene Derivatives

S1.1. General Information

Tetrahydrofuran (THF) and toluene were dried using a PureSolv solvent purification system. All other solvents and reagents used were purchased from commercial suppliers and used without further purification. ^{1}H-NMR spectra were obtained at room temperature on a Bruker 400 MHz or 500 MHz spectrometer. ^{13}C-NMR spectra were obtained at 100 or 125 MHz respectively. All NMR spectra were processed using *MestReNova* NMR software. Chemical shifts are reported in parts per million (ppm) and coupling constants (*J*) reported in Hz. Splitting patterns are reported as follows: singlet (s), doublet (d), triplet (t), quadruplet (q), quintuplet (quint), doublet of doublets (dd), doublet of doublets of doublets (ddd), multiplet (m), etc. NMR signals were assigned using the appropriate 2D NMR experiments (*i.e.* HSQC and HMBC when necessary). TLC analysis was carried out on aluminium sheets coated with silica gel and visualized using potassium permanganate solution and/or UV light. Infra-red spectra were recorded as evaporated films or neat using FT/IR spectrometers. Melting points were measured on solids as obtained after chromatography. Mass spectra were obtained using positive or negative electrospray (ESI), atmospheric pressure chemical ionization (APCI) or atmospheric solids analysis probe (ASAP).

S1.2. Aqueous solubility determination

To vials charged with cationic pyrene salts and fitted with a stirring bar was added D_2O (0.5 mL) prior to sealing them under air. The resulting suspensions were shortly sonicated and then stirred at room temperature for 72 h. The suspensions were allowed to settle and the supernatant was filtered through cotton. The concentration of the saturated solution was determined by ^{1}H-NMR using nitromethane as an internal standard. Compounds **IMI$_2$**, **TMA$_3$** and **PRD$_3$** (marked with asterisk (*)) showed much higher solubility than the other compounds and a saturated solution could not be formed as viscous honey-like solutions formed; in these cases the maximum concentration achieved while the mixture could still be stirred was measured.

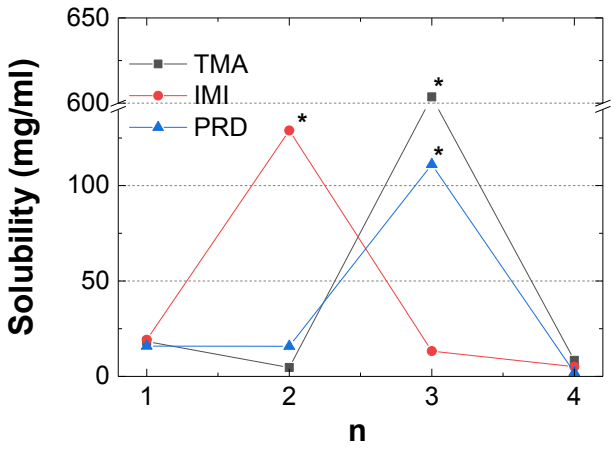

Figure S1 Aqueous solubility of cationic pyrenes.

S1.3. Synthesis and Characterization

1-(Bromomethyl)pyrene (S1)

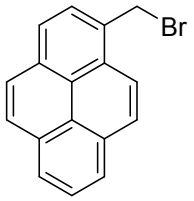

To a suspension of 1-pyrenemethanol (5.00 g, 21.5 mmol) in dry toluene (250 mL) at 0 ˚C, PBr_3 (1.0 mL, 10.8 mmol) was added dropwise. The resulting mixture was stirred at 0 ˚C for 1.5 h and then at room temperature for 1 h. The reaction was quenched by careful addition of saturated aqueous Na_2CO_3 (25 mL). Layers were separated and the organic fraction was washed with H_2O (2 × 12 mL) and brine (2 × 12 mL). The organic layer was concentrated to obtain the title product as an off-white solid (6.21 g, 98%), mp (toluene): decomposes above 125 ºC. ^{1}H-NMR (400 MHz, $CDCl_3$) δ 5.28 (s, C*H*$_2$, 2 H), 8.02-8.16 (m, Ar*H*, 5 H), 8.21-8.30 (m, Ar*H*, 3 H), 8.41 (d, *J* = 9.2 Hz, Ar*H*, 1 H) ppm; ^{13}C-NMR (125 MHz, $CDCl_3$) δ 32.2 (*C*H$_2$), 122.8 (Ar*C*H), 124.6 (Ar*C*), 124.9 (Ar*C*H), 125.1 (Ar*C*), 125.6 (Ar*C*H), 125.6 (Ar*C*H), 126.3 (Ar*C*H), 127.3 (Ar*C*H), 127.7 (Ar*C*H), 128.0 (Ar*C*H), 128.2 (Ar*C*H), 129.1 (Ar*C*), 130.6 (Ar*C*), 130.8 (Ar*C*), 131.2 (Ar*C*), 132.0 (Ar*C*) ppm; IR ν_{max} (neat/cm^{-1}): 3037, 1917, 1587, 1418, 1311, 1201, 1184, 1084, 840; HRMS calcd for $C_{17}H_{12}Br$ [M]$^+$: 295.0117, found 295.0112.

General procedure A: Alkylation of amines and *N*-heterocycles

***N*,*N*,*N*-Trimethyl-*N*-(1-pyrenylmethyl)ammonium bromide (TMA_1)**

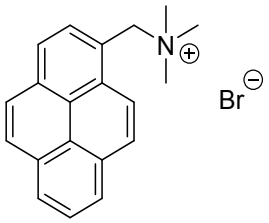

A solution of trimethylamine in ethanol (4.2 M, 14.7 mL, 62.0 mmol) was added to a flask charged with **S1** (1.00 g, 3.39 mmol). The flask was sealed under air and the mixture stirred at 60 ºC for 18 h. After cooling to room temperature volatiles were removed under vacuum. The resulting solid was triturated in Et_2O, filtered and washed with more Et_2O. The title product was obtained as an off-white solid (1.25 mg, 98%), mp (MeOH): decomposes above 170 ºC. ^{1}H-NMR (400 MHz, DMSO-d_6) δ 3.17 (s, N(CH_3)$_3$, 9 H), 5.35 (s, CH_2, 2 H), 8.17 (t, *J* = 7.6 Hz, Ar*H*, 1 H), 8.26-8.31 (m, Ar*H*, 2 H), 8.35 (d, *J* = 8.8 Hz, Ar*H*, 1 H), 8.38-8.47 (m, Ar*H*, 4 H), 8.78 (d, *J* = 9.2 Hz, Ar*H*, 1 H) ppm; ^{13}C-NMR (100 MHz, DMSO-d_6) δ 52.1 (N(*C*H$_3$)$_3$), 64.3 (Ar*C*H$_2$N), 121.8 (Ar*C*), 123.4 (Ar*C*H), 123.6 (Ar*C*), 124.2 (Ar*C*), 124.8 (Ar*C*H), 126.0 (Ar*C*H), 126.3 (Ar*C*H), 126.8 (Ar*C*H), 127.2 (Ar*C*H), 128.9 (Ar*C*H), 128.9 (Ar*C*H), 129.9 (Ar*C*), 130.6 (Ar*C*), 131.5 (Ar*C*), 132.3 (Ar*C*H), 132.4 (Ar*C*) ppm; IR ν_{max} (neat/cm^{-1}): 3402, 3003, 2922, 1594, 1481, 973; HRMS calcd for $C_{20}H_{20}N^+$ [M]$^+$: 274.1590, found 274.1580.

^{1}H-NMR (500 MHz, MeOD-d_4) δ 3.24 (s, N(CH_3)$_3$, 9 H), 5.36 (s, CH_2, 2 H), 8.13 (t, *J* = 7.8 Hz, Ar*H*, 1 H), 8.19 (d, *J* = 9.0 Hz, Ar*H*, 1 H), 8.22-8.29 (m, Ar*H*, 2 H), , 8.31-8.40 (m, Ar*H*, 4 H), 8.60 (d, *J* = 9.5 Hz, Ar*H*, 1 H) ppm; ^{13}C-NMR (125 MHz, MeOD-d_4) δ 53.6 (t, *J* = 4.0 Hz, N(*C*H$_3$)$_3$), 67.0 (t, *J* = 2.4 Hz, Ar*C*H$_2$N), 121.9 (Ar*C*), 123.6 (Ar*C*H), 125.5 (Ar*C*), 125.9 (Ar*C*H), 126.2 (Ar*C*), 127.3 (Ar*C*H), 127.7 (Ar*C*H), 127.9 (Ar*C*H), 128.3 (Ar*C*H), 130.5 (Ar*C*H), 1230.8 (Ar*C*H), 131.7 (Ar*C*), 132.6 (Ar*C*), 133.1 (Ar*C*H), 133.2 (Ar*C*), 134.8 (Ar*C*) ppm

1-Methyl-3-(1-pyrenylmethyl)-1*H*-imidazolium bromide (IMI_1)

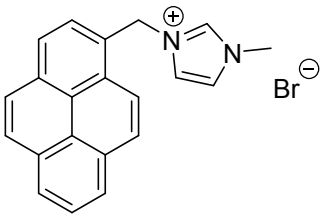

Prepared according to general procedure A using **S1** (2.00 g, 6.78 mmol) in THF (18.2 mL) and 1-methylimidazole (540 µL, 6.78 mmol). After 16 h at 60 ˚C volatiles were removed, the solid resuspended in Et_2O, filtered and washed with more Et_2O. After cooling to room

temperature, the resulting suspension was filtered under vacuum and the solid was washed with Et_2O. The title product was obtained as a white solid (2.42 g, 95%), mp (THF): 190-193 ºC. ^{1}H-NMR (400 MHz, DMSO-d_6) δ 3.82 (s, NCH_3, 3 H), 6.22 (s, ArCH_2N, 2 H), 7.74 (s, Ar*H*, 1 H), 7.88 (s, Ar*H*, 1 H), 8.10-8.19 (m, Ar*H*, 2 H), 8.21-8.31 (m, Ar*H*, 2 H), 8.32-8.43 (m, Ar*H*, 4 H), 8.48 (d, *J* = 9.6 Hz, Ar*H*, 1 H), 9.17 (s, Ar*H*, 1 H) ppm; ^{13}C-NMR (100 MHz, DMSO-d_6) δ 35.9 (N*C*H$_3$), 49.9 (Ar*C*H$_2$N), 122.4 (Ar*C*H), 122.6 (Ar*C*H), 123.7 (Ar*C*H), 123.9 (Ar*C*H), 124.1 (Ar*C*), 125.2 (Ar*C*), 125.8 (Ar*C*H), 126.0 (Ar*C*H), 126.7 (Ar*C*H), 127.3 (Ar*C*H), 127.3 (Ar*C*), 127.9 (Ar*C*H), 128.2 (Ar*C*H), 128.6 (Ar*C*), 128.8 (Ar*C*H), 130.1 (Ar*C*), 130.7 (Ar*C*), 131.5 (Ar*C*), 136.7 (Ar*C*H) ppm; IR ν_{max} (neat/cm^{-1}): 3051, 1571, 1554, 1416, 1168, 1157, 856; HRMS calcd for $C_{21}H_{17}N^+$ [M]$^+$: 297.1386, found 297.1375.

^{1}H-NMR (500 MHz, MeOD-d_4) δ 3.87 (s, NCH_3, 3 H), 6.19 (s, ArCH_2N, 2 H), 7.58 (s, Ar*H*, 1 H), 7.69 (s, Ar*H*, 1 H), 8.07-8.18 (m, Ar*H*, 3 H), 8.21 (d, *J* = 8.5 Hz, Ar*H*, 1 H), 8.26-8.36 (m, Ar*H*, 5 H) ppm, full H/D exchange is observed in position 2 of the imidazolium ring; ^{13}C-NMR (125 MHz, MeOD-d_4) δ 36.5 (N*C*H$_3$), 52.1 (Ar*C*H$_2$N), 122.7 (Ar*C*H), 123.9 (Ar*C*H), 125.2 (Ar*C*H), 125.6 (Ar*C*), 126.2 (Ar*C*), 126.4 (Ar*C*H), 127.0 (Ar*C*), 127.1 (Ar*C*H), 127.3 (Ar*C*H), 127.8 (Ar*C*H), 128.3 (Ar*C*H), 129.4 (Ar*C*H), 129.7 (Ar*C*H), 130.5 (Ar*C*H), 130.6 (Ar*C*), 132.0 (Ar*C*), 132.6 (Ar*C*), 134.0 (Ar*C*) ppm, full H/D exchange is observed in position 2 of the imidazolium ring.

1-(1-Pyrenylmethyl)pyridinium bromide (PRD_1)

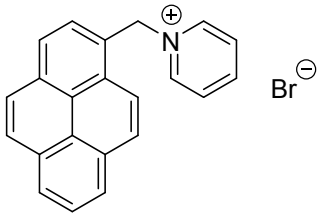

Prepared according to general procedure A using **S1** (2.00 g, 6.78 mmol) in THF (18.2 mL) and pyridine (548 µL, 6.78 mmol). After 16 h at 60 ˚C volatiles were removed, the solid resuspended in Et_2O, filtered and washed with more Et_2O. After cooling to room temperature, the resulting suspension was filtered under vacuum and the solid was washed with Et_2O. The title product was obtained as a yellow solid (2.42 g, 98%), mp (THF): 190-195 ºC. ^{1}H-NMR (400 MHz, DMSO-d_6) δ 6.69 (s, ArCH_2N, 2 H), 8.12-8.22 (m, Ar*H*, 4 H), 8.27 (d, *J* = 9.0 Hz, Ar*H*, 1 H), 8.30 (d, *J* = 9.0 Hz, Ar*H*, 1 H), 8.36-8.46 (m, Ar*H*, 4 H), 8.48 (d, *J* = 9.2 Hz, Ar*H*, 1 H), 8.63 (t, *J* = 7.8 Hz, Ar*H*, 1 H), 9.18 (d, *J* = 6.4 Hz, Ar*H*, 2 H) ppm; ^{13}C-NMR (100 MHz, DMSO-d_6) δ 61.1 (Ar*C*H$_2$N), 122.2 (Ar*C*H), 123.6 (Ar*C*), 124.1 (Ar*C*), 125.4 (Ar*C*H), 126.0 (Ar*C*H), 126.3 (Ar*C*H), 126.3 (Ar*C*), 126.8 (Ar*C*H), 127.2 (Ar*C*H), 128.4 (Ar*C*H), 128.5 (Ar*C*H), 128.6 (Ar*C*H), 129.0 (Ar*C*), 129.2 (Ar*C*H), 130.1 (Ar*C*), 130.7 (Ar*C*), 131.9 (Ar*C*), 144.8 (Ar*C*H), 146.1 (Ar*C*H) ppm; IR ν_{max} (neat/cm^{-1}): 3013, 1626, 1482, 1140; HRMS calcd for $C_{22}H_{16}N^+$ [M]$^+$: 294.1277, found 294.1265.

General procedure B: $LiAlH_4$ reduction of carboxylic acids

2-(1-Pyrenyl)ethanol (S2)

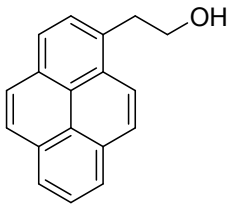

To a stirring suspension of $LiAlH_4$ (877 mg, 23.1 mmol) in dry THF (19 mL) placed in a water bath at room temperature, a solution of 1-pyreneacetic acid (1.50 g, 5.76 mmol) in dry THF (19 mL) was added dropwise. After 3 h the reaction was quenched by very careful dropwise addition of MeOH (3 mL) and diluted aqueous HCl. The product was extracted with Et_2O (× 3) and the combined organic layers were washed with H_2O, dried ($MgSO_4$) and concentrated *in vacuo*. The crude product was purified by silica flash column chromatography (CH_2Cl_2) to yield the title product as a bright yellow solid (1.27 g, 90%), mp (CH_2Cl_2): 93-96 ºC. ^{1}H-NMR (400 MHz, $CDCl_3$) δ 1.45 (t, *J* = 6.8 Hz, O*H*, 1 H), 3.65 (t, *J* = 6.8 Hz, ArC*H*$_2$CH$_2$OH, 2 H), 4.12 (q, *J* = 6.8 Hz, ArCH$_2$C*H*$_2$OH, 2 H), 7.93 (d, *J* = 7.6 Hz, Ar*H*, 1 H), 8.02 (t, *J* = 7.6 Hz, Ar*H*, 1 H), 8.06 (s, Ar*H*,2 H), 8.11-8.22 (m, Ar*H*,4 H), 8.33 (d, *J* = 9.2 Hz, Ar*H*, 1 H) ppm; ^{13}C-NMR (100 MHz, $CDCl_3$) δ 36.7 (Ar*C*H$_2$CH$_2$OH), 63.9 (ArCH$_2$*C*H$_2$OH), 123.2 (Ar*C*H), 124.9(Ar*C*H), 124.9(Ar*C*H), 124.9(Ar*C*), 125.1(Ar*C*H), 125.1(Ar*C*), 125.9(Ar*C*H), 127.0(Ar*C*H), 127.4(Ar*C*H), 127.6(Ar*C*H), 128.0(Ar*C*H), 129.2(Ar*C*), 130.3(Ar*C*), 130.8(Ar*C*), 131.4(Ar*C*), 132.4 (Ar*C*) ppm; IR ν_{max} (neat/cm^{-1}): 3331, 3039, 2947, 2877, 1603, 1182, 1040, 840; HRMS calcd for $C_{18}H_{14}OK$ $[M+K]^+$: 285.0676, found 285.0677.

General procedure C: synthesis of alkyl bromides

1-(2-Bromoethyl)pyrene (S3)

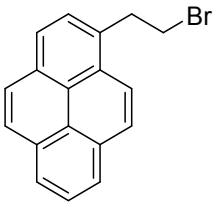

To a solution of **S2** (1.27 g, 5.14 mmol) in dry CH_2Cl_2 (79 mL) at 0 ˚C, PBr_3 (1.2 mL, 12.9 mmol) was added dropwise. The resulting solution was allowed to warm to room temperature. After 6 h it was cooled to 0 ˚C and quenched with aqueous sat. $NaHCO_3$. Layers were separated and the aqueous fraction was extracted with CH_2Cl_2 (× 3). The combined organic layers were dried ($MgSO_4$) and concentrated *in vacuo*. The crude product was purified by silica flash column chromatography (hexane/CH_2Cl_2, 50:50) to yield the title product as a yellow solid (380 mg, 24%), mp (CH_2Cl_2): 96-99 ºC. ^{1}H-NMR (400 MHz, $CDCl_3$) δ 3.79 (t, *J* = 8.0 Hz, C*H*$_2$, 2 H), 3.92 (t, *J* = 8.0 Hz, C*H*$_2$, 2 H), 7.92 (d, *J* = 8.0 Hz, Ar*H*, 1 H), 8.00-8.10 (m, Ar*H*, 3 H), 8.13-8.23 (m, Ar*H*, 4 H), 8.25 (d, *J* = 9.2 Hz, Ar*H*, 1 H) ppm; ^{13}C-NMR (125 MHz, $CDCl_3$) δ 32.4 (*C*H$_2$), 37.2 (*C*H$_2$), 122.6 (Ar*C*H), 124.9 (Ar*C*), 124.9 (Ar*C*H), 125.1 (Ar*C*H), 125.1 (Ar*C*), 125.3 (Ar*C*H), 126.0 (Ar*C*H), 127.2 (Ar*C*H), 127.4 (Ar*C*H), 127.6 (Ar*C*H), 128.0 (Ar*C*H), 128.8 (Ar*C*), 130.6 (Ar*C*), 130.8 (Ar*C*), 131.3 (Ar*C*), 132.7 (Ar*C*) ppm; IR ν_{max} (neat/cm^{-1}): 3038, 2962, 1902, 1603, 1587, 1433, 1305, 1216; HRMS calcd for $C_{18}H_{14}Br$ [M+H]$^+$: 309.0273, found 309.0281.

***N*,*N*-Dimethyl-2-(1-pyrenyl)acetamide (2)**

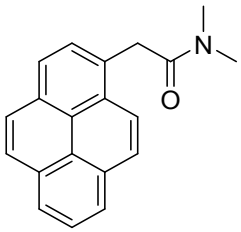

A solution of 1-pyreneacetic acid (1.0 g, 3.84 mmol), $NHMe_2$·HCl (376 mg, 4.61 mmol) and HOBt·H_2O (646 mg, 4.22 mmol) in dry THF (7.7 mL) was stirred at room temperature for 30 min. Then, NEt_3 (1.07 mL, 7.68 mmol) and *N*,*N'*-diisopropylcarbodiimide (653 µL, 4.22 mmol) were added and the resulting mixture was stirred at room temperature. After 20 h the reaction mixture was diluted with Et_2O and filtered through cotton. The resulting solution was washed with dilute aqueous HCl, aqueous sat. $NaHCO_3$ and brine, dried ($MgSO_4$) and concentrated *in vacuo*. The crude product was purified by silica flash column chromatography (CH_2Cl_2/MeOH, 100:0 to 99:1) to yield the title product as a yellow solid (940 mg, 85%), mp (CH_2Cl_2): 142-145 ºC. ^{1}H-NMR (400 MHz, $CDCl_3$) δ 3.06 (s, CON(C*H*$_3$)$_a$(CH$_3$)$_b$, 3 H), 3.07 (s, CON(CH$_3$)$_a$(C*H*$_3$)$_b$, 3 H), 4.45 (s, ArC*H*$_2$, 2 H), 7.90 (d, *J* =

8.0 Hz, Ar*H*, 1 H), 8.02 (t, *J* = 7.6 Hz, Ar*H*, 1 H), 8.06 (s, Ar*H*, 2 H), 8.12-8.22 (m, 4 H), 8.27 (d, *J* = 9.2 Hz, Ar*H*, 1 H), ppm; ^{13}C-NMR (125 MHz, $CDCl_3$) δ 35.8 (CON(CH_3)$_a$(CH_3)$_b$), 37.8 (CON(CH_3)$_a$(CH_3)$_b$), 39. (ArCH_2), 123.0 (Ar*C*H), 124.8 (Ar*C*), 124.9 (Ar*C*H), 125.0 (Ar*C*H), 125.1 (Ar*C*), 125.2(Ar*C*H), 125.9 (Ar*C*H), 127.0 (Ar*C*H), 127.1 (Ar*C*H), 127.4 (Ar*C*H), 127.9 (Ar*C*H), 129.1 (Ar*C*), 129.2 (Ar*C*), 130.5 (Ar*C*), 130.8 (Ar*C*), 131.3 (Ar*C*), 171.2 (*C*ONMe$_2$) ppm; IR ν_{max} (neat/cm^{-1}): 3040, 2926, 1641, 1393, 1133, 839; HRMS calcd for C20H17ONNa [M+Na]$^+$: 310.1207, found 310.1203.

_N_-(2-(1-Pyrenyl)ethyl)-_N_,_N_-dimethylamine (3)

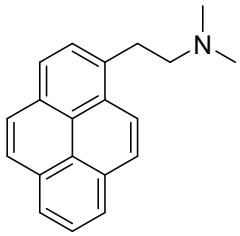

To a stirring solution of of **2** (800 mg, 2.78 mmol) in dry THF (18.5 mL) at 0 ˚C was added $LiAlH_4$ (423 mg, 11.1 mmol) in little portions. After the addition, the reaction mixture was allowed to warm to room temperature. After 20 h the mixture was cooled to 0 ˚C and the reaction was quenched by very careful dropwise addition of MeOH and aqueous NaOH. The product was extracted with Et_2O (× 5) and the combined organic layers were washed with brine, dried ($MgSO_4$) and concentrated *in vacuo*. The crude product was purified by silica flash column chromatography (CH_2Cl_2/MeOH, 100:0 to 94:6) to yield the title product as an orange solid (636 mg, 84%), mp (CH_2Cl_2): 43-47 ºC. ^{1}H-NMR (400 MHz, $CDCl_3$) δ 2.45 (s, N(CH_3)$_2$, 6 H), 2.73-2.83 (m, ArCH_2CH_2, 2 H), 3.51-3.59 (m, ArCH_2CH_2, 2 H), 7.91 (d, *J* = 7.6 Hz, Ar*H*, 1 H), 7.97-8.07 (m, Ar*H*, 3 H), 8.10-8.15 (m, Ar*H*, 2 H), 8.16-8.21 (m, Ar*H*, 2 H), 8.31 (d, *J* = 9.2 Hz, Ar*H*, 1 H) ppm; ^{13}C-NMR (125 MHz, $CDCl_3$) δ 32.0 (ArCH_2CH_2), 45.5 (N(CH_3)$_2$), 61.4 (ArCH_2CH_2), 123.2 (Ar*C*H), 124.7 (Ar*C*H), 124.9 (Ar*C*H), 124.9 (Ar*C*H), 125.0 (Ar*C*), 125.1 (Ar*C*), 125.8 (Ar*C*H), 126.7 (Ar*C*H), 127.4 (Ar*C*H), 127.5 (Ar*C*H), 127.5 (Ar*C*H), 128.8 (Ar*C*), 130.0 (Ar*C*), 130.9 (Ar*C*), 131.4 (Ar*C*), 134.4 (Ar*C*) ppm; IR ν_{max} (neat/cm^{-1}): 3040, 2939, 2766, 1674, 1460, 1182, 1041, 841; HRMS calcd for $C_{20}H_{19}NK$ [M+K]$^+$: 312.1149, found 312.1150.

***N*-(2-(1-Pyrenyl)ethyl)-*N*,*N*,*N*-trimethyl ammonium iodide (4)**

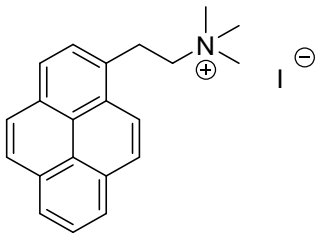

To a stirring solution of **3** (300 mg, 1.10 mmol) in dry acetone (13.7 mL) at room temperature was added methyl iodide (410 µL, 6.58 mmol). After 18 h volatiles were removed under vacuum and THF was added. The precipitated product was filtered under vacuum and washed with more THF. After drying, the title product was obtained as an off-white solid (433 mg, 97%), mp (THF): decomposes above 250 ºC. ^{1}H-NMR (400 MHz, MeOD-d_4) δ 3.38 (s, N(CH_3)$_3$, 9 H), 3.74-3.83 (m, ArCH_2CH$_2$, 2 H), 3.88-3.97 (m, ArCH$_2$CH_2, 2 H), 8.03-8.09 (m, Ar*H*, 2 H), 8.10 (d, *J* = 9.2 Hz, Ar*H*, 1 H), 8.13 (d, *J* = 9.2 Hz, Ar*H*, 1 H), 8.21-8.30 (m, Ar*H*, 4 H), 8.35 (d, *J* = 10.0 Hz, Ar*H*, 1 H) ppm; ^{13}C-NMR (125 MHz, MeOD-d_4) δ 27.7 (ArCH$_2$CH$_2$), 53.7 (t, *J* = 4.0 Hz, N(*C*H$_3$)$_3$), 68.0 (t, *J* = 2.5 Hz, ArCH$_2$*C*H$_2$), 123.3 (Ar*C*H), 125.9 (Ar*C*), 126.3 (Ar*C*), 126.3 (Ar*C*H), 126.4 (Ar*C*H), 126.7 (Ar*C*H), 127.4 (Ar*C*H), 128.4 (Ar*C*H), 128.6 (Ar*C*H), 129.0 (Ar*C*H), 129.6 (Ar*C*H), 130.3 (Ar*C* × 2), 132.1 (Ar*C*), 132.4 (Ar*C*), 132.8 (Ar*C*) ppm; IR ν_{max} (neat/cm^{-1}): 3042, 3003, 2955, 1457, 1405, 1179, 967, 943, 912, 842; HRMS calcd for $C_{21}H_{22}N$ [M]$^+$: 288.1747, found 288.1733.

***N*-(2-(1-Pyrenyl)ethyl)-*N*,*N*,*N*-trimethyl ammonium bromide (TMA_2)**

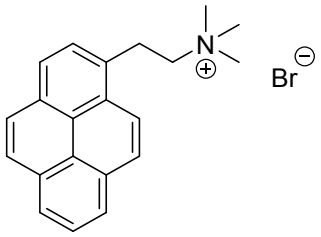

To a solution of **4** (50 mg, 0.120 mmol) in MeOH (0.24 mL) was added aqueous HBr (62%, 0.24 mL) and the resulting mixture was stirred at 55 ˚C. After 1.5 h the reaction mixture was allowed to cool to room temperature and then diluted with MeOH and acetone. Volatiles were removed under vacuum and the crude product was triturated in THF to obtain the title product as an off-white solid (39 mg, 88%), mp (Et_2O) decomposes above 210 ºC. ^{1}H-NMR (500 MHz, $CDCl_3$) δ 3.38 (s, N(CH_3)$_3$, 9 H), 3.75-3.81 (m, ArCH_2CH$_2$, 2 H), 3.88-3.95 (m, ArCH$_2$CH_2, 2 H), 8.03-8.08 (m, Ar*H*, 2 H), 8.10 (d, *J* = 9.0 Hz, Ar*H*, 1 H), 8.13 (d, *J* = 9.0 Hz, Ar*H*, 1 H), 8.22-8.29 (m, Ar*H*, 4 H), 8.35 (d, *J* = 9.0 Hz, Ar*H*, 1 H) ppm; ^{13}C-NMR (125 MHz, $CDCl_3$) δ 27.7 (ArCH$_2$CH$_2$), 53.7 (t, *J* = 4.0 Hz, N(*C*H$_3$)$_3$), 68.0 (t, *J* = 2.5 Hz, ArCH$_2$*C*H$_2$), 123.3 (Ar*C*H), 125.9 (Ar*C*), 126.3 (Ar*C*), 126.3 (Ar*C*H), 126.4 (Ar*C*H), 126.6 (Ar*C*H), 127.4 (Ar*C*H), 128.4 (Ar*C*H), 128.6 (Ar*C*H), 129.0 (Ar*C*H), 129.6 (Ar*C*H), 130.3 (Ar*C* × 2), 132.1 (Ar*C*), 132.4 (Ar*C*), 132.8 (Ar*C*) ppm; IR ν_{max} (neat/cm^{-1}): 3036, 3011, 1603, 1479, 974, 914, 847; HRMS calcd for $C_{21}H_{22}N$ [M]$^+$: 288.1747, found 288.1739.

1-Methyl-3-(2-(1-Pyrenyl)ethyl)imidazolium bromide (IMI_2)

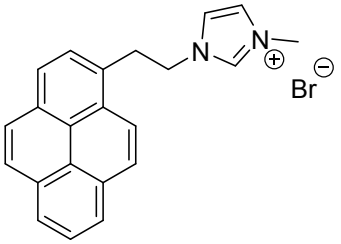

Prepared according to general procedure A using **S3** (50 mg, 0.162 mmol) and neat 1-methylimidazole (200 µL, 2.51 mmol). After 4.5 h at 55 ˚C THF was added. The precipitated product was filtered under vacuum and washed with more THF. After drying, the title product was obtained as an off-white solid (53 mg, 84%), mp (THF): 162-165 ºC. ^{1}H-NMR (500 MHz, MeOD-d_4) δ 3.71 (s, Ar(N)CH_3, 3 H), 3.84 (t, J = 7.0 Hz, ArCH_2CH$_2$N, 2 H), 4.60 (t, J = 7.0 Hz, ArCH$_2$CH_2N, 2 H), 7.40 (bs, ArH, 1 H), 7.46 (bs, ArH, 1 H), 7.96-8.08 (m, ArH, 4 H), 8.10 (d, J = 9.5 Hz, ArH, 1 H), 8.14-8.21 (m, ArH, 3 H), 8.63 (s, ArH, 1 H) ppm, partial H/D exchange is observed in position 2 of the imidazolium ring; ^{13}C-NMR (125 MHz, MeOD-d_4) δ 34.5 (ArCH$_2$CH$_2$), 36.3 (NCH$_3$), 52.0 (ArCH$_2$$CH_2$), 123.3 (Ar$C$H), 123.9 (Ar$C$H), 124.7 (Ar$C$H), 125.8 (Ar$C$), 126.0 (Ar$C$), 126.1 (Ar$C$H), 126.2 (Ar$C$H), 126.4 (Ar$C$H), 127.3 (Ar$C$H), 128.4 (Ar$C$H), 128.4 (Ar$C$H), 128.7 (Ar$C$H), 129.2 (Ar$C$H), 130.2 (Ar$C$), 131.5 (Ar$C$), 132.0 (Ar$C$), 132.1 (Ar$C$), 132.6 (Ar$C$), 137.8 (Ar$C$) ppm, partial H/D exchange is observed in position 2 of the imidazolium ring; IR ν_{max} (neat/cm^{-1}): 3040, 1564, 1456, 1165, 848; HRMS calcd for $C_{22}H_{19}N_2$ $[M]^+$: 311.1543, found 311.1530.

***N*-(2-(1-Pyrenyl)ethyl)pyridinium bromide (PRD_2)**

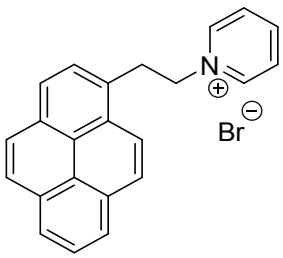

Prepared according to general procedure A using **S3** (50 mg, 0.162 mmol) and neat pyridine (200 µL, 2.47 mmol). After 16 h at 80 ˚C volatiles were removed, the solid resuspended in Et_2O, filtered and washed with more Et_2O. After drying, the title product was obtained as an off-white solid (54 mg, 86%), mp (Et_2O): 235-239 ºC. ^{1}H-NMR (400 MHz, MeOD-d_4) δ 4.11 (t, J = 6.8 Hz, ArCH_2CH$_2$N, 2 H), 5.14 (t, J = 6.8 Hz, ArCH_2CH$_2$N, 2 H), 7.73 (d, J = 8.0 Hz, ArH, 1 H), 7.88 (t, J = 7.2 Hz, ArH, 2 H), 8.01-8.09 (m, ArH, 2 H), 8.10-8.13 (m, ArH, 2 H), 8.15 (d, J = 9.4 Hz, ArH, 1 H), 8.20 (d, J = 9.4 Hz, ArH, 1 H), 8.22-8.27 (m, ArH, 2 H), 8.45 (tt, J = 7.7, 1.2 Hz, ArH, 1 H), 8.67 (d, J = 5.6 Hz, ArH, 2 H) ppm; ^{13}C-NMR (125 MHz, MeOD-d_4) δ 35.3 (ArCH$_2$CH$_2$), 64.2 (ArCH$_2$$CH_2$), 123.0 (Ar$C$H), 125.8 (Ar$C$), 126.1 (Ar$C$), 126.2 (Ar$C$H), 126.4 (Ar$C$H), 126.7 (Ar$C$H), 127.5 (Ar$C$H), 128.4 (Ar$C$H), 128.8 (Ar$C$H),

128.9 (Ar*C*H), 129.2 (Ar*C*H), 129.6 (Ar*C*H), 130.4 (Ar*C*), 130.5 (Ar*C*), 132.1 (Ar*C*), 132.5 (Ar*C*), 132.7 (Ar*C*), 146.0 (Ar*C*H), 147.0 (Ar*C*H) ppm; IR ν_{max} (neat/cm^{-1}): 3040, 1632, 1486, 1172, 850; HRMS calcd for $C_{23}H_{18}N$ $[M]^+$: 308.1434, found 308.1432.

(*E*)-3-(1-Pyrenyl)acrylic acid (S4)

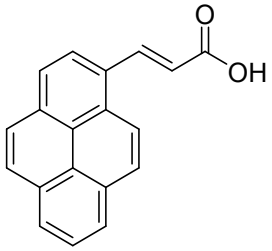

To a mixture of pyrene-1-carboxaldehyde (5.00 g, 21.7 mmol) and pyridine (10.5 mL, 130.2 mmol) was added malonic acid (11.3 g, 108.6 mmol). The mixture was stirred in an open flask at 100 ˚C for 16 h. After cooling to room temperature the reaction was quenched with 2 M aqueous HCl and then filtered under vacuum. The solid was washed with more 2 M aqueous HCl. After drying, the title product was obtained as a bright yellow solid (5.80 g, 98%), mp (H_2O): >260 ºC. ^{1}H-NMR (400 MHz, DMSO-d_6) δ 6.83 (d, *J* = 15.6 Hz, Ar$CH_2C\mathit{H}_2$, 1 H), 8.12 (t, *J* = 7.6 Hz, Ar*H*, 1 H), 8.22 (d, *J* = 8.8 Hz, Ar*H*, 1 H), 8.27 (d, *J* = 8.8 Hz, Ar*H*, 1 H), 8.30-8.34 (m, Ar*H*, 2 H), 8.35-8.40 (m, Ar*H*, 2 H), 8.50-8.57 (2, Ar*H*, 2 H), 8.71 (d, *J* = 15.6 Hz, Ar$C\mathit{H}_2CH_2$, 1 H), 12.61 (bs, $CO_2\mathit{H}$, 1 H) ppm; ^{13}C-NMR (125 MHz, DMSO-d_6) δ 121.7 (Ar$CH_2\mathit{C}H_2$), 122.3 (Ar*C*H), 123.8 (Ar*C*), 124.0 (Ar*C*), 124.6 (Ar*C*H), 125.3 (Ar*C*H), 125.9 (Ar*C*H), 126.1 (Ar*C*H), 126.6 (Ar*C*H), 127.4 (Ar*C*H), 127.9 (Ar*C*), 128.5 (Ar*C*H), 128.7 (Ar*C*H), 128.9 (Ar*C*), 130.2 (Ar*C*), 130.8 (Ar*C*), 132.1 (Ar*C*), 139.9 (Ar$\mathit{C}H_2CH_2$), 167.6 ($\mathit{C}O_2H$) ppm; IR ν_{max} (neat/cm^{-1}): 1675, 1609, 1278, 1175, 971, 841, 836; HRMS calcd for $C_{19}H_{11}O_2$ $[M–H]^–$: 271.0765, found 271.0767.

3-(1-Pyrenyl)propionic acid (S5)

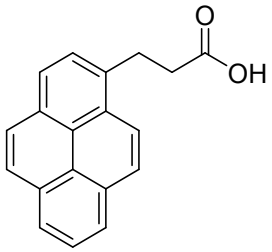

To a stirring suspension of **S4** (6.34 g, 23.3 mmol) in AcOH (900 mL) under N_2 was added PtO_2 (634 mg, 10 wt%). Then, the atmosphere was replaced by H_2 (1 atm) doing 3 vacuum/refill cycles. After 18 h stirring at room temperature the initial yellow suspension turned into a dark grey suspension and the atmosphere was replaced by N_2 again. The mixture was filtered through cotton and Et_2O was used to wash it. After concentrating to dryness under vacuum, the solid residue was dissolved in Et_2O, washed with H_2O (× 3), dried ($MgSO_4$) and concentrated *in vacuo*. The title product was obtained as a pale yellow solid (6.09 g, 95%), which was used in the next step without further purification.

3-(1-Pyrenyl)-1-propanol (S6)

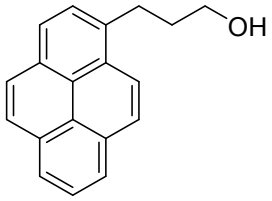

Prepared according to general procedure B using a solution of $LiAlH_4$ (3.36 g, 88.7 mmol) in dry THF (100 mL) and a solution of **S5** (6.08 g, 22.2 mmol) acid in dry THF (50 mL). Reaction set at 0 ˚C and stirred for 18 h at room temperature. The crude product was purified by silica column chromatography (CH_2Cl_2). The title product was obtained as a pale yellow solid (5.25 g, 91%), mp (CH_2Cl_2): 87-90 ºC. ^{1}H-NMR (400 MHz, $CDCl_3$) δ 1.38 (s, O*H*, 1 H), 2.08-2.20 (m, $ArCH_2CH_2CH_2$, 2 H), 3.48 (t, *J* = 7.6 Hz, $ArCH_2CH_2CH_2$, 2 H), 3.81 (t, *J* = 6.4 Hz, $ArCH_2CH_2CH_2$, 2 H), 7.91 (d, *J* = 8.0 Hz, Ar*H*, 1 H), 7.96-8.08 (m, Ar*H*, 3 H), 8.09-8.24 (m, Ar*H*, 4 H), 8.32 (d, *J* = 9.2 Hz, Ar*H*, 1 H) ppm; ^{13}C-NMR (125 MHz, $CDCl_3$) δ 29.6 ($ArCH_2CH_2CH_2$), 34.6 ($ArCH_2CH_2CH_2$), 62.4 ($ArCH_2CH_2CH_2$), 123.3 (Ar*C*H), 124.7 (Ar*C*H), 124.8 (Ar*C*H), 124.9 (Ar*C*H), 125.0 (Ar*C*), 125.1 (Ar*C*), 125.8 (Ar*C*H), 126.6 (Ar*C*H), 127.3 (Ar*C*H), 127.3 (Ar*C*H), 127.5 (Ar*C*H), 128.7 (Ar*C*), 129.9 (Ar*C*), 130.9 (Ar*C*), 131.4 (Ar*C*), 136.1 (Ar*C*) ppm; IR ν_{max} (neat/cm^{-1}): 3340, 3037, 2937, 2873, 1434, 1183, 1058, 841; HRMS calcd for $C_{19}H_{17}O$ $[M+H]^+$: 261.1274, found 261.1277.

1-(3-Bromopropyl)pyrene (S7)

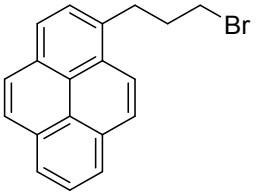

To a solution of **S6** (781 mg, 3.00 mmol), in dry CH_2Cl_2 (8.6 mL) under N_2 were added tetrabromomethane (995 mg, 3.00 mmol) and triphenylphosphine (1.57 g, 6.00 mmol) and the resulting solution was stirred at room temperature. After 40 min the mixture was diluted with EtOAc and the resulting precipitate was removed by filtration through Celite. The crude product was purified by silica column chromatography (hexane/CH_2Cl_2, 100:0 to 50:50). The title product was obtained as a pale yellow oil (781 mg, 81%). ^{1}H-NMR (400 MHz, $CDCl_3$) δ 2.42 (quint, *J* = 6.9 Hz, $ArCH_2CH_2CH_2$, 2 H), 3.46-3.58 (m, $ArCH_2CH_2CH_2$ + $ArCH_2CH_2CH_2$, 4 H), 7.91 (d, *J* = 7.6 Hz, Ar*H*, 1 H), 7.98-8.08 (m, Ar*H*, 3 H), 8.10-8.16 (m, Ar*H*, 2 H), 8.17-8.23 (m, Ar*H*, 2 H), 8.30 (d, *J* = 9.2 Hz, Ar*H*, 1 H) ppm; ^{13}C-NMR (125 MHz, $CDCl_3$) δ 31.6 ($ArCH_2CH_2CH_2$), 33.5 ($ArCH_2CH_2CH_2$), 34.4 ($ArCH_2CH_2CH_2$), 123.1 (Ar*C*H), 124.8 (Ar*C*H), 124.8 (Ar*C*H), 124.9 (Ar*C*), 125.0 (Ar*C*H), 125.1 (Ar*C*), 125.9 (Ar*C*H), 126.8 (Ar*C*H), 127.4 (Ar*C*H), 127.4 (Ar*C*H), 127.5 (Ar*C*H), 128.7 (Ar*C*), 130.1

(Ar*C*), 130.8 (Ar*C*), 131.4 (Ar*C*), 134.7 (Ar*C*) ppm; IR ν_{max} (neat/cm^{-1}): 3039, 2930, 1602, 1434, 1243, 1182, 841; HRMS calcd for $C_{19}H_{16}Br$ $[M+H]^+$: 323.0430, found 323.0438.

_N_-(3-(1-Pyrenyl)propyl)-_N_,_N_,_N_-trimethyl ammonium bromide (TMA_3)

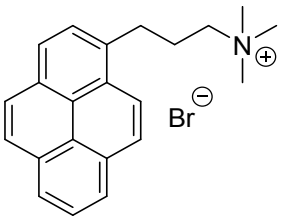

Prepared according to general procedure A using **S7** (300 mg, 0.928 mmol) and a solution of NMe_3 in EtOH (4.2 M, 5.0 mL, 21.0 mmol). After 17 h at 55 ˚C volatiles were removed, the solid resuspended in Et_2O, filtered and washed with more Et_2O. The title product was obtained as a white solid (302 mg, 85%), mp (Et_2O): 214-217 ºC. ^{1}H-NMR (400 MHz, MeOD-d_4) δ 2.30-2.42 (m, $ArCH_2CH_2CH_2$, 2 H), 3.12 (s, $N(CH_3)_3$, 9 H), 3.44-3.58 (m, $ArCH_2CH_2CH_2$ + $ArCH_2CH_2CH_2$, 4 H), 7.98 (d, *J* = 7.6 Hz, Ar*H*, 1 H), 8.03 (t, *J* = 7.6 Hz, Ar*H*, 1 H), 8.08 (s, Ar*H*, 2 H), 8.17-8.25 (m, Ar*H*, 4 H), 8.38 (d, *J* = 9.2 Hz, Ar*H*, 1 H) ppm; ^{13}C-NMR (125 MHz, MeOD-d_4) δ 26.1 ($ArCH_2CH_2CH_2$), 30.6 (t, *J* = 1.6 Hz, $ArCH_2CH_2CH_2$), 53.6 (t, *J* = 4.0 Hz,$N(CH_3)_3$), 67.5 (t, *J* = 2.9 Hz,$ArCH_2CH_2CH_2$), 123.9 (Ar*C*H), 126.0 (Ar*C*), 126.1 (Ar*C*H), 126.1 (Ar*C*H), 126.3 (Ar*C*H), 126.3 (Ar*C*), 127.2 (Ar*C*H), 128.1 (Ar*C*H), 128.4 (Ar*C*H), 128.5 (Ar*C*H), 128.9 (Ar*C*H), 130.0 (Ar*C*), 131.8 (Ar*C*), 132.2 (Ar*C*), 132.8 (Ar*C*), 135.3 (Ar*C*) ppm; IR ν_{max} (neat/cm^{-1}): 3011, 2952, 1602, 1482, 848; HRMS calcd for $C_{22}H_{24}N$ $[M]^+$: 302.1903, found 302.1891.

1-Methyl-3-(3-(1-Pyrenyl)propyl)imidazolium bromide (IMI_3)

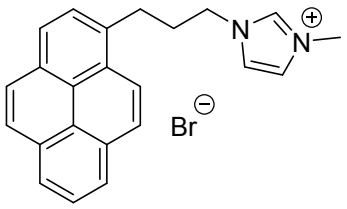

Prepared according to general procedure A using **S7** (100 mg, 0.309 mmol) and neat 1-methylimidazole (670 µL, 8.41 mmol). After 17 h at 55 ˚C volatiles were removed, the solid resuspended in Et_2O, filtered and washed with more Et_2O. The title product was obtained as an off-white solid (89 mg, 71%), mp (Et_2O): 180-184 ºC. ^{1}H-NMR (400 MHz, MeOD-d_4) δ 2.50 (quint, *J* = 7.4 Hz, $ArCH_2CH_2CH_2$, 2 H), 3.50 (t, *J* = 7.4 Hz, $ArCH_2CH_2CH_2$, 2 H), 3.72 (s, $Ar(N)CH_3$, 3 H), 4.37 (t, *J* = 7.4 Hz, $ArCH_2CH_2CH_2$, 2 H), 7.39 (d, *J* = 1.8 Hz, Ar*H*, 1 H), 7.59 (d, *J* = 1.8 Hz, Ar*H*, 1 H), 7.93 (d, *J* = 7.6 Hz, Ar*H*, 1 H), 8.03 (t, *J* = 7.6 Hz, Ar*H*, 1 H), 8.08 (s, Ar*H*, 2 H), 8.14-8.26 (m, 4 H), 8.31 (d, *J* = 9.2 Hz, Ar*H*, 1 H) ppm, full H/D

exchange is observed in position 2 of the imidazolium ring; ^{13}C-NMR (125 MHz, MeOD-d_4) δ 31.0 (Ar*C*H_2CH_2CH_2), 32.6 (ArCH_2*C*H_2CH_2), 36.2 (Ar(N)*C*H_3), 50.6 (ArCH_2CH_2*C*H_2), 123.5 (Ar*C*H), 124.0 (Ar*C*H), 124.7 (Ar*C*H), 126.0 (Ar*C*), 126.1 (Ar*C*H), 126.1 (Ar*C*H), 126.2 (Ar*C*), 126.3 (Ar*C*H), 127.2 (Ar*C*H), 128.1 (Ar*C*H), 128.4 (Ar*C*H), 128.5 (Ar*C*H), 128.8 (Ar*C*H), 129.9 (Ar*C*), 131.7 (Ar*C*), 132.2 (Ar*C*), 132.8 (Ar*C*), 135.6 (Ar*C*) ppm, full H/D exchange is observed in position 2 of the imidazolium ring and C-2 is not observed; IR ν_{max} (neat/cm^{-1}): 3049, 2942, 1546, 1458, 1246, 1184, 1103, 849; HRMS calcd for $C_{23}H_{21}N_2$ $[M]^+$: 325.1699, found 325.1684.

_N_-(3-(1-Pyrenyl)propyl)pyridinium bromide (PRD_3)

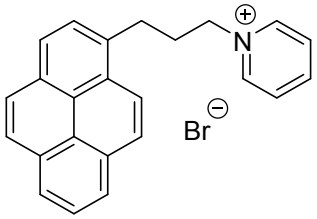

Prepared according to general procedure A using **S7** (100 mg, 0.309 mmol) and neat pyridine (670 □L, 8.28 mmol). After 17 h at 55 ˚C volatiles were removed, the solid resuspended in Et_2O, filtered and washed with more Et_2O. The title product was obtained as an off-white solid (96 mg, 77%),, mp (Et_2O): decomposes above 45 ºC. ^{1}H-NMR (400 MHz, MeOD-d_4) δ 2.63 (quint, *J* = 7.6 Hz, ArCH$_2$C*H*$_2$CH$_2$, 2 H), 3.55 (t, *J* = 7.6 Hz, ArC*H*$_2$CH$_2$CH$_2$, 2 H), 4.81 (t, *J* = 7.6 Hz, ArCH$_2$CH$_2$C*H*$_2$, 2 H), 7.92-7.99 (m, Ar*H*, 3 H), 8.00-8.10 (m, Ar*H*, 3 H), 8.13-8.25 (m, Ar*H*, 4 H), 8.32 (d, *J* = 9.6 Hz, Ar*H*, 1 H), 8.43 (t, *J* = 8.0 Hz, Ar*H*, 1 H), 8.96 (d, *J* = 5.6 Hz, Ar*H*, 2 H) ppm; ^{13}C-NMR (125 MHz, MeOD-d_4) δ 30.9 (Ar*C*H$_2$CH$_2$CH$_2$), 33.9 (ArCH$_2$*C*H$_2$CH$_2$), 62.9 (ArCH$_2$CH$_2$*C*H$_2$), 123.9 (Ar*C*H), 126.0 (Ar*C*), 126.1 (Ar*C*H), 126.1 (Ar*C*H), 126.2 (Ar*C*), 126.3 (Ar*C*H), 127.2 (Ar*C*H), 128.1 (Ar*C*H), 128.4 (Ar*C*H), 128.4 (Ar*C*H), 128.9 (Ar*C*H), 129.3 (Ar*C*H), 129.9 (Ar*C*), 131.8 (Ar*C*), 132.2 (Ar*C*), 132.8 (Ar*C*), 135.2 (Ar*C*), 145.9 (Ar*C*H), 146.6 (Ar*C*H) ppm; IR ν_{max} (neat/cm^{-1}): 3035, 1633, 1488, 1121, 974, 850; HRMS calcd for $C_{24}H_{20}N$ $[M]^+$: 322.1590, found 322.1578.

4-(1-Pyrenyl)-1-butanol (S8)

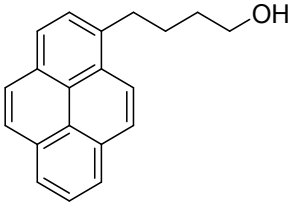

Prepared according to general procedure B using a solution of $LiAlH_4$ (263 mg, 6.94 mmol) in dry THF (7.5 mL) and a solution of 3-(1-pyrenyl)butyric acid (500 mg, 1.73 mmol) in dry

THF (4.0 mL). Reaction set at 0 ˚C and stirred for 19 h at room temperature. The crude product was purified by silica column chromatography (CH_2Cl_2). The title product was obtained as a pale yellow oil (448 mg, 94%). ^{1}H-NMR (400 MHz, $CDCl_3$) δ 1.25 (bs, O*H*, 1 H), 1.70-1.84 (m, CH_2, 2 H), 1.90-2.04 (m, CH_2, 2 H), 3.40 (t, *J* = 7.6 Hz, ArCH_2CH$_2$CH$_2$CH$_2$, 2 H), 3.73 (t, *J* = 6.2 Hz, ArCH$_2$CH$_2$CH$_2$CH_2, 2 H), 7.89 (d, *J* = 8.0 Hz, Ar*H*, 1 H), 7.97-8.08 (m, Ar*H*, 3 H), 8.09-8.15 (m, Ar*H*, 2 H), 8.15-8.21 (m, Ar*H*, 2 H), 8.30 (d, *J* = 9.2 Hz, Ar*H*, 1 H) ppm; ^{13}C-NMR (125 MHz, $CDCl_3$) δ 28.0 (*C*H$_2$), 32.7 (*C*H$_2$), 33.2 (Ar*C*H$_2$CH$_2$CH$_2$CH$_2$), 62.9 (ArCH$_2$CH$_2$CH$_2$*C*H$_2$), 123.4 (Ar*C*H), 124.7 (Ar*C*H), 124.8 (Ar*C*H), 124.8 (Ar*C*H), 125.0 (Ar*C*), 125.1 (Ar*C*), 125.8 (Ar*C*H), 126.6 (Ar*C*H), 127.2 (Ar*C*H), 127.2 (Ar*C*H), 127.5 (Ar*C*H), 128.6 (Ar*C*), 129.8 (Ar*C*), 130.9 (Ar*C*), 131.4 (Ar*C*), 136.6 (Ar*C*) ppm; IR ν_{max} (neat/cm^{-1}): 3323, 3039, 2934, 2862, 1603, 1458, 1182, 1060, 841; HRMS calcd for $C_{20}H_{19}O$ $[M+H]^+$: 275.1430, found 275.1428.

1-(4-Bromobutyl)pyrene (S9)

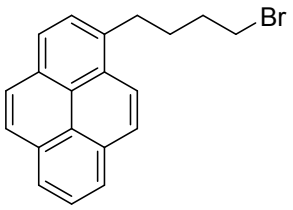

Prepared according to general procedure C using **S8** (400 mg, 1.46 mmol), PBr_3 (137 µL, 1.46 mmol) and CH_2Cl_2 (4.0 mL). Reaction set at 0 ˚C and stirred at room temperature for 17 h and then at 40 ˚C for 4 h. The crude product was purified by silica column chromatography (hexane/CH_2Cl_2, 50:50). The title product was obtained as a pale yellow oil (220 mg, 45%), mp (CH_2Cl_2): 68-70 ºC. ^{1}H-NMR (400 MHz, $CDCl_3$) δ 1.98-2.10 (m, ArCH$_2$CH_2CH$_2$CH$_2$ + ArCH$_2$CH$_2$CH_2CH$_2$, 4 H), 3.34-3.44 (m, ArCH$_2$CH$_2$CH$_2$CH_2, 2 H), 3.45-3.53 (m, ArCH_2CH$_2$CH$_2$CH$_2$, 2 H), 7.88 (d, *J* = 8.0 Hz, Ar*H*, 1 H), 7.98-8.08 (m, Ar*H*, 3 H), 8.13 (d, *J* = 8.0 Hz, Ar*H*, 2 H), 8.16-8.21 (m, Ar*H*, 2 H), 8.28 (d, *J* = 9.6 Hz, Ar*H*, 1 H) ppm; ^{13}C-NMR (125 MHz, $CDCl_3$) δ 30.2 (ArCH$_2$CH$_2$*C*H$_2$CH$_2$), 32.6 (ArCH$_2$*C*H$_2$CH$_2$CH$_2$), 32.6 (ArCH$_2$CH$_2$CH$_2$*C*H$_2$), 33.6 (Ar*C*H$_2$CH$_2$CH$_2$CH$_2$), 123.2 (Ar*C*H), 124.7 (Ar*C*H), 124.8 (Ar*C*H), 124.9 (Ar*C*H), 125.0 (Ar*C*), 125.1 (Ar*C*), 125.8 (Ar*C*H), 126.7 (Ar*C*H), 127.3 (Ar*C*H), 127.3 (Ar*C*H), 127.5 (Ar*C*H), 128.6 (Ar*C*), 129.9 (Ar*C*), 130.9 (Ar*C*), 131.4 (Ar*C*), 136.0 (Ar*C*) ppm; IR ν_{max} (neat/cm^{-1}): 3039, 2937, 2862, 1603, 1458, 1434, 1245, 1182, 841; HRMS calcd for $C_{20}H_{17}Br$ $[M]^+$: 336.0508, found 336.0507.

***N*-(4-(1-Pyrenyl)butyl)-*N*,*N*,*N*-trimethyl ammonium bromide (TMA_4)**

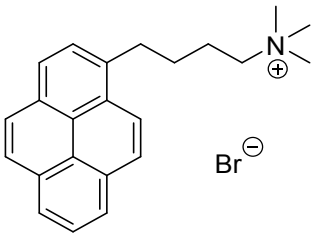

Prepared according to general procedure A using **S9** (120 mg, 0.356 mmol) and a solution of NMe_3 in EtOH (4.2 M, 1.9 mL, 8.05 mmol). After 21 h at 55 ˚C volatiles were removed, the solid resuspended in Et_2O, filtered and washed with more Et_2O. The title product was obtained as a white solid (142 mg, 97%), mp (Et_2O): 187-190 ºC. ^{1}H-NMR (400 MHz, MeOD-d_4) δ 1.84-2.05 (m, $ArCH_2CH_2CH_2CH_2$ + $ArCH_2CH_2CH_2CH_2$, 4 H), 3.11 (s, $N(CH_3)_3$, 9 H), 3.36-3.43 (m, $ArCH_2CH_2CH_2CH_2$, 2 H), 3.43-3.50 (m, $ArCH_2CH_2CH_2CH_2$, 2 H), 7.94 (d, *J* = 8.0 Hz, Ar*H*, 1 H), 8.01 (t, *J* = 7.6 Hz, Ar*H*, 1 H), 8.03-8.09 (m, Ar*H*, 2 H), 8.13-8.23 (m, Ar*H*, 4 H), 8.35 (d, *J* = 9.2 Hz, Ar*H*, 1 H) ppm; ^{13}C-NMR (125 MHz, MeOD-d_4) δ 23.9 ($ArCH_2CH_2CH_2CH_2$), 29.5 (t, *J* = 1.5 Hz $ArCH_2CH_2CH_2CH_2$), 33.6 ($ArCH_2CH_2CH_2CH_2$), 53.5 (t, *J* = 4.0 Hz $N(CH_3)_3$), 67.7 (t, *J* = 2.9 Hz $ArCH_2CH_2CH_2CH_2$), 124.3 (Ar*C*H), 125.9 (Ar*C*H), 126.0 (Ar*C*H), 126.1 (Ar*C*H), 126.1 (Ar*C*), 126.3 (Ar*C*), 127.1 (Ar*C*H), 127.8 (Ar*C*H), 128.5 (Ar*C*H), 128.5 (Ar*C*H), 128.5 (Ar*C*H), 129.9 (Ar*C*), 131.5 (Ar*C*), 132.3 (Ar*C*), 132.8 (Ar*C*), 137.0 (Ar*C*) ppm; IR ν_{max} (neat/cm^{-1}): 3011, 2945, 2874, 1602, 1486, 1417, 1183, 966, 907, 848; HRMS calcd for $C_{23}H_{26}N$ $[M]^+$: 316.2060, found 316.2055.

1-Methyl-3-(4-(1-Pyrenyl)butyl)imidazolium bromide (IMI_4)

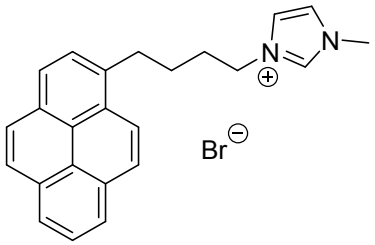

Prepared according to general procedure A using **S9** (30 mg, 0.089 mmol) and neat 1-methylimidazole (200 µL, 2.51 mmol). After 21 h at 55 ˚C volatiles were removed, the solid resuspended in Et_2O, filtered and washed with more Et_2O. The title product was obtained as a white solid (36 mg, 86%.), mp (Et_2O): 158-161 ºC. ^{1}H-NMR (400 MHz, MeOD-d_4) δ 1.85-2.98 (m, $ArCH_2CH_2CH_2CH_2$, 2 H), 2.00-2.11 (m, $ArCH_2CH_2CH_2CH_2$, 2 H), 3.45 (t, *J* = 7.2 Hz, $ArCH_2CH_2CH_2CH_2$, 2 H), 3.82 (s, Ar(N)CH_3, 3 H), 4.24 (t, *J* = 7.2 Hz, $ArCH_2CH_2CH_2CH_2$, 2 H), 7.47 (d, *J* = 2.0 Hz, Ar*H*, 1 H), 7.57 (d, *J* = 2.0 Hz, Ar*H*, 1 H), 7.91 (d, *J* = 7.6 Hz, Ar*H*, 1 H), 8.01 (t, *J* = 7.6 Hz, Ar*H*, 1 H), 8.06 (s, Ar*H*, 2 H), 8.12-8.23 (m, Ar*H*, 4 H), 8.31 (d, *J* = 9.6 Hz, Ar*H*, 1 H) ppm, full H/D exchange is observed in position

2 of the imidazolium ring; ^{13}C-NMR (125 MHz, MeOD-d_4) δ 29.4 (ArCH$_2$*C*H$_2$CH$_2$CH$_2$), 30.9 (ArCH$_2$CH$_2$*C*H$_2$CH$_2$), 35.5 (Ar*C*H$_2$CH$_2$CH$_2$CH$_2$), 36.3 (Ar(N)*C*H$_3$), 50.8 (ArCH$_2$CH$_2$CH$_2$*C*H$_2$), 123.6 (Ar*C*H), 124.2 (Ar*C*H), 124.9 (Ar*C*H), 125.9 (Ar*C*H), 125.9 (Ar*C*H), 126.1 (Ar*C*), 126.1 (Ar*C*H), 126.3 (Ar*C*), 127.1 (Ar*C*H), 127.8 (Ar*C*H), 128.5 (Ar*C*H), 128.5 (Ar*C*H), 128.6 (Ar*C*H), 129.8 (Ar*C*), 131.5 (Ar*C*), 132.3 (Ar*C*), 132.8 (Ar*C*), 137.1 (Ar*C*) ppm, full H/D exchange is observed in position 2 of the imidazolium ring and C-2 is not observed; IR ν_{max} (neat/cm^{-1}): 3038, 2934, 1545, 1458, 851; HRMS calcd for $C_{24}H_{23}N_2$ [M]$^+$: 339.1856, found 339.1855.

_N_-(4-(1-Pyrenyl)butyl)pyridinium bromide (PRD$_4$)

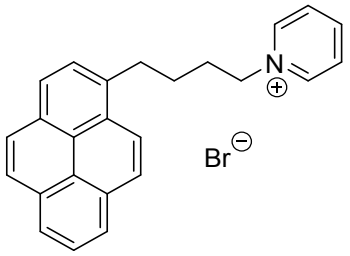

Prepared according to general procedure A using **S9** (30 mg, 0.089 mmol) and neat pyridine (200 □L, 2.47 mmol). After 21 h at 55 ˚C volatiles were removed, the solid resuspended in Et_2O, filtered and washed with more Et_2O. The title product was obtained as a white solid (37 mg, quant.), mp (Et_2O): decomposes above 250 ºC. ^{1}H-NMR (400 MHz, MeOD-d_4) δ 1.90-2.03 (m, ArCH$_2$C*H*$_2$CH$_2$CH$_2$, 2 H), 2.12-2.26 (m, ArCH$_2$CH$_2$C*H*$_2$CH$_2$, 2 H), 3.47 (t, *J* = 7.6 Hz, ArC*H*$_2$CH$_2$CH$_2$CH$_2$, 2 H), 4.66 (t, *J* = 7.6 Hz, ArCH$_2$CH$_2$CH$_2$C*H*$_2$, 2 H), 7.90 (d, *J* = 7.6 Hz, Ar*H*, 1 H), 7.97-8.04 (m, Ar*H*, 3 H), 8.06 (s, Ar*H*, 2 H), 8.10-8.16 (m, Ar*H*, 2 H), 8.20 (d, *J* = 8.0 Hz, Ar*H*, 2 H), 8.30 (d, *J* = 9.6 Hz, Ar*H*, 1 H), 8.47 (tt, *J* = 8.0, 1.2 Hz, Ar*H*, 1 H), 8.92 (d, *J* = 5.2 Hz, Ar*H*, 2 H) ppm; ^{13}C-NMR (125 MHz, MeOD-d_4) δ 27.8 (ArCH$_2$*C*H$_2$CH$_2$CH$_2$), 30.8 (ArCH$_2$CH$_2$*C*H$_2$CH$_2$), 32.1 (Ar*C*H$_2$CH$_2$CH$_2$CH$_2$), 61.6 (ArCH$_2$CH$_2$CH$_2$*C*H$_2$), 122.8 (Ar*C*H), 124.5 (Ar*C*H), 124.5 (Ar*C*H), 124.7 (Ar*C*H), 124.7 (Ar*C*H), 124.9 (Ar*C*), 125.7 (Ar*C*), 126.4 (Ar*C*H), 127.1 (Ar*C*H), 127.1 (Ar*C*H), 127.2 (Ar*C*H), 128.0 (Ar*C*H), 128.4 (Ar*C*), 130.1 (Ar*C*), 130.8 (Ar*C*), 131.4 (Ar*C*), 135.4 (Ar*C*), 144.4 (Ar*C*H), 145.3 (Ar*C*H) ppm; IR ν_{max} (neat/cm^{-1}): 3028, 2939, 1624, 1602, 1479, 1465, 1184, 849; HRMS calcd for $C_{25}H_{22}N$ [M]$^+$: 336.1747, found 336.1744.

S1.4. NMR Spectra

1-(Bromomethyl)pyrene (S1)

^{1}H-NMR (400 MHz, $CDCl_3$)

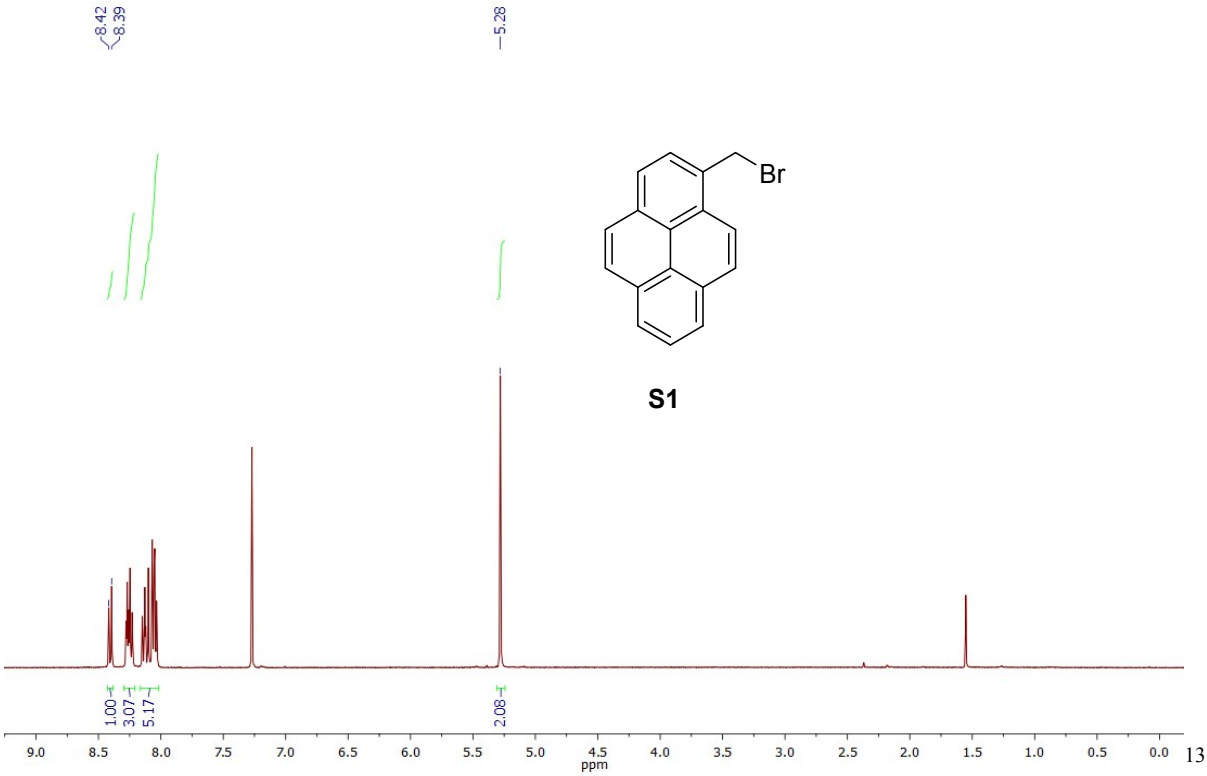

S1

13

C-NMR (125 MHz, $CDCl_3$)

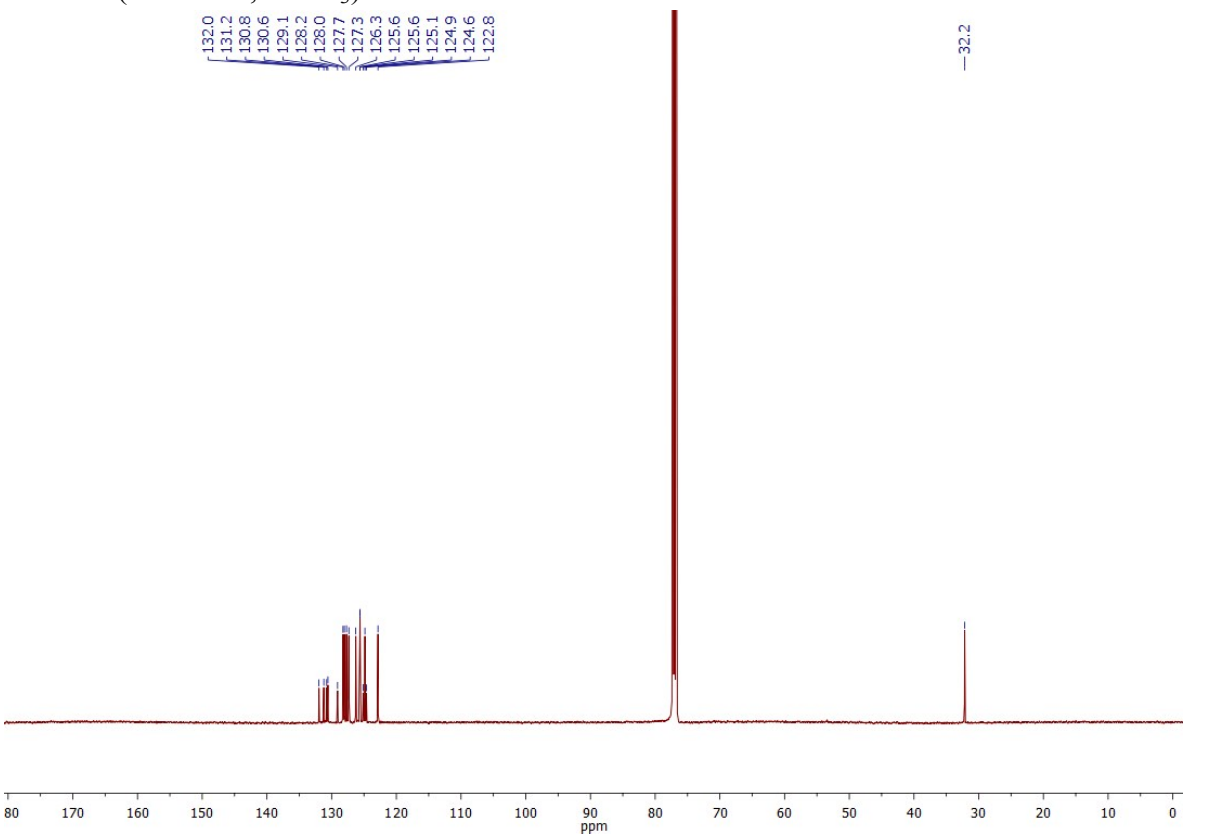

***N*,*N*,*N*-Trimethyl-*N*-(1-pyrenylmethyl)ammonium bromide (TMA_1)**

^{1}H-NMR (400 MHz, DMSO-d_6)

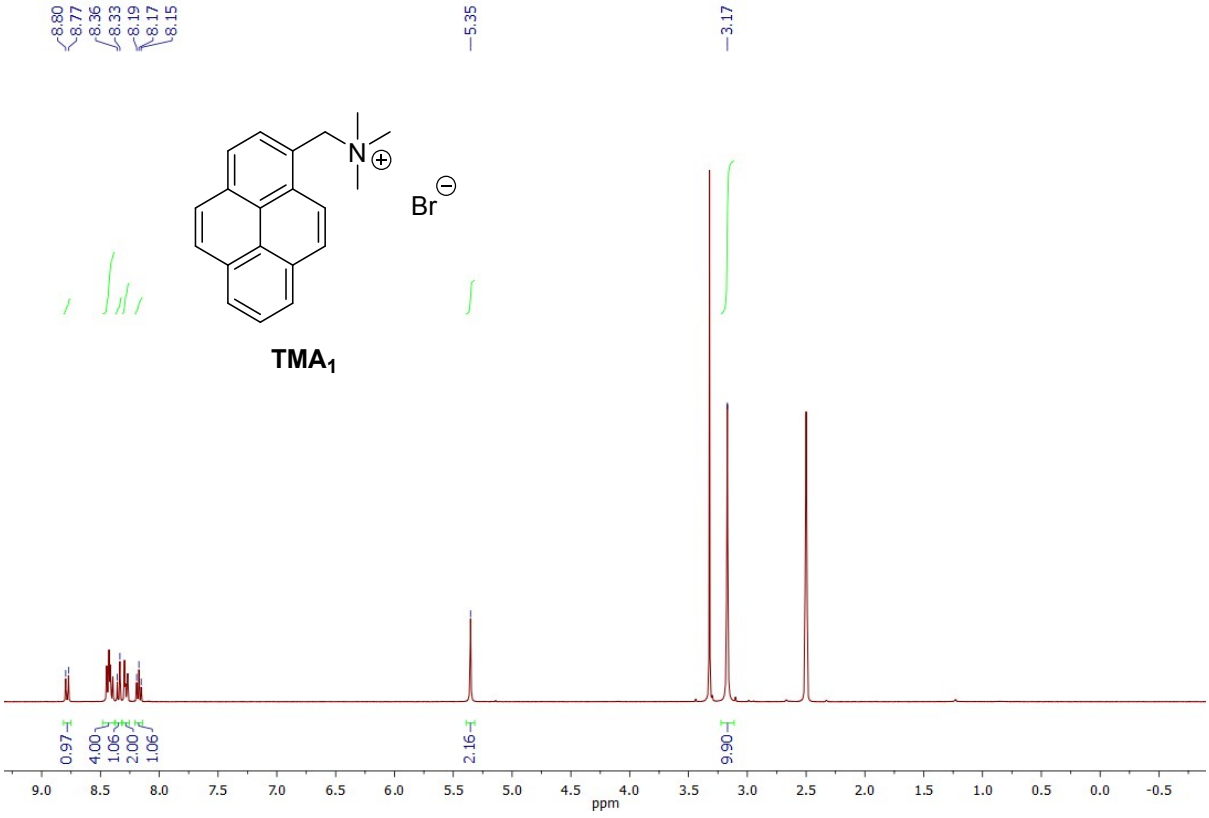

TMA_1

^{13}C-NMR (100 MHz, DMSO-d_6)

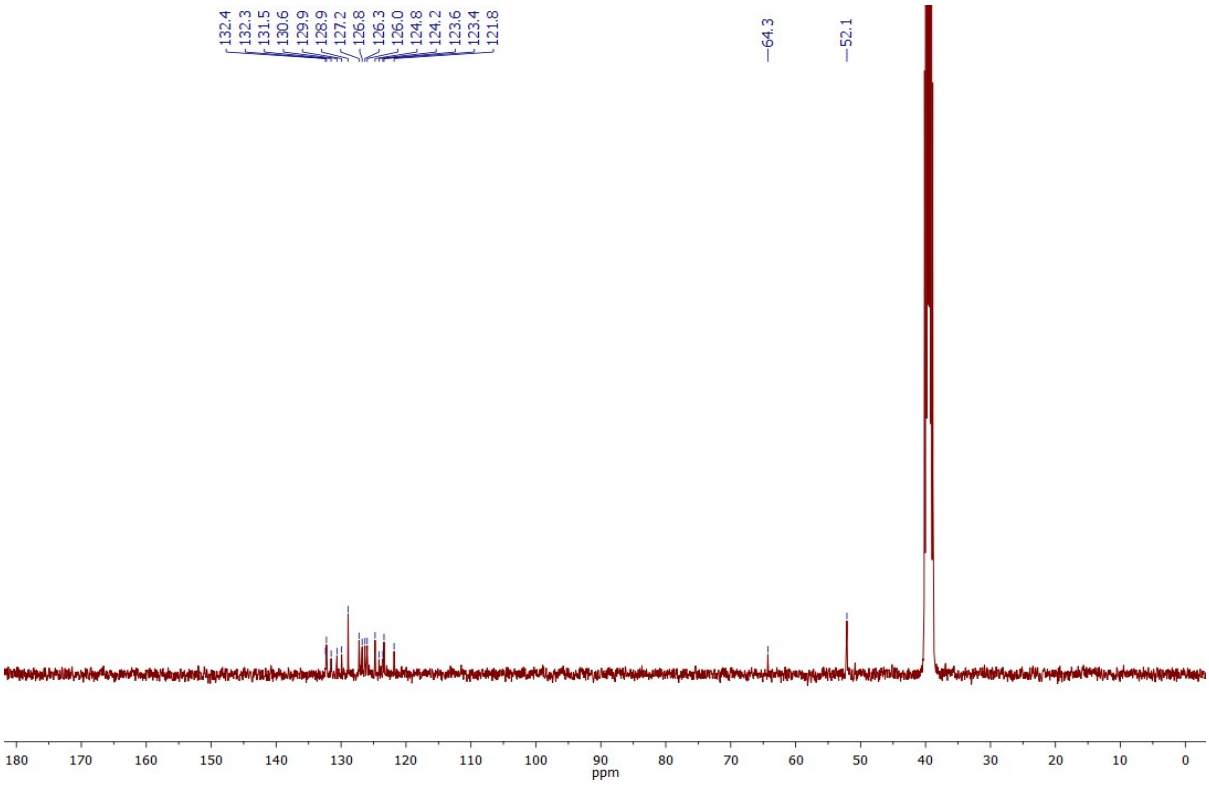

^{1}H-NMR (500 MHz, MeOD-d_4)

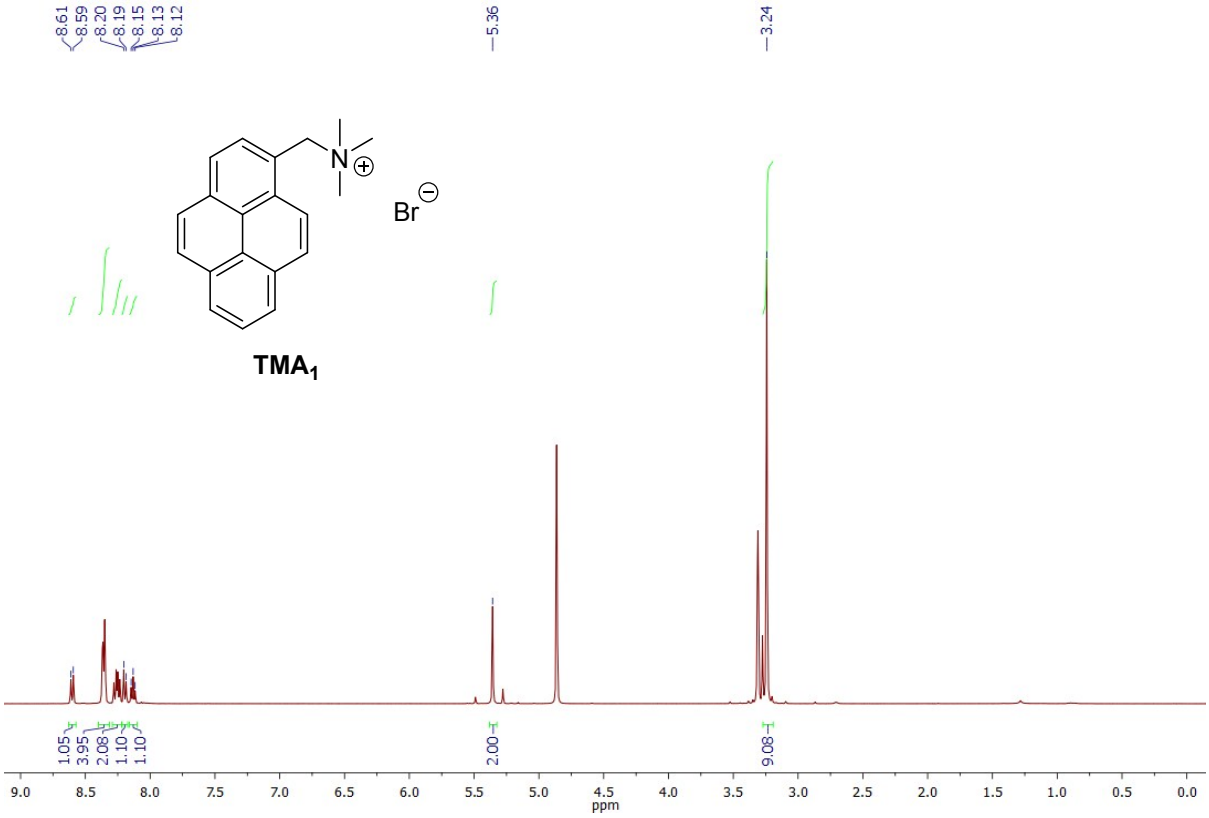

TMA$_1$

^{13}C-NMR (125 MHz, MeOD-d_4)

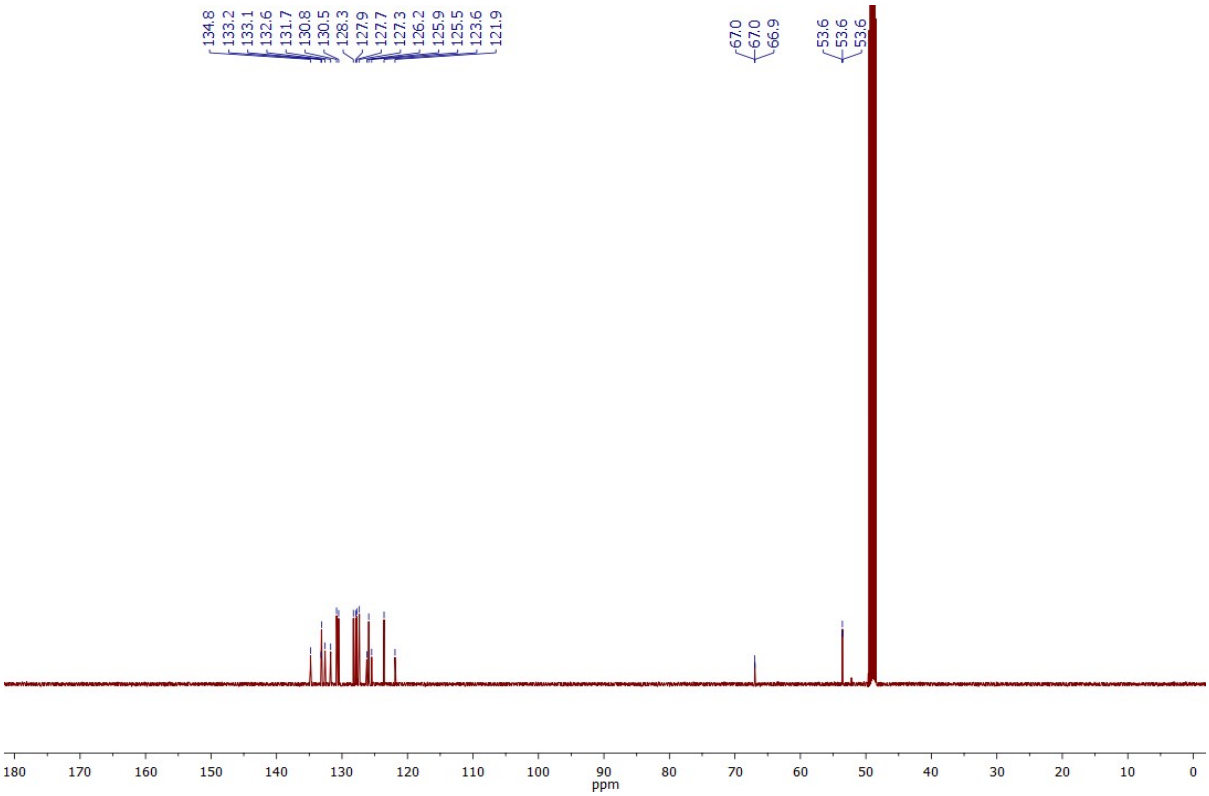

1-Methyl-3-(1-pyrenylmethyl)-1*H*-imidazolium bromide (IMI_1)

^{1}H-NMR (400 MHz, DMSO-d_6)

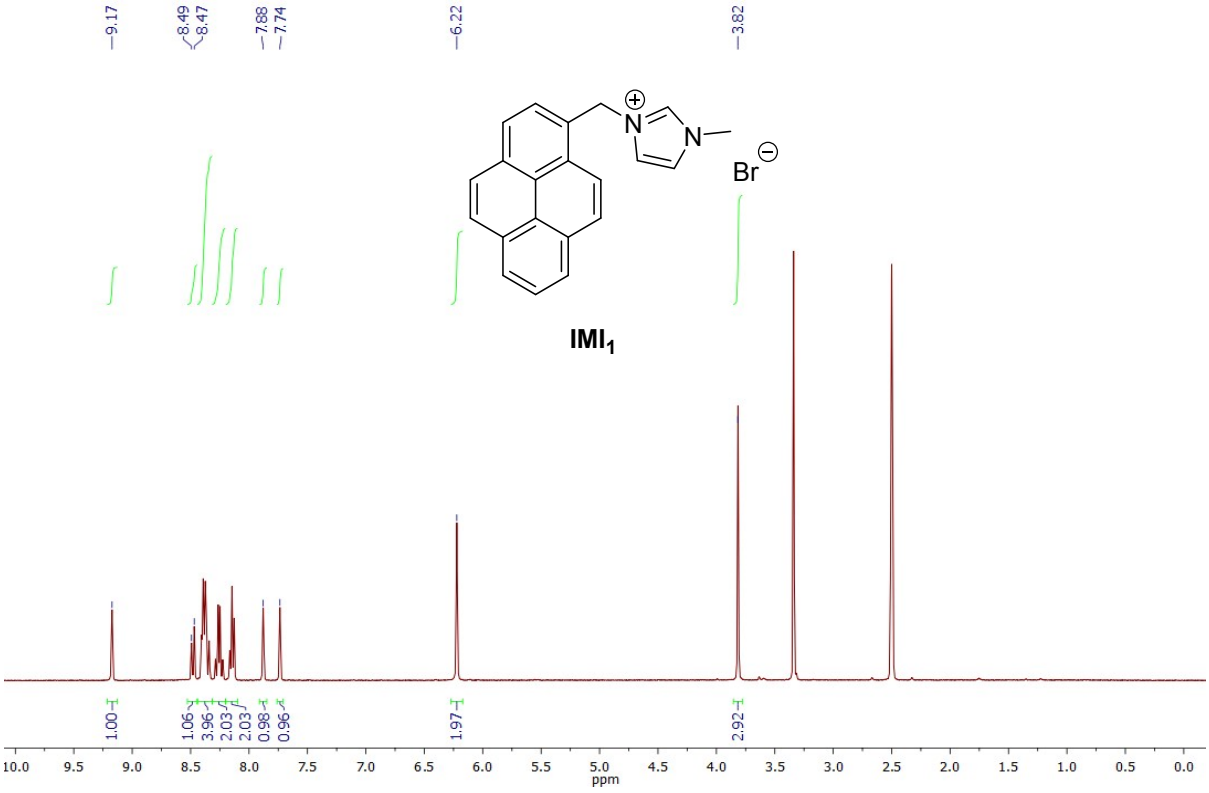

^{13}C-NMR (100 MHz, DMSO-d_6)

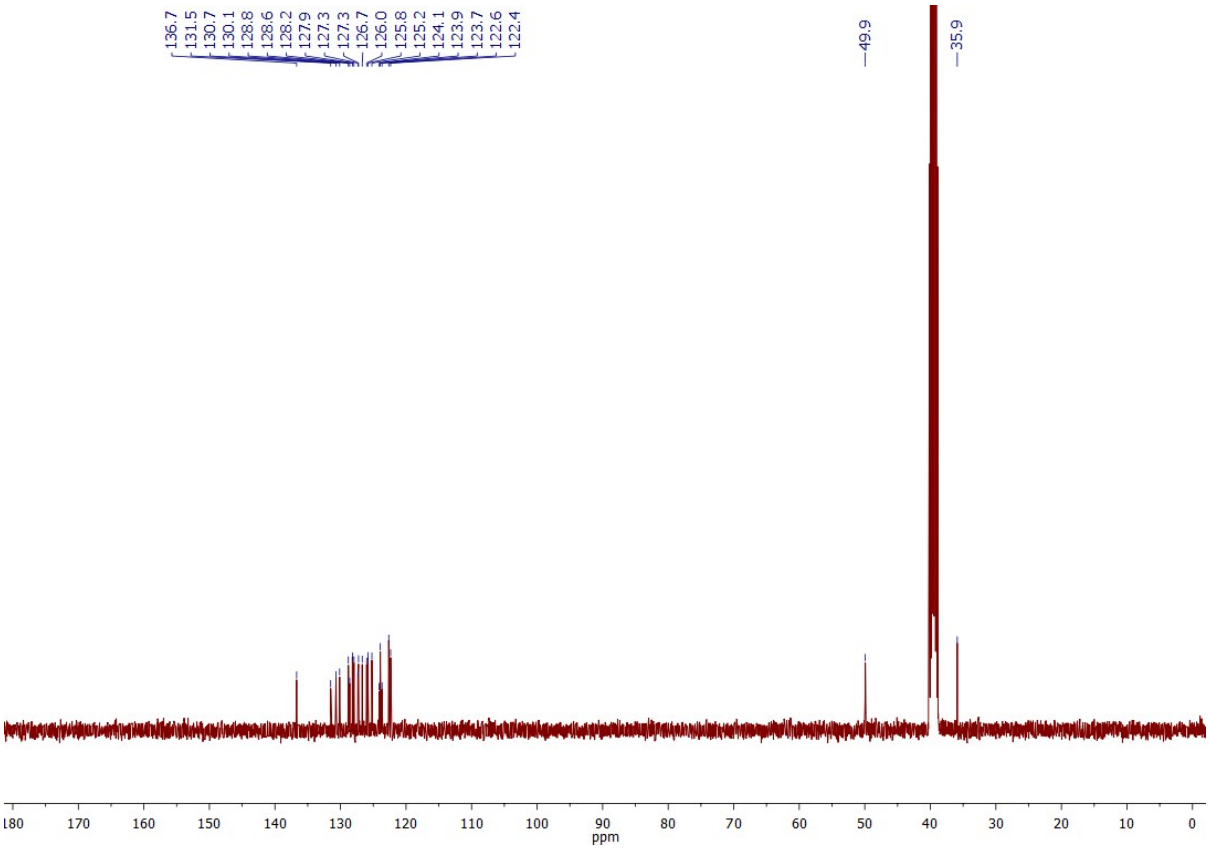

^{1}H-NMR (500 MHz, MeOD-d_4)

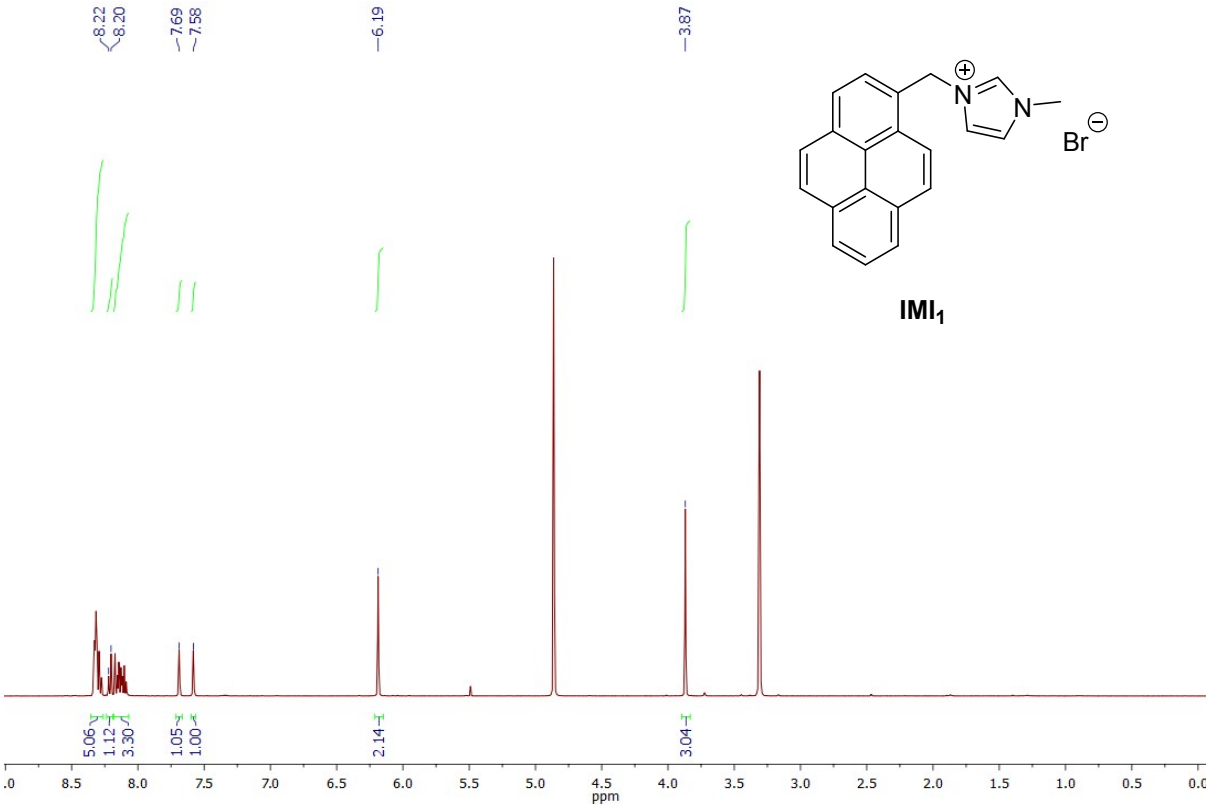

IMI$_1$

^{13}C-NMR (125 MHz, MeOD-d_4)

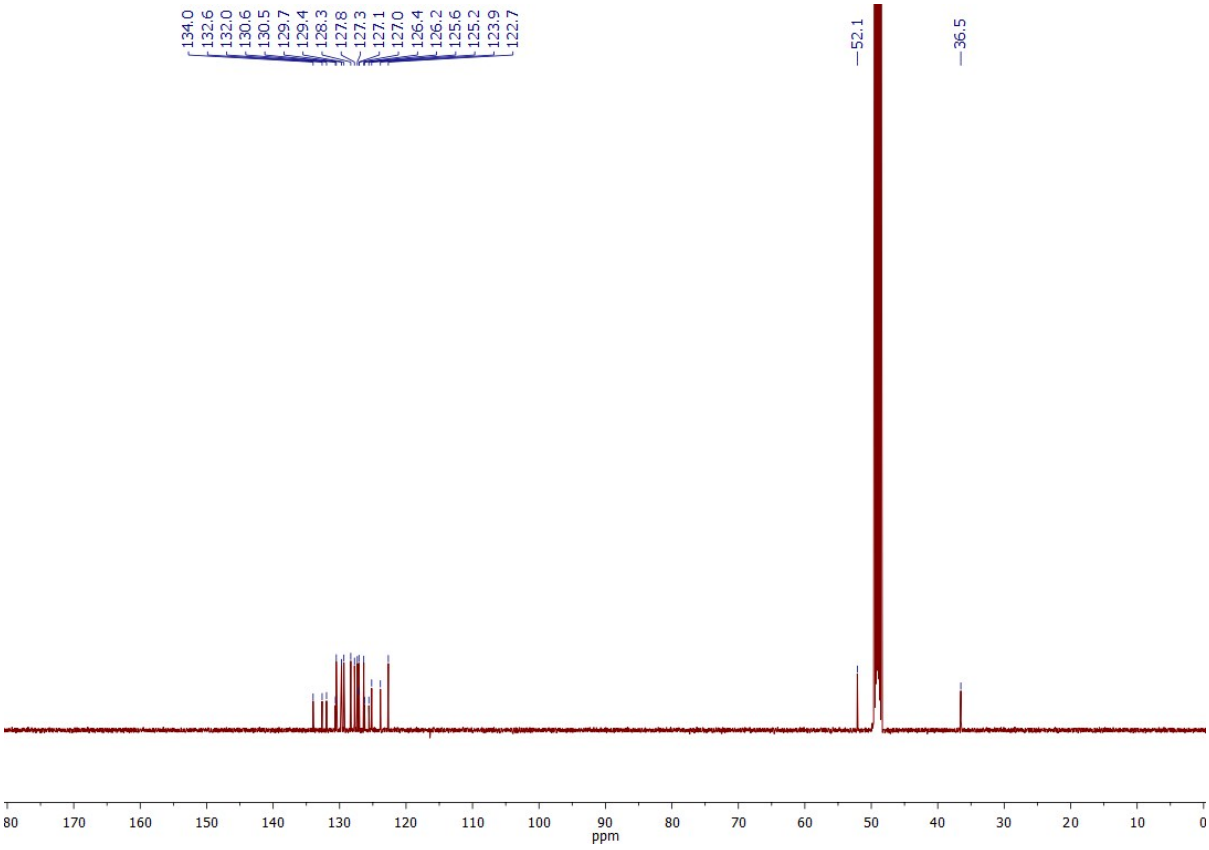

1-(1-Pyrenylmethyl)pyridinium bromide (PRD_1)

^{1}H-NMR (400 MHz, DMSO-d_6)

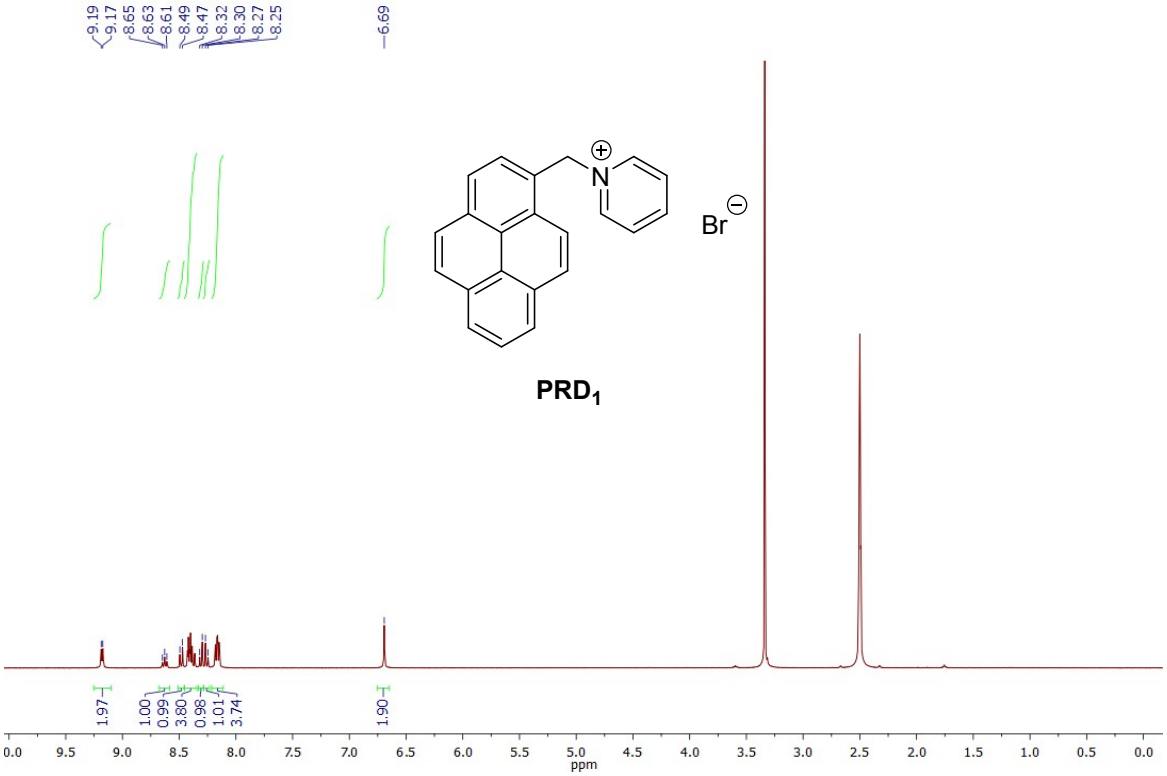

^{13}C-NMR (100 MHz, DMSO-d_6)

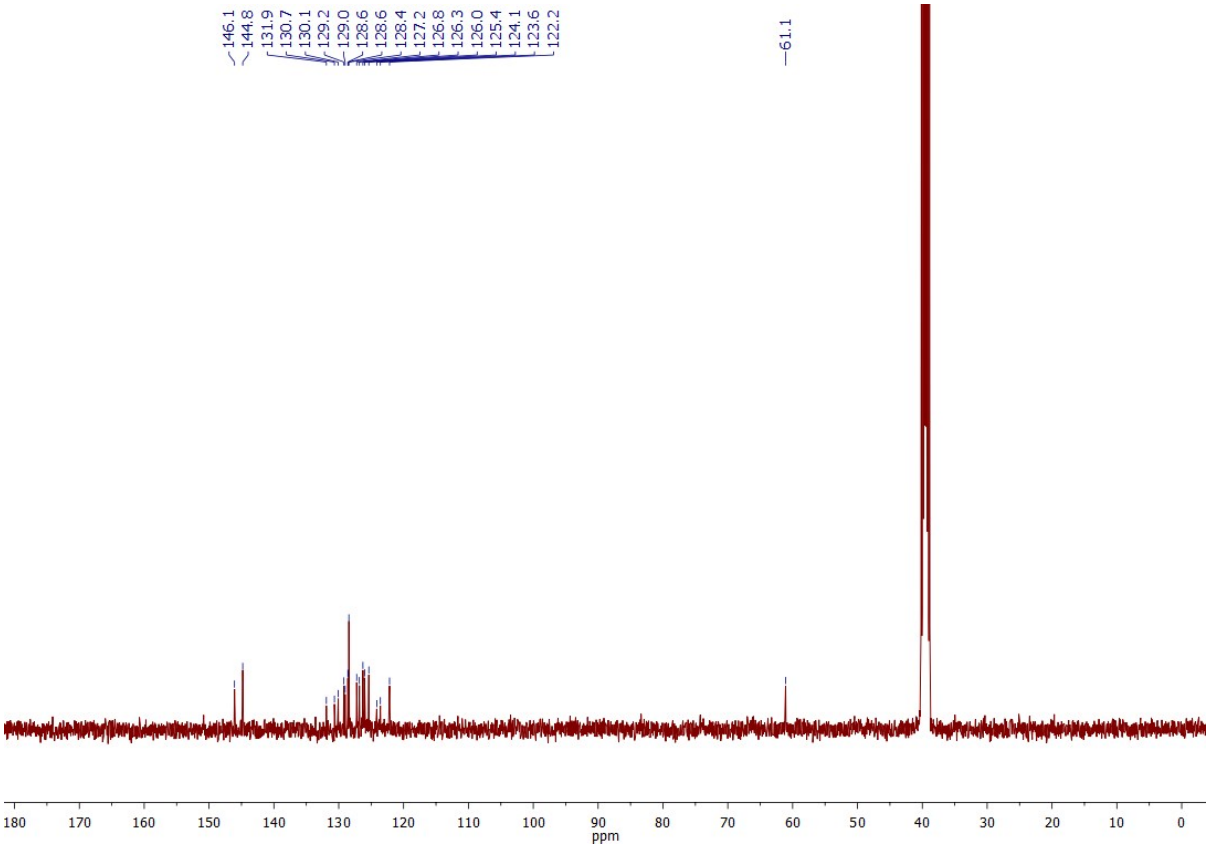

2-(1-Pyrenyl)ethanol (S2)

^{1}H-NMR (400 MHz, $CDCl_3$)

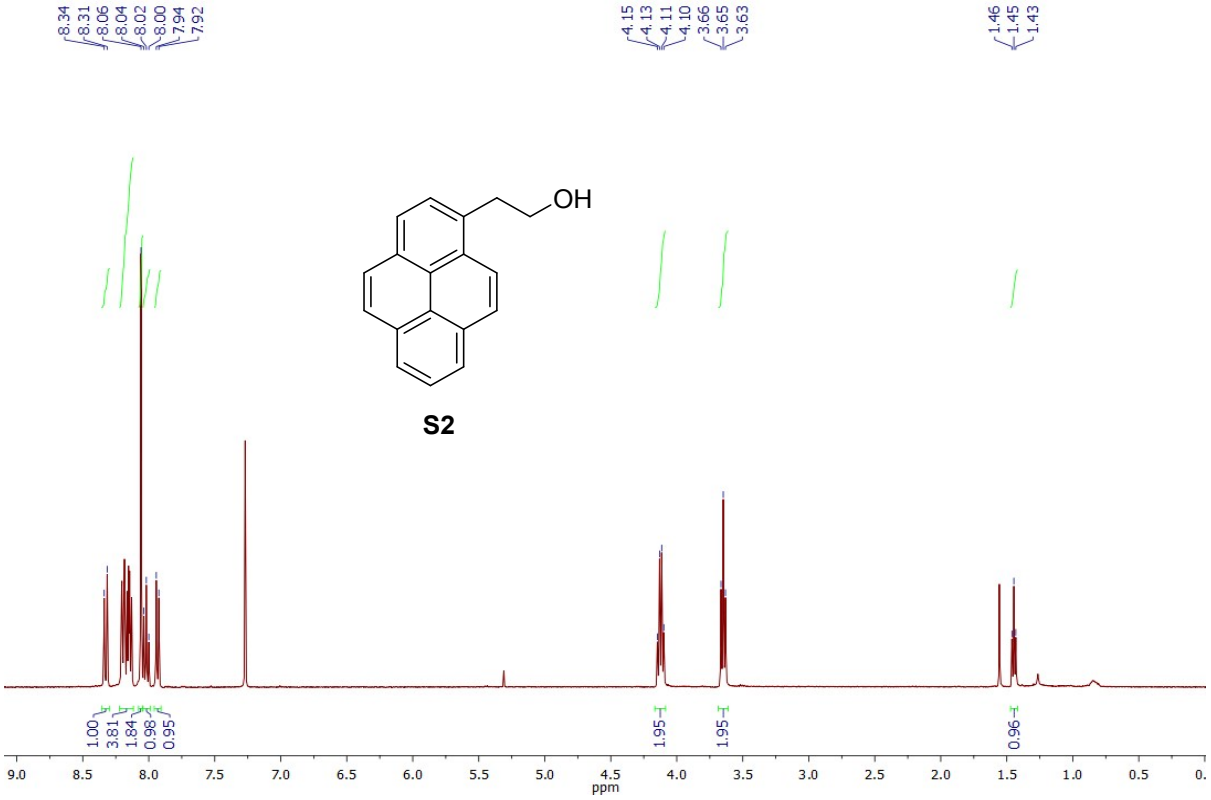

^{13}C-NMR (100 MHz, $CDCl_3$)

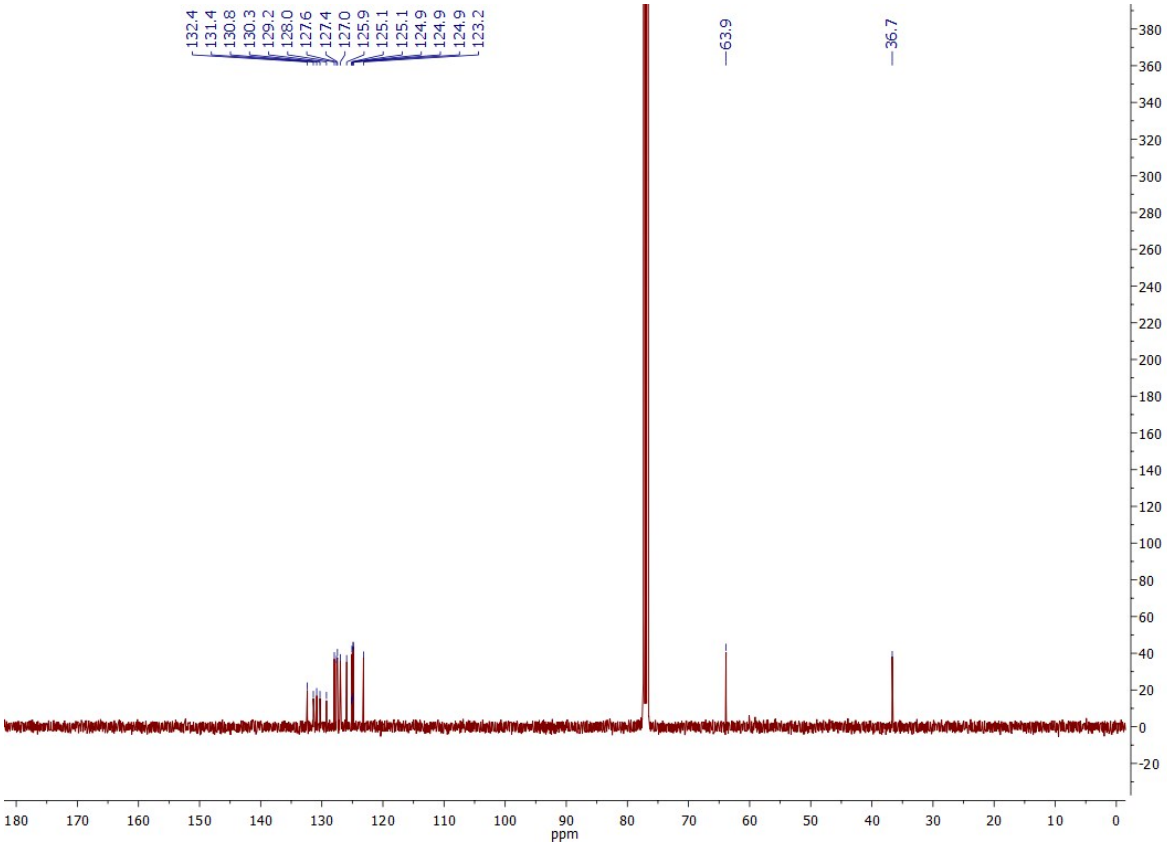

1-(2-Bromoethyl)pyrene (S3)

^{1}H-NMR (400 MHz, $CDCl_3$)

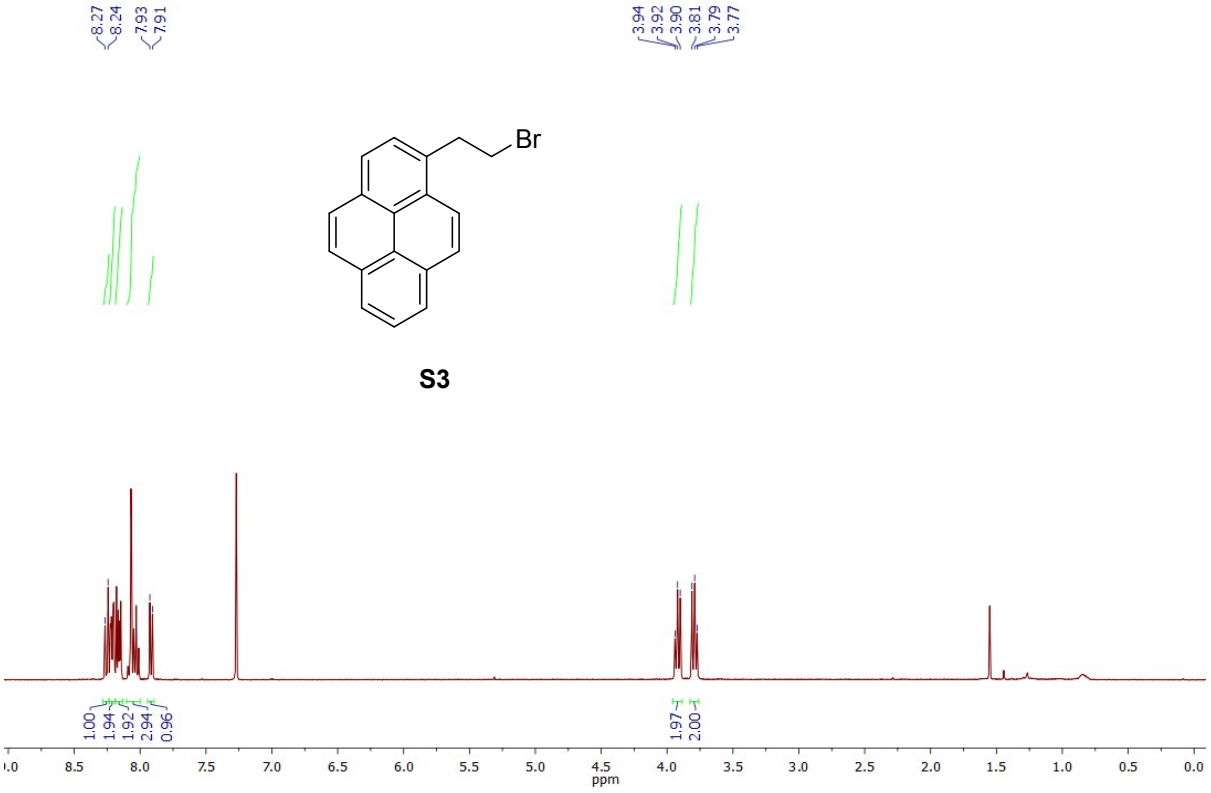

^{13}C-NMR (125 MHz, $CDCl_3$)

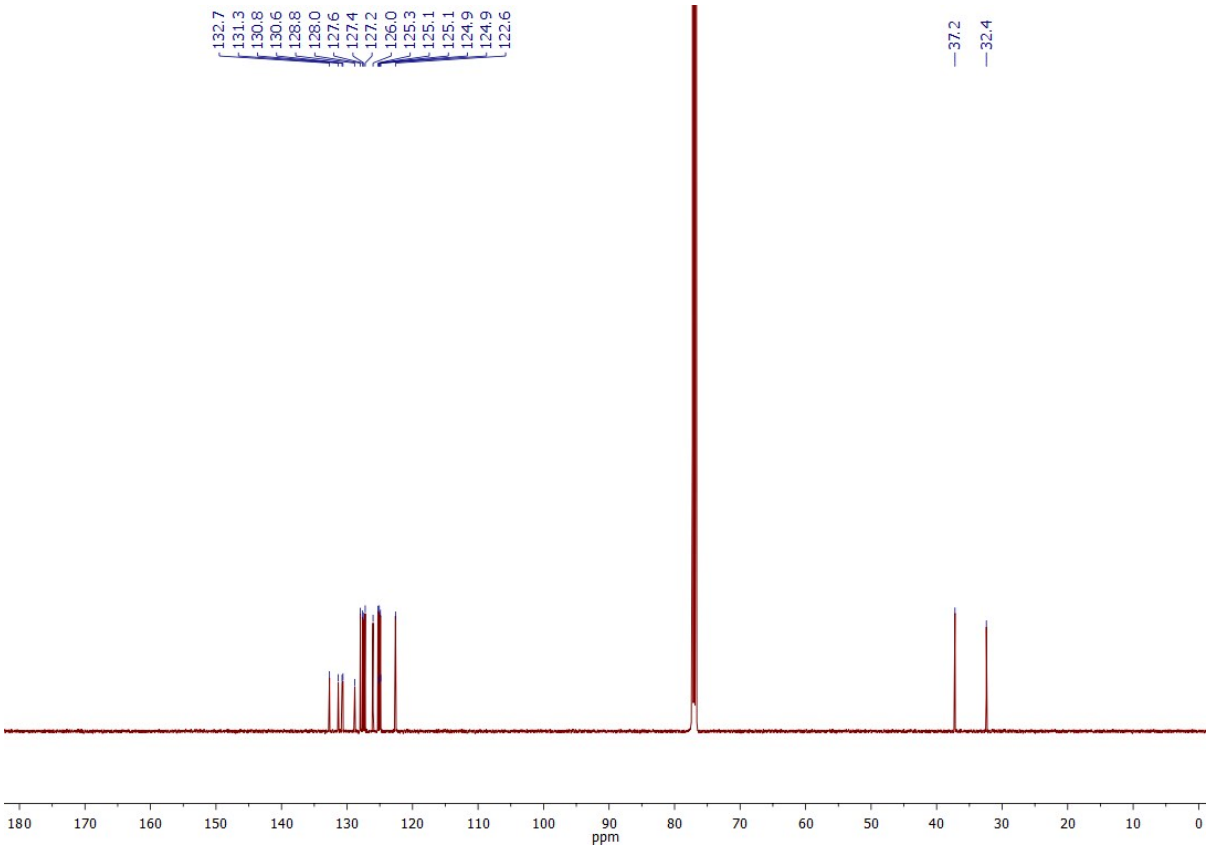

***N*,*N*-Dimethyl-2-(1-pyrenyl)acetamide (2)**

^{1}H-NMR (400 MHz, $CDCl_3$)

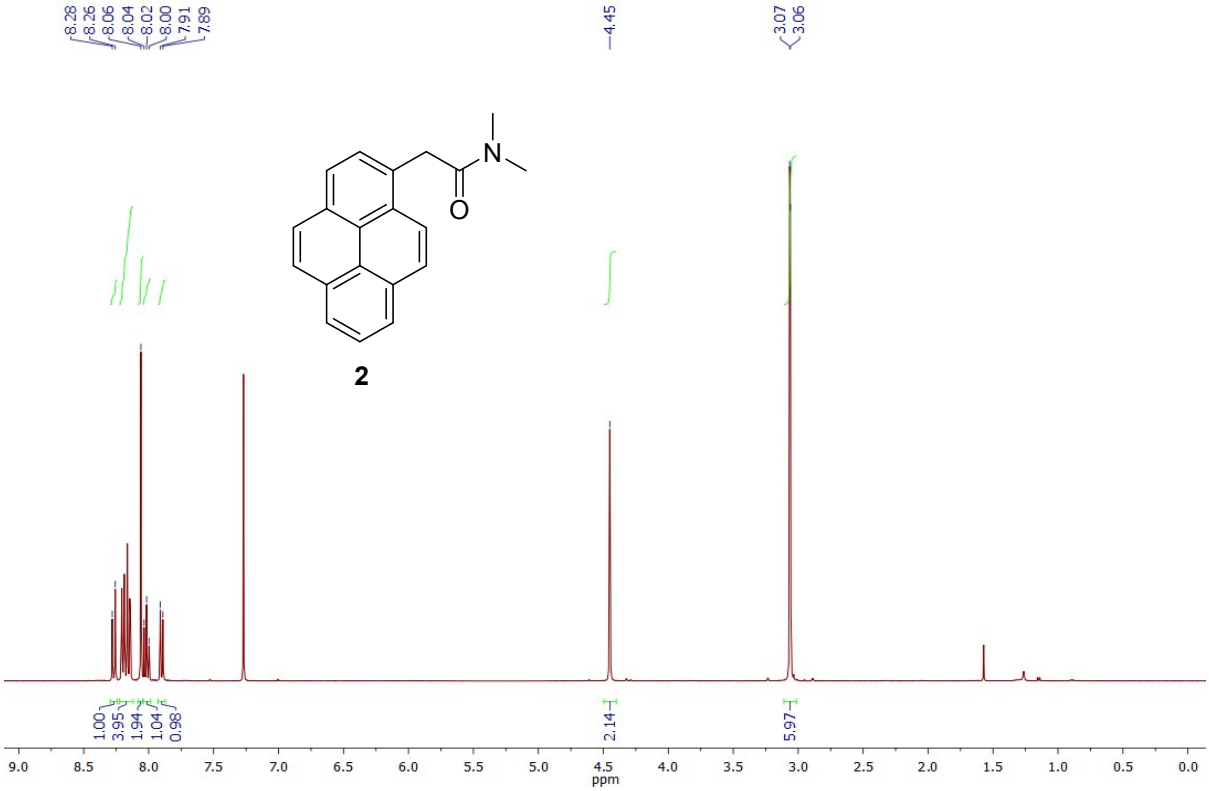

^{13}C-NMR (125 MHz, $CDCl_3$)

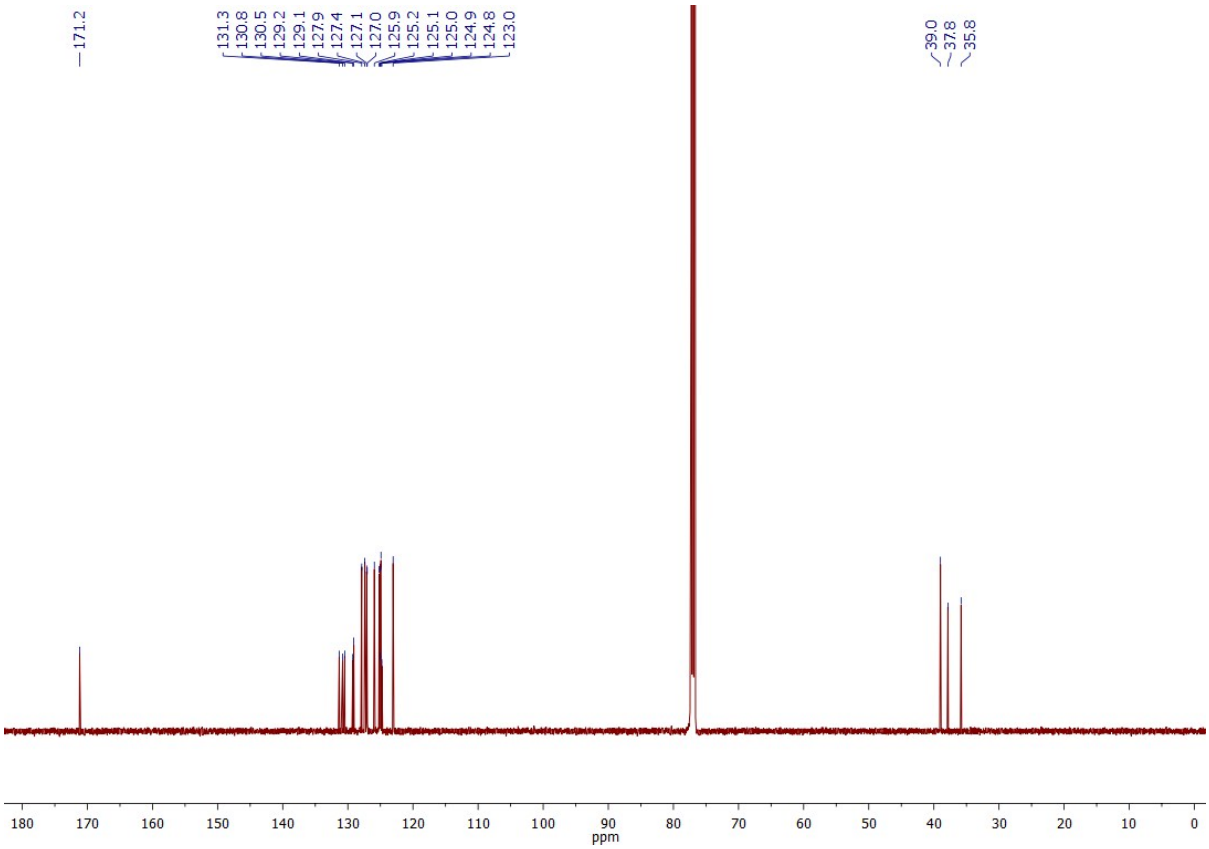

N-(2-(1-Pyrenyl)ethyl)-*N*,*N*-dimethylamine (3)

^{1}H-NMR (400 MHz, $CDCl_3$)

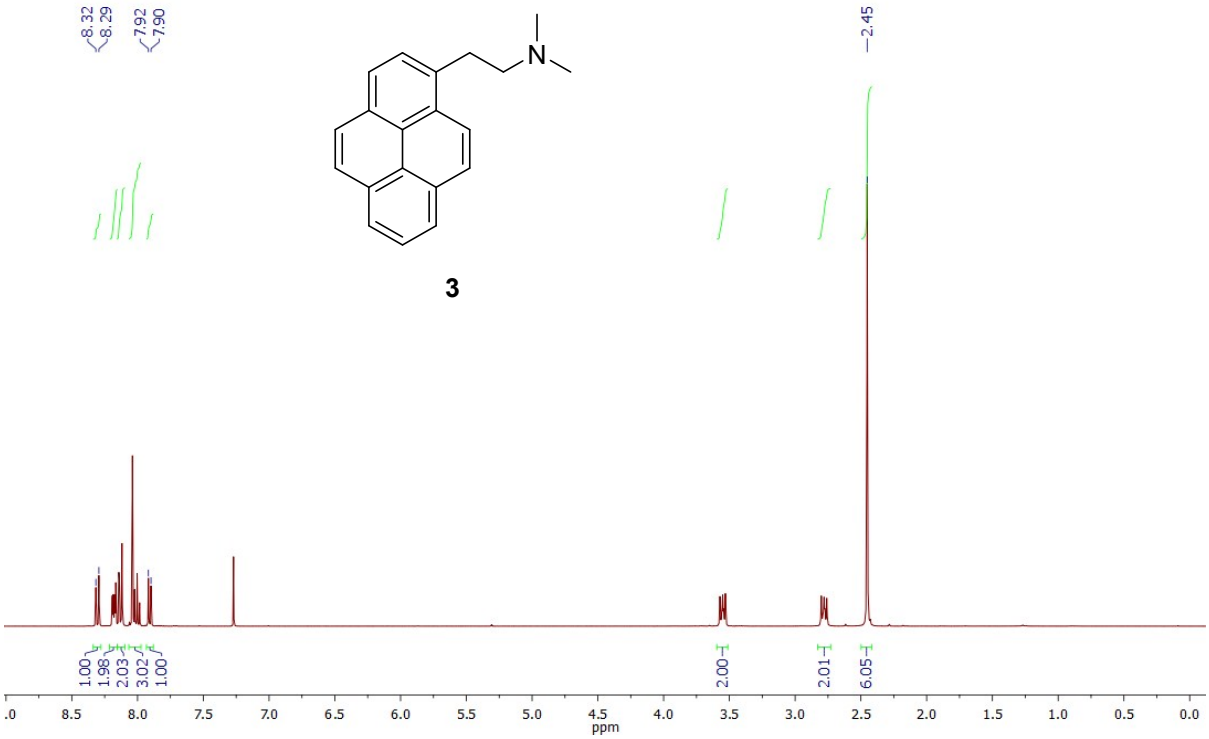

^{13}C-NMR (125 MHz, $CDCl_3$)

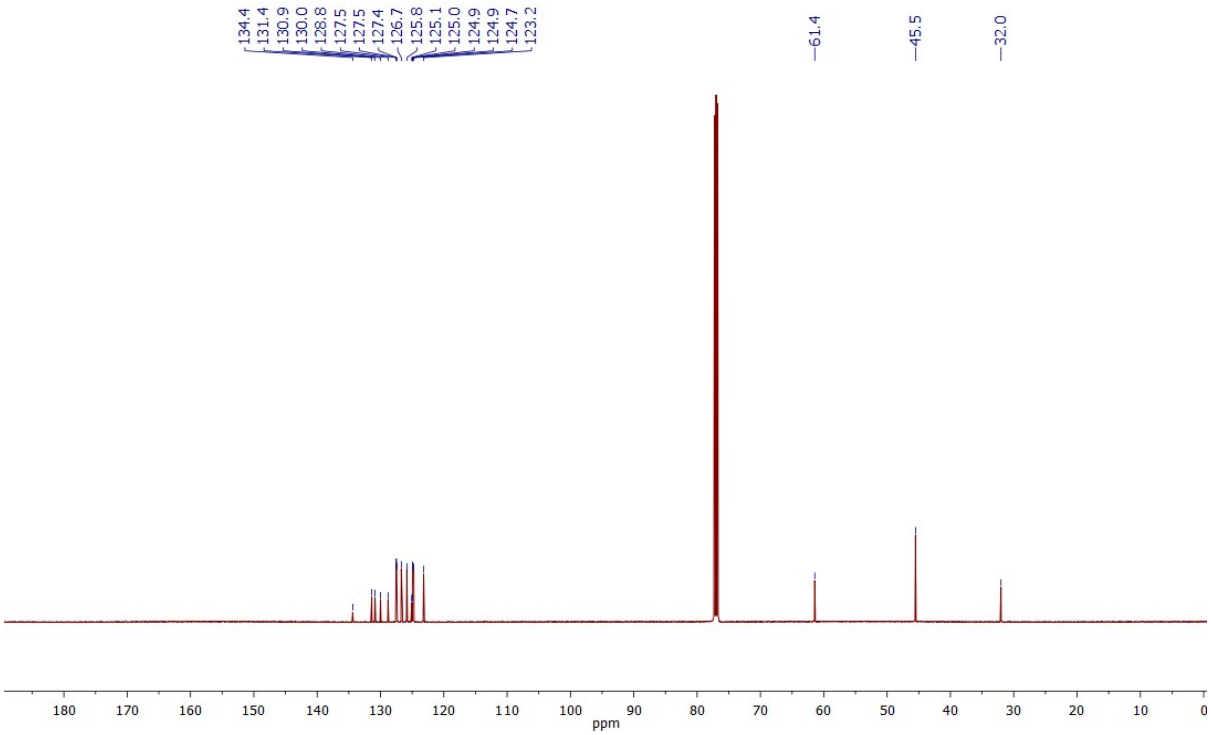

_N_-(2-(1-Pyrenyl)ethyl)-_N_,_N_,_N_-trimethyl ammonium iodide (4)

^{1}H-NMR (400 MHz, MeOD-d_4)

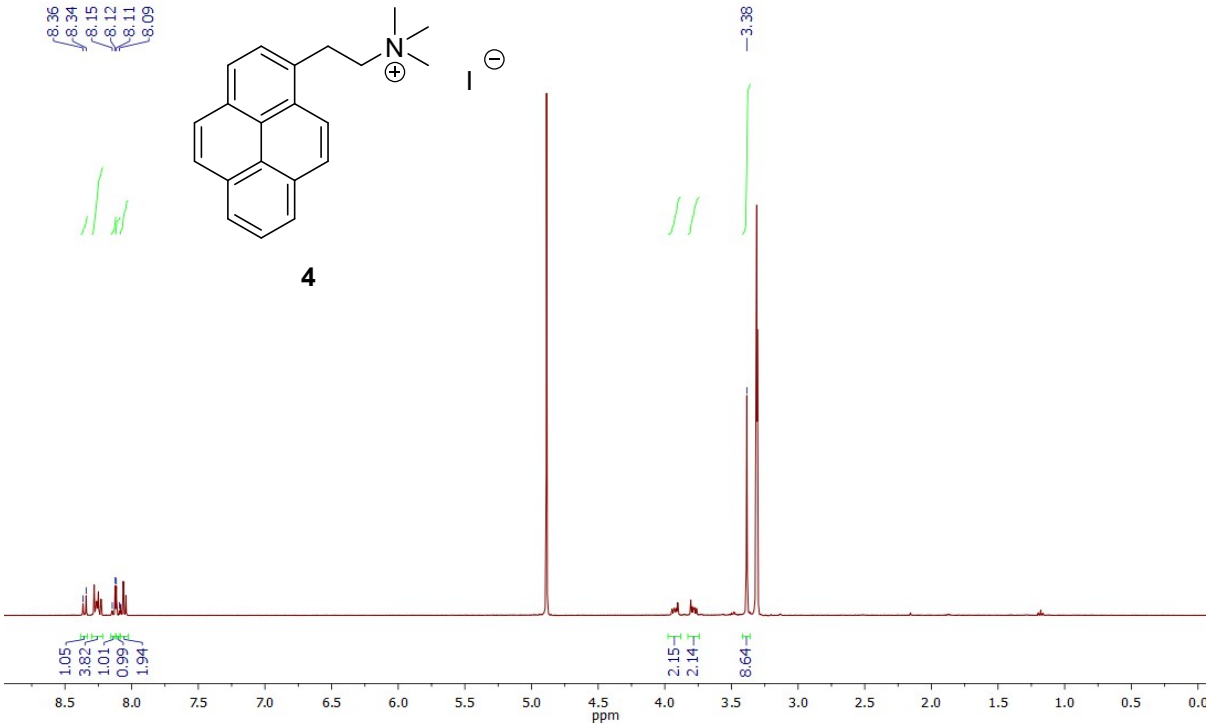

^{13}C-NMR (125 MHz, MeOD-d_4)

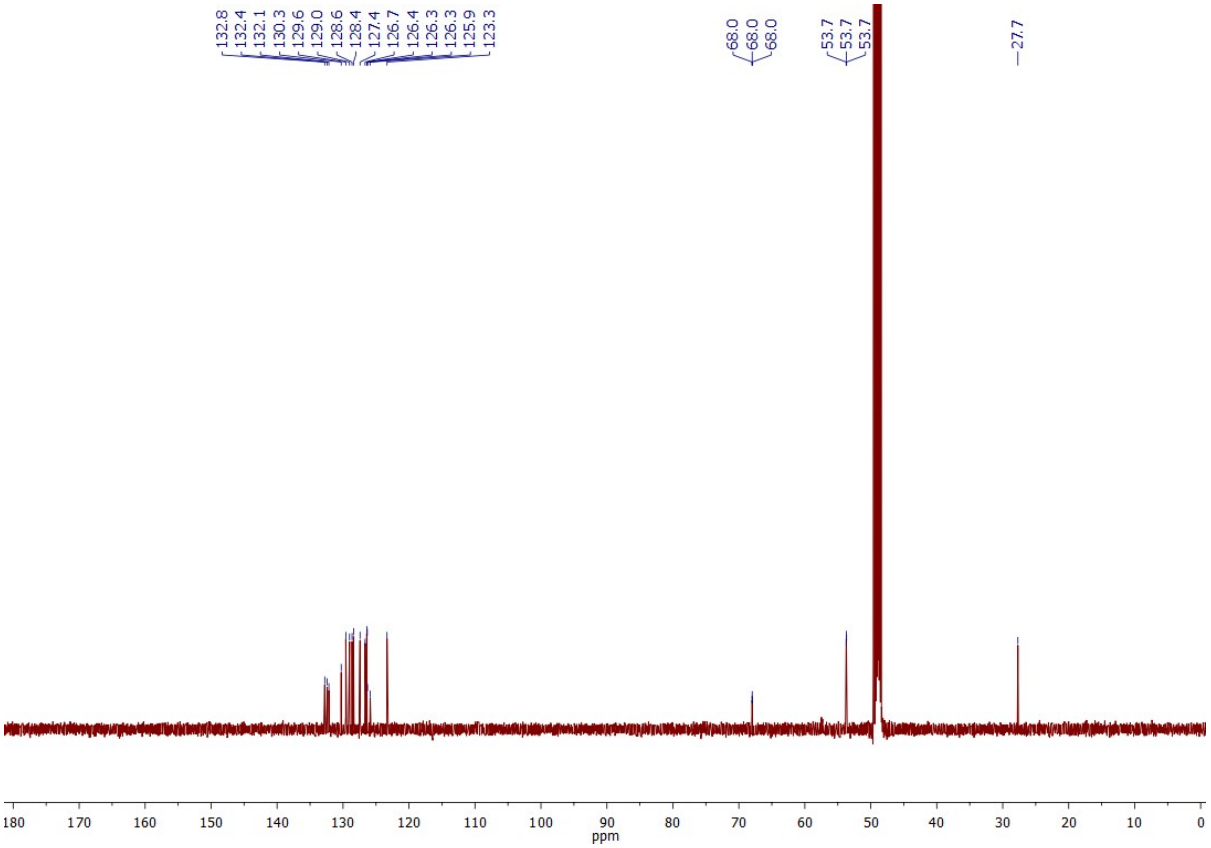

_N_-(2-(1-Pyrenyl)ethyl)-_N_,_N_,_N_-trimethyl ammonium bromide (TMA_2)

^{1}H-NMR (500 MHz, MeOD-d_4)

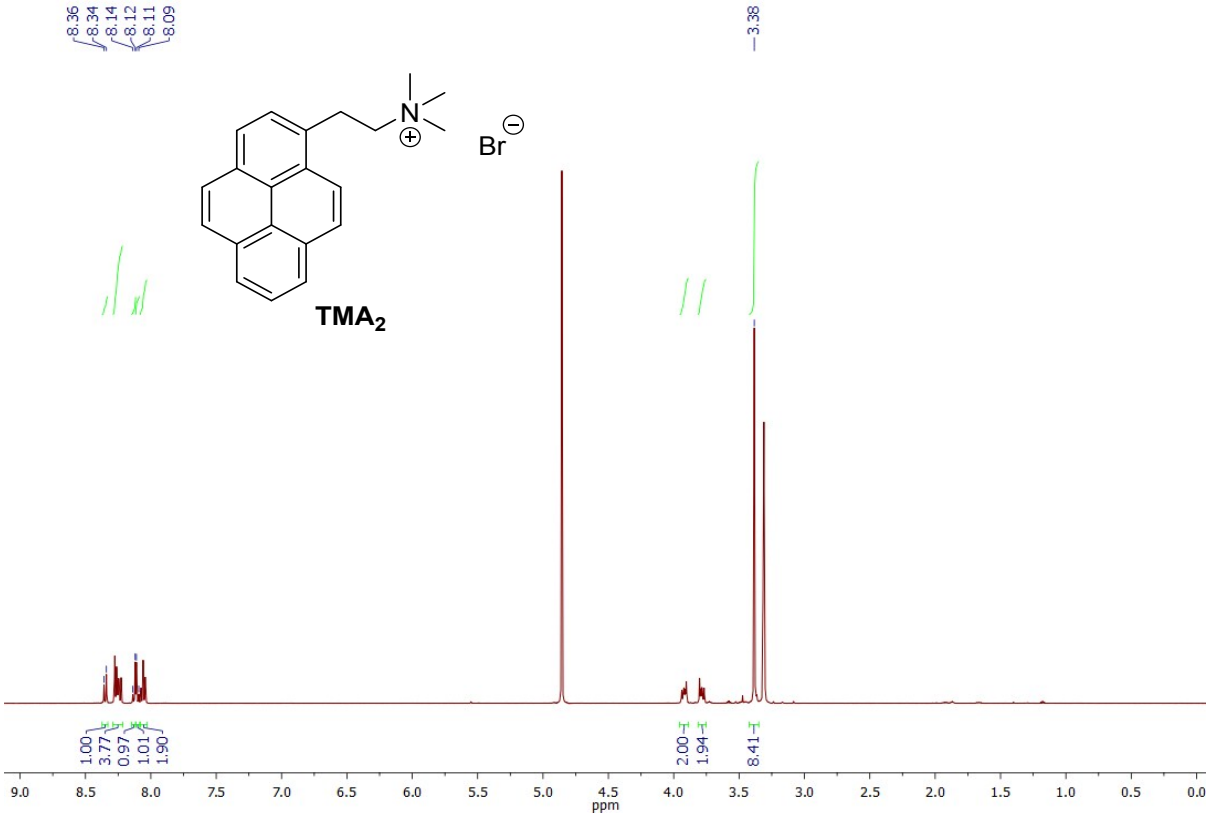

^{13}C-NMR (125 MHz, MeOD-d_4)

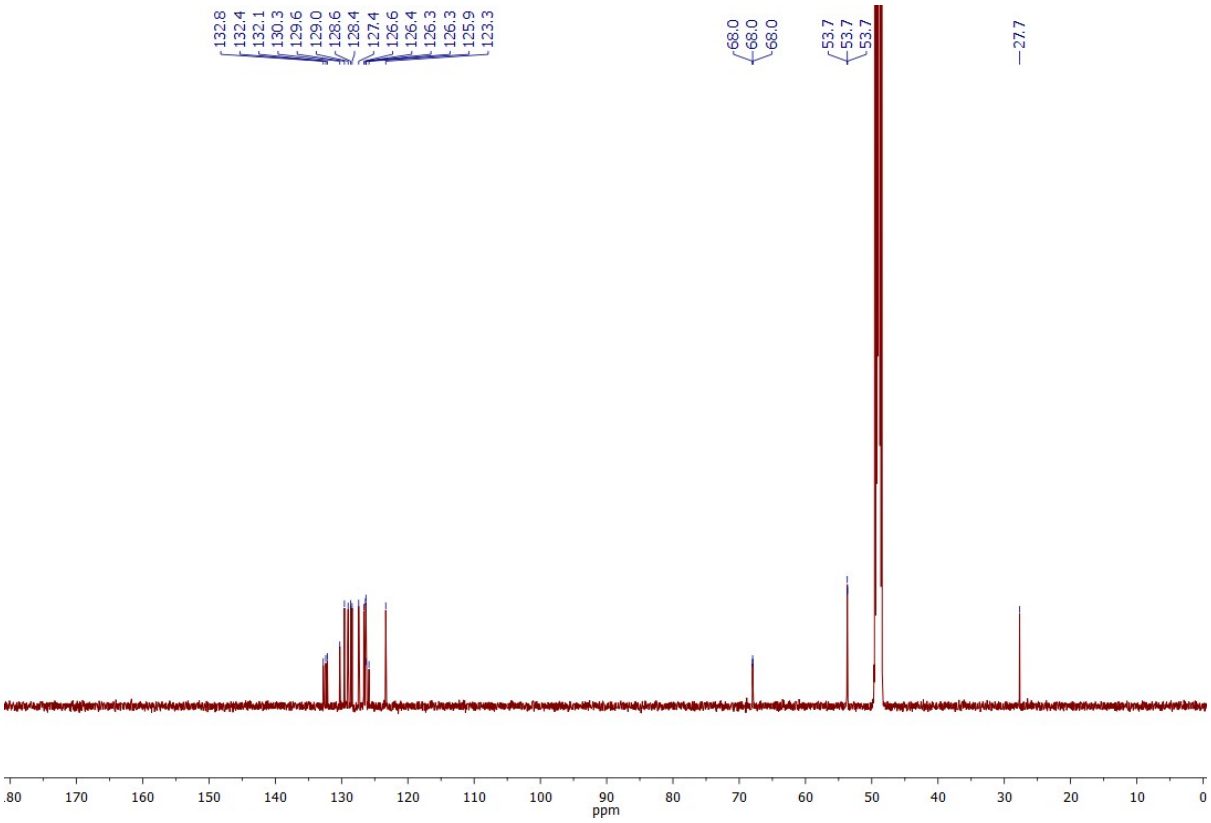

1-Methyl-3-(2-(1-Pyrenyl)ethyl)imidazolium bromide (IMI_2)

^{1}H-NMR (500 MHz, MeOD-d_4)

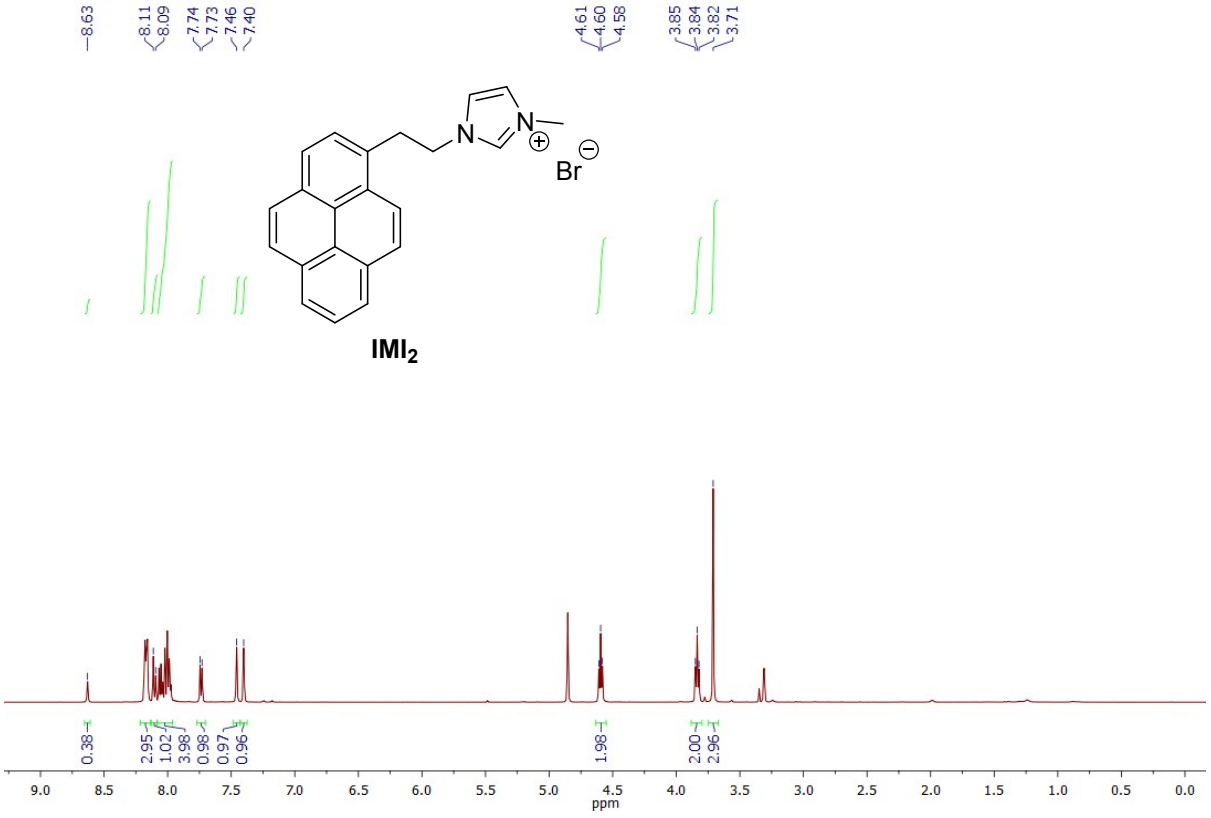

IMI_2

^{13}C-NMR (125 MHz, MeOD-d_4)

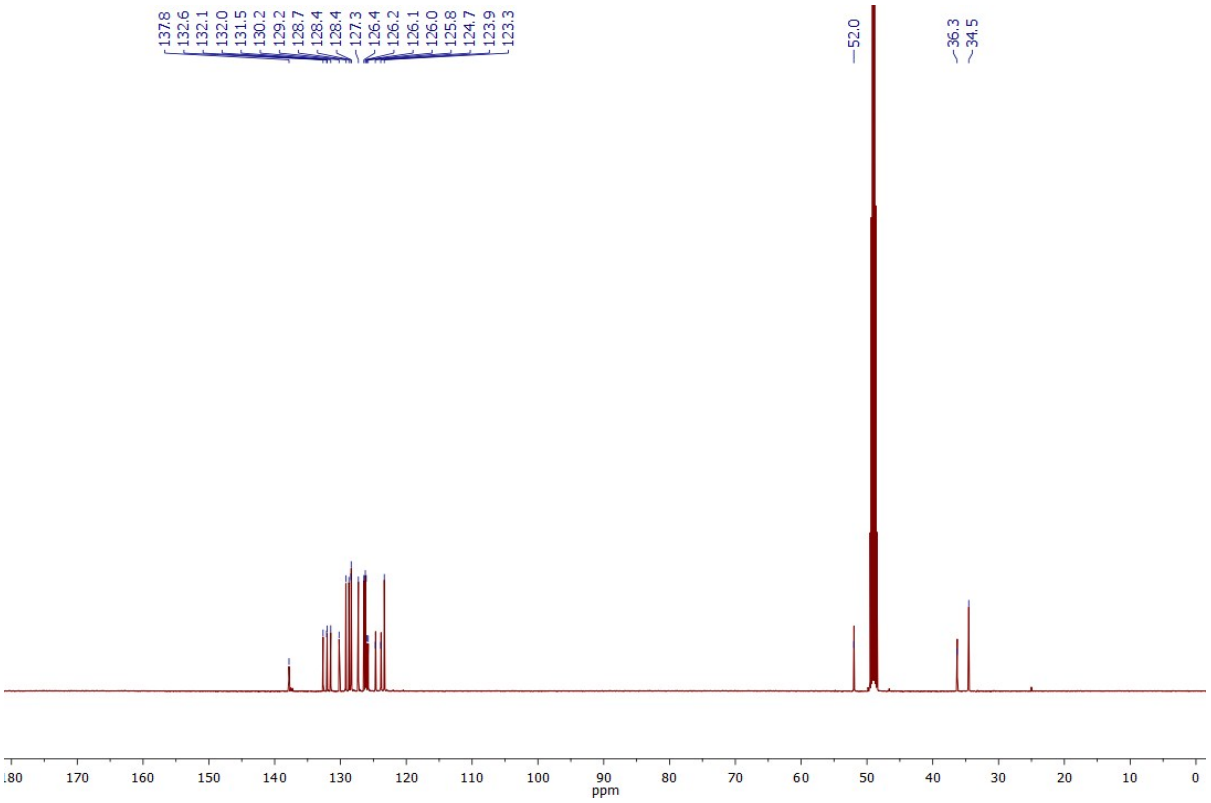

N-(2-(1-Pyrenyl)ethyl)pyridinium bromide (PRD_2)

^{1}H-NMR (400 MHz, MeOD-d_4)

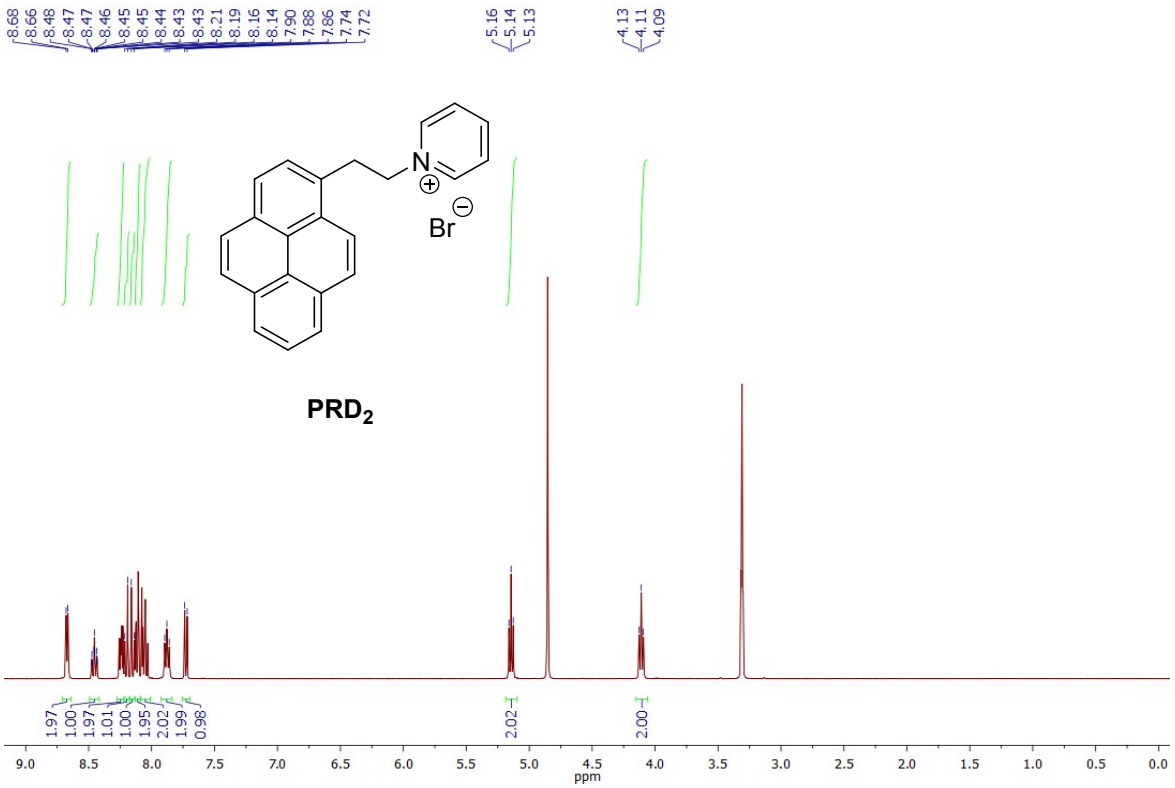

^{13}C-NMR (125 MHz, MeOD-d_4)

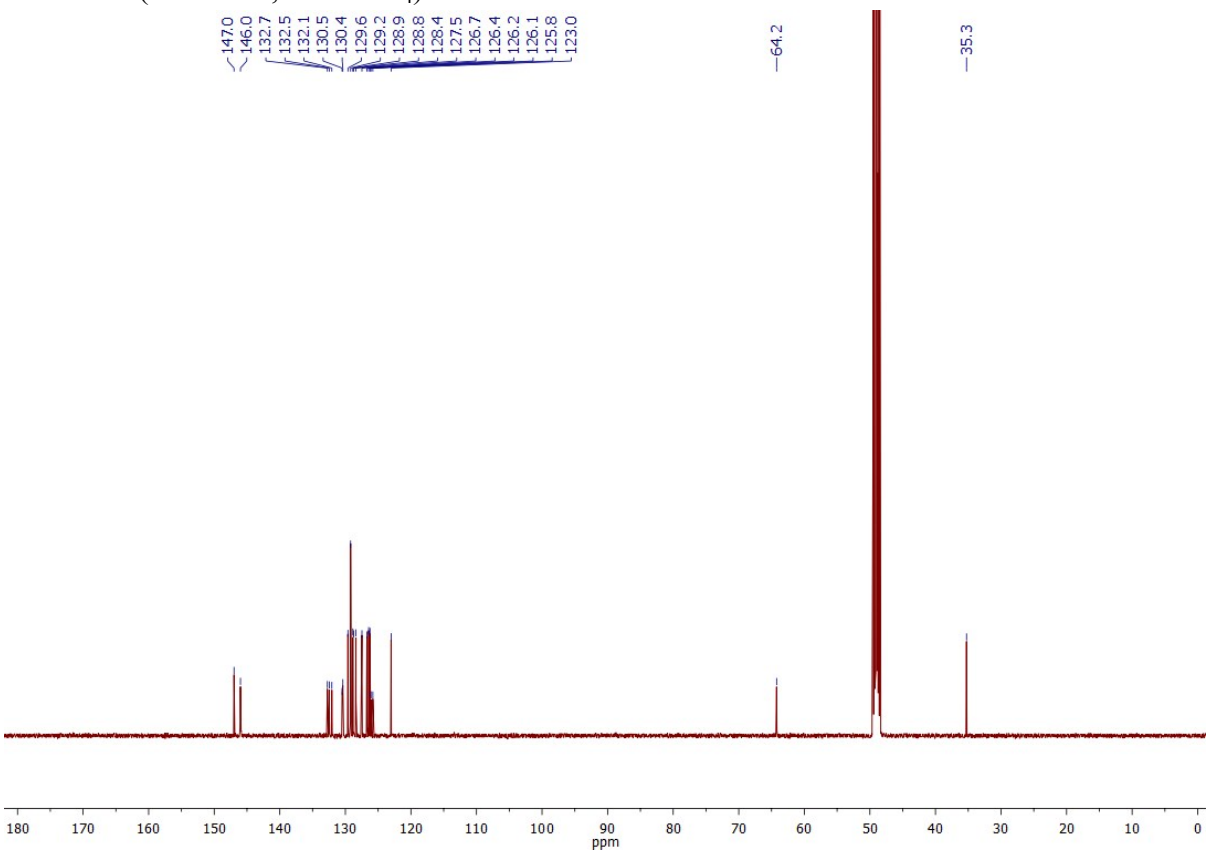

(*E*)-3-(1-Pyrenyl)acrylic acid (S4)

^{1}H-NMR (400 MHz, DMSO-d_6)

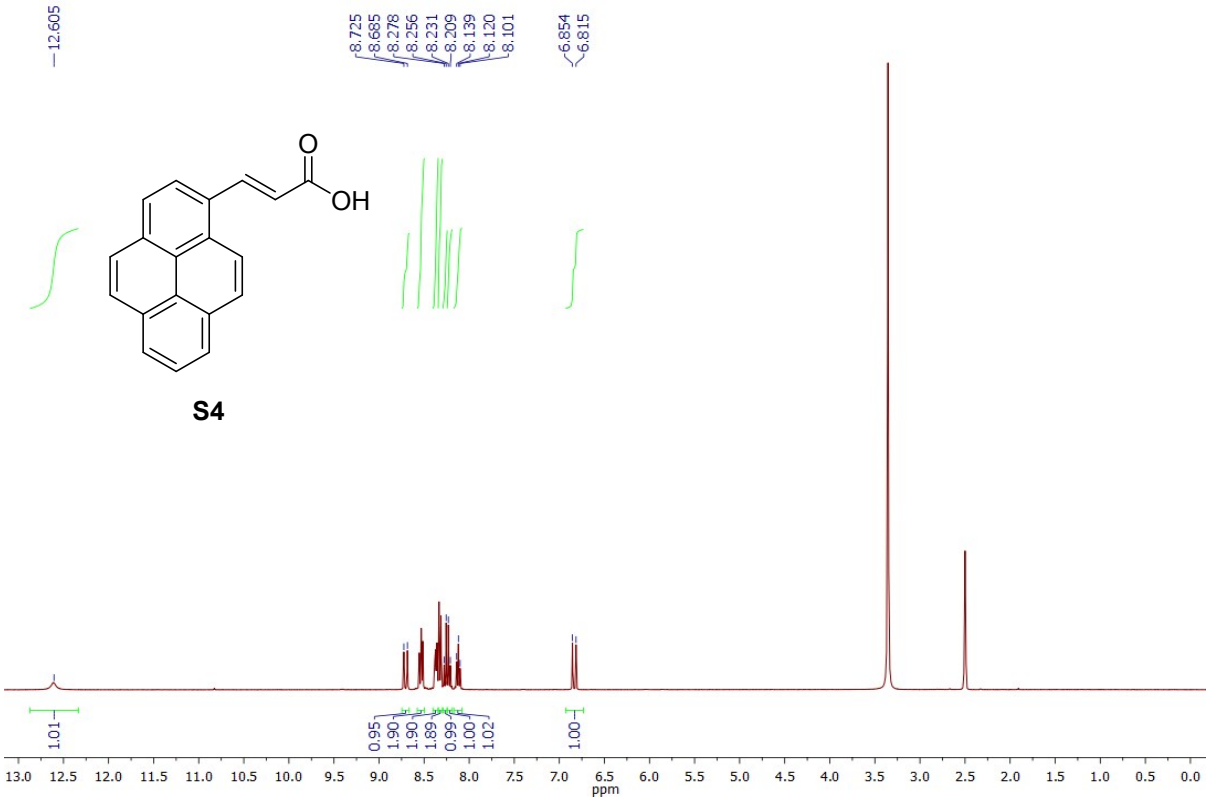

^{13}C-NMR (125 MHz, DMSO-d_6)

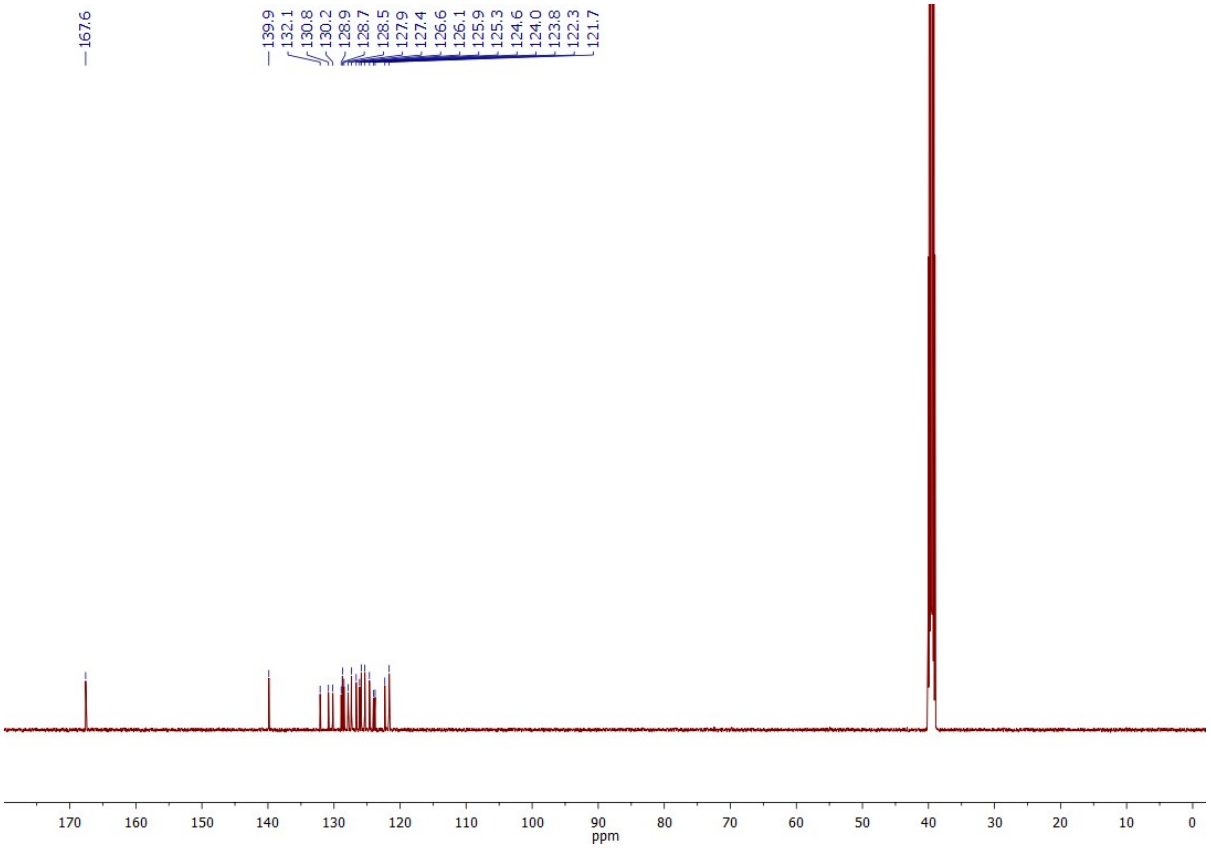

3-(1-Pyrenyl)-1-propanol (S6)

^{1}H-NMR (400 MHz, $CDCl_3$)

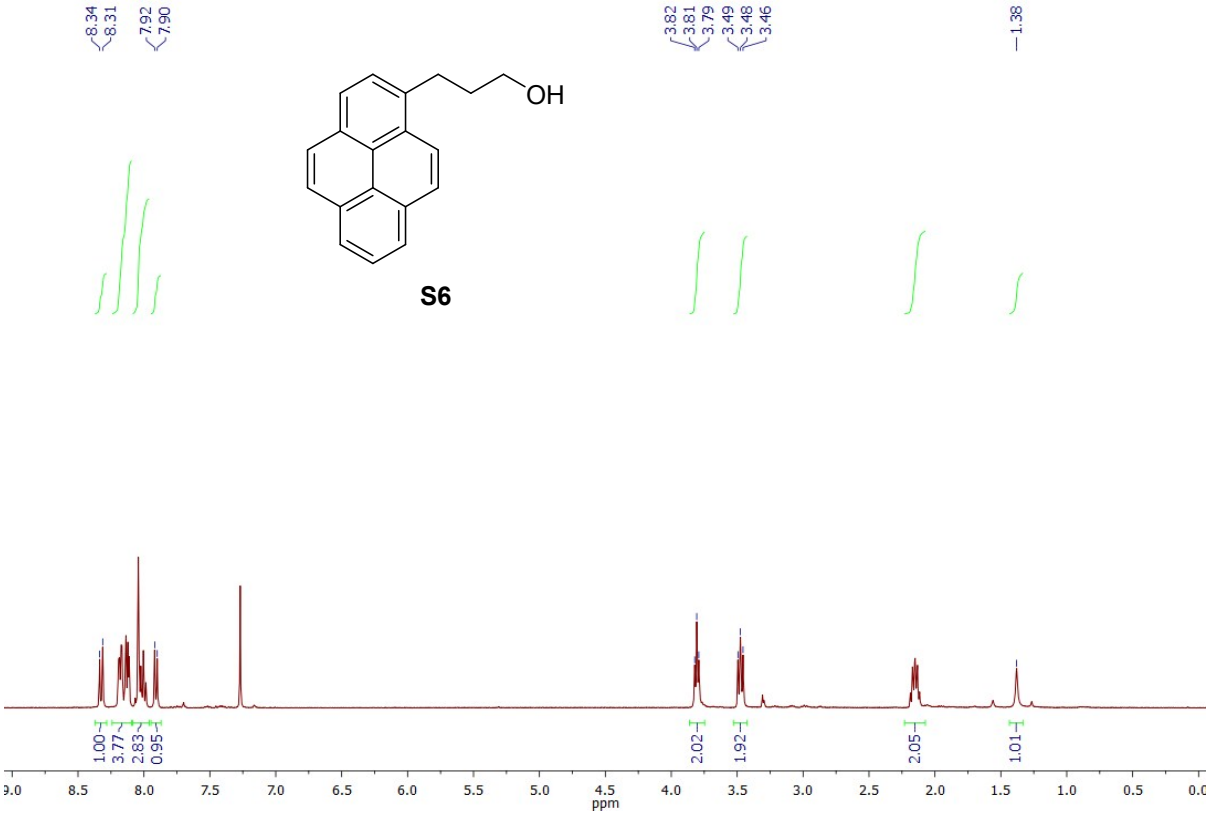

^{13}C-NMR (125 MHz, $CDCl_3$)

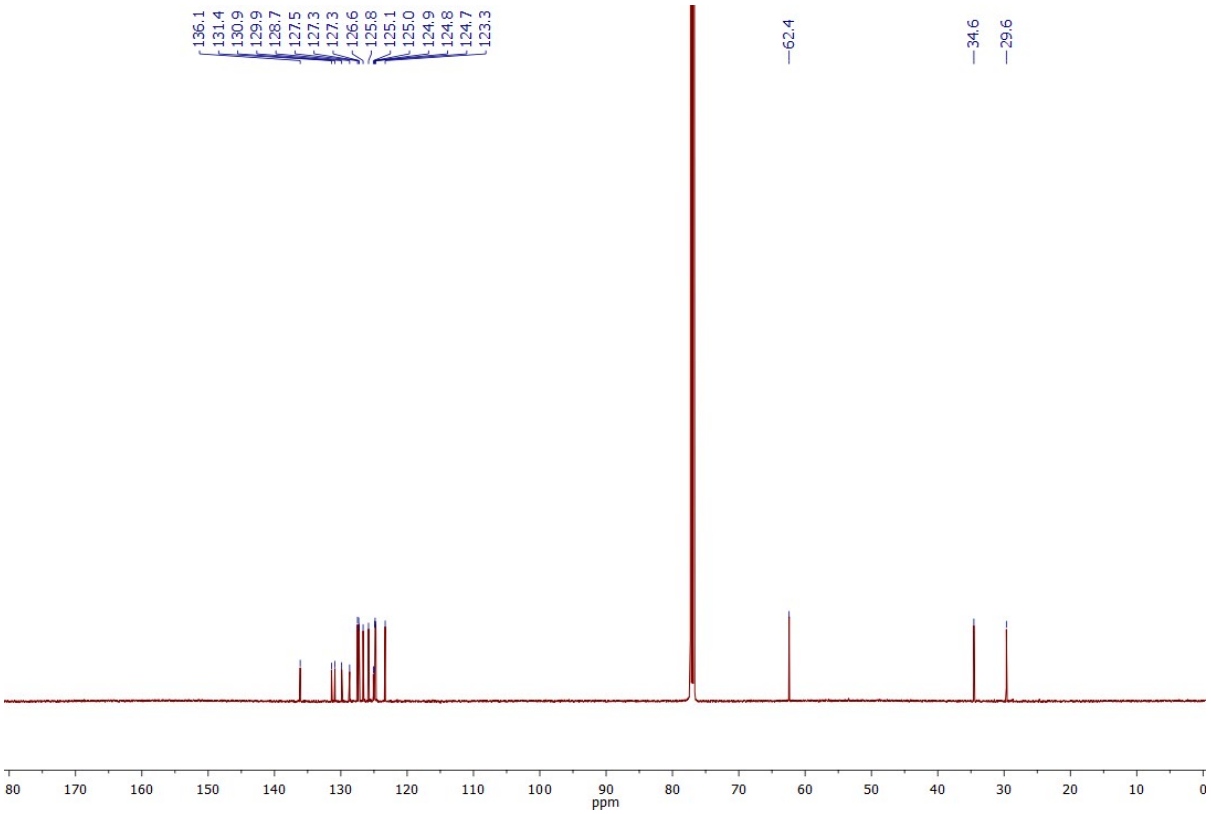

1-(3-Bromopropyl)pyrene (S7)

^{1}H-NMR (400 MHz, $CDCl_3$)

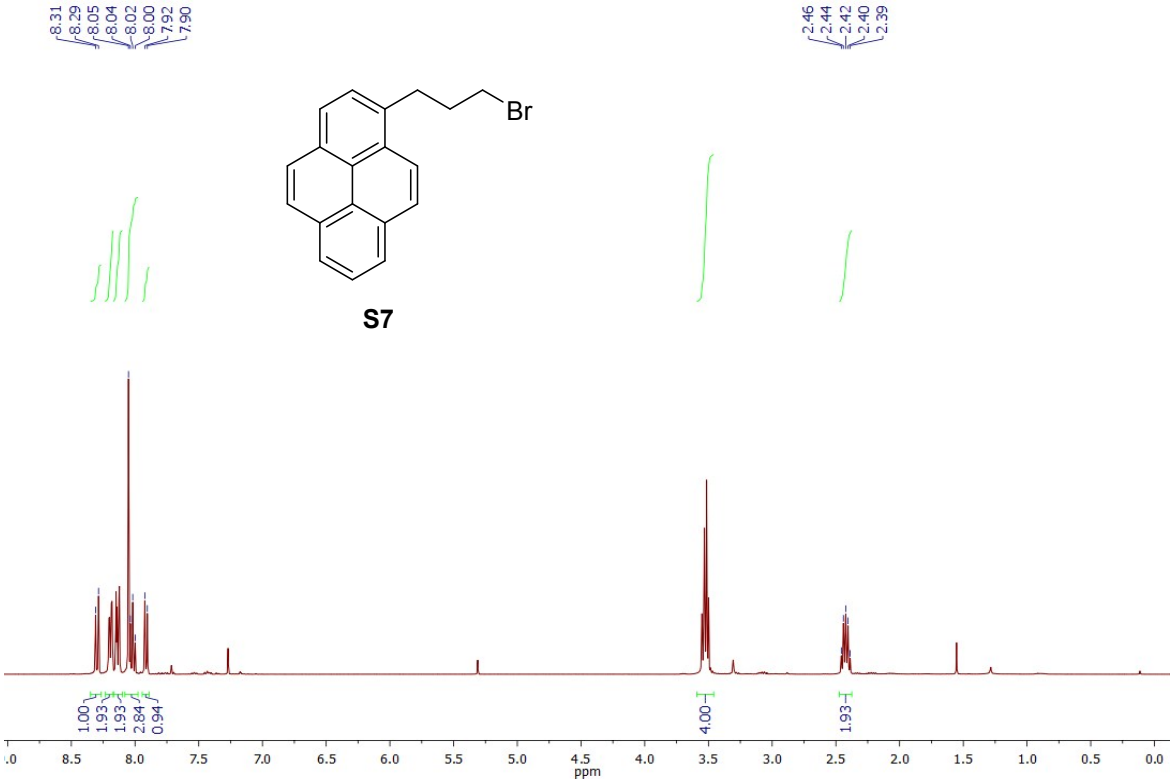

^{13}C-NMR (125 MHz, $CDCl_3$)

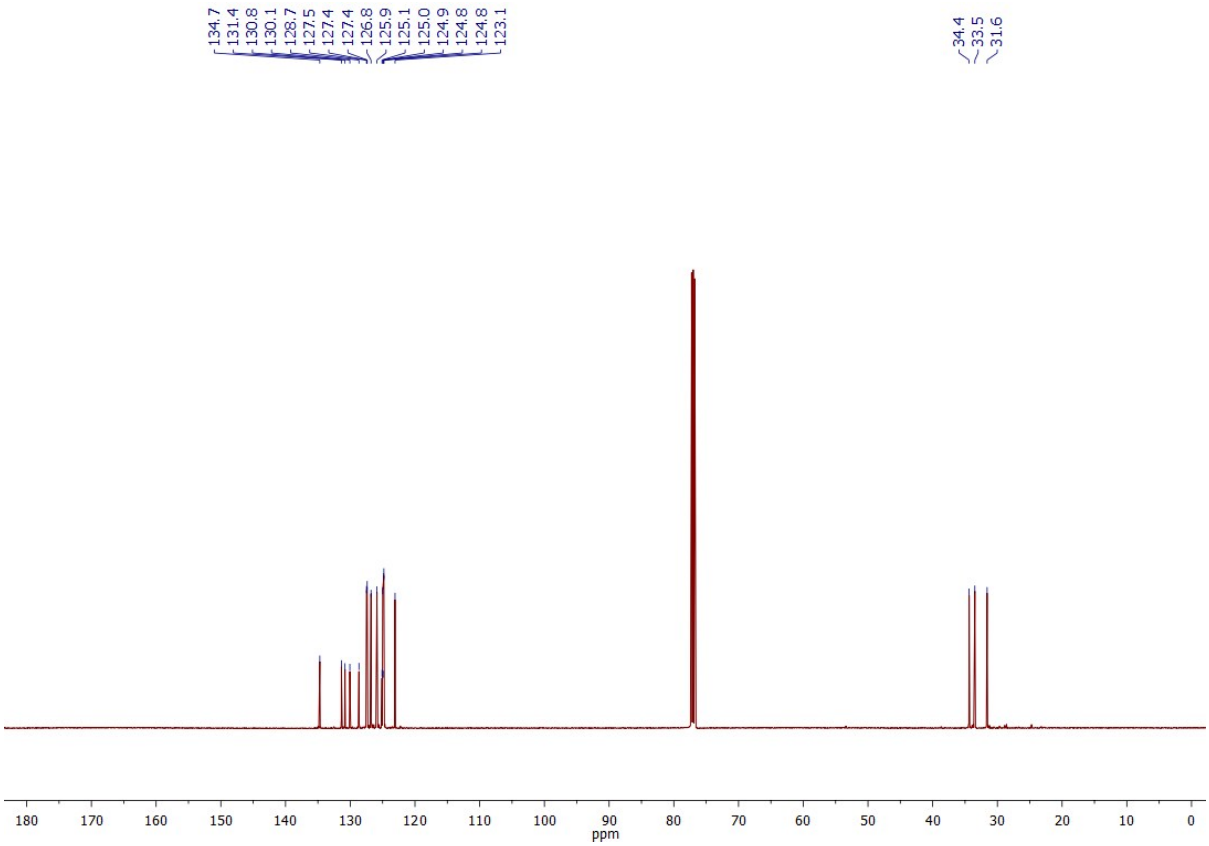

_N_-(3-(1-Pyrenyl)propyl)-_N_,_N_,_N_-trimethyl ammonium bromide (TMA_3)

^{1}H-NMR (400 MHz, MeOD-d_4)

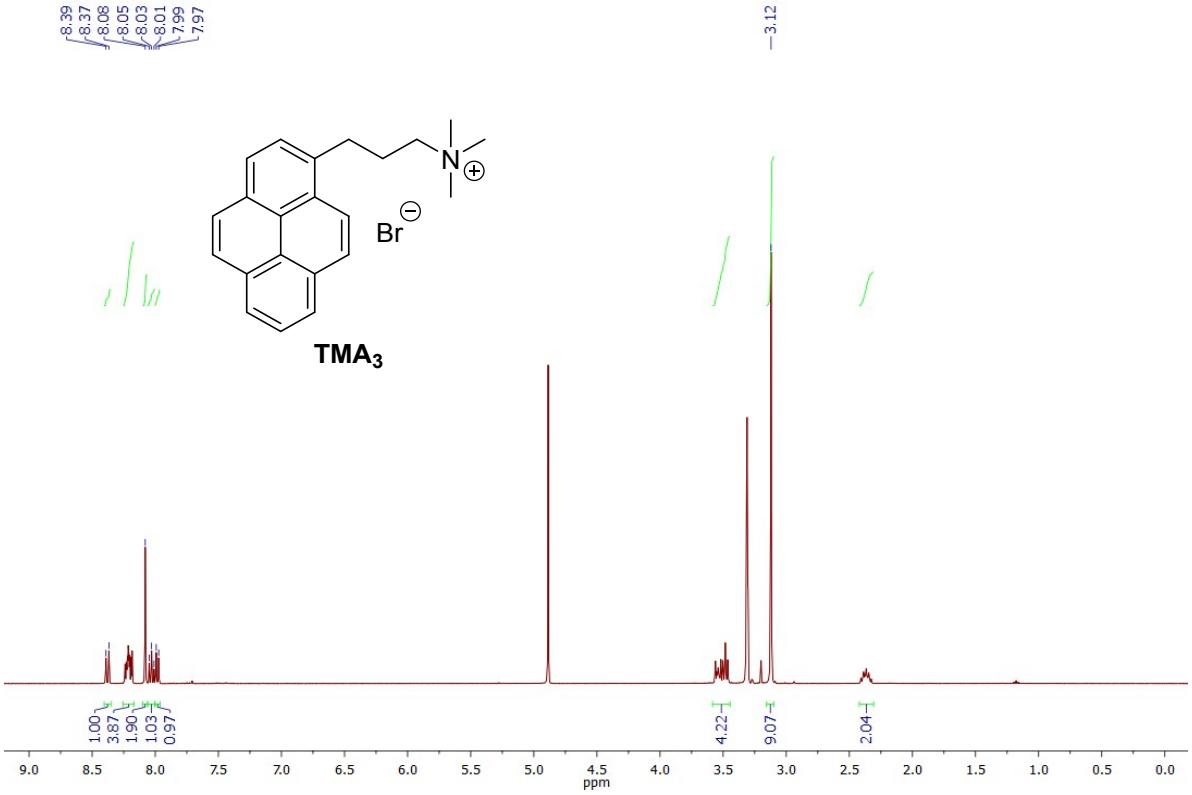

^{13}C-NMR (125 MHz, MeOD-d_4)

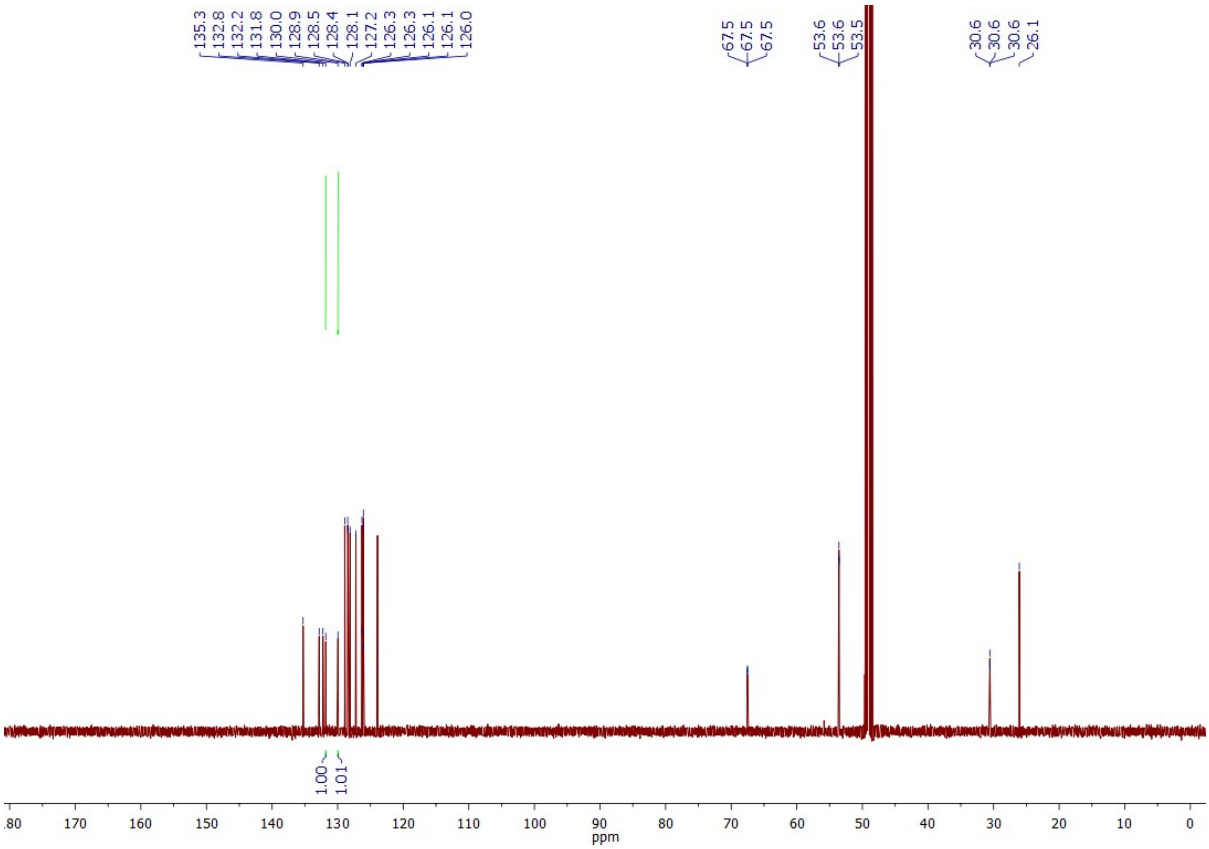

1-Methyl-3-(3-(1-Pyrenyl)propyl)imidazolium bromide (IMI_3)

^{1}H-NMR (400 MHz, MeOD-d_4)

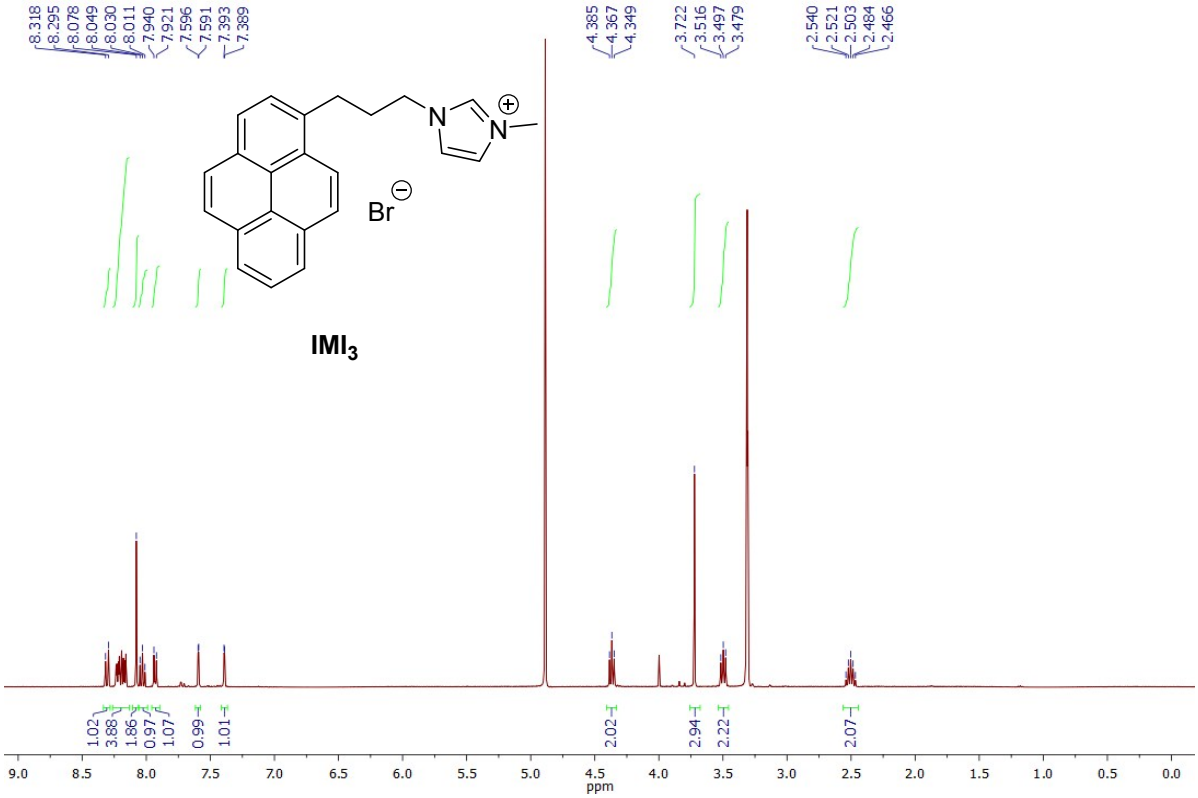

^{13}C-NMR (125 MHz, MeOD-d_4)

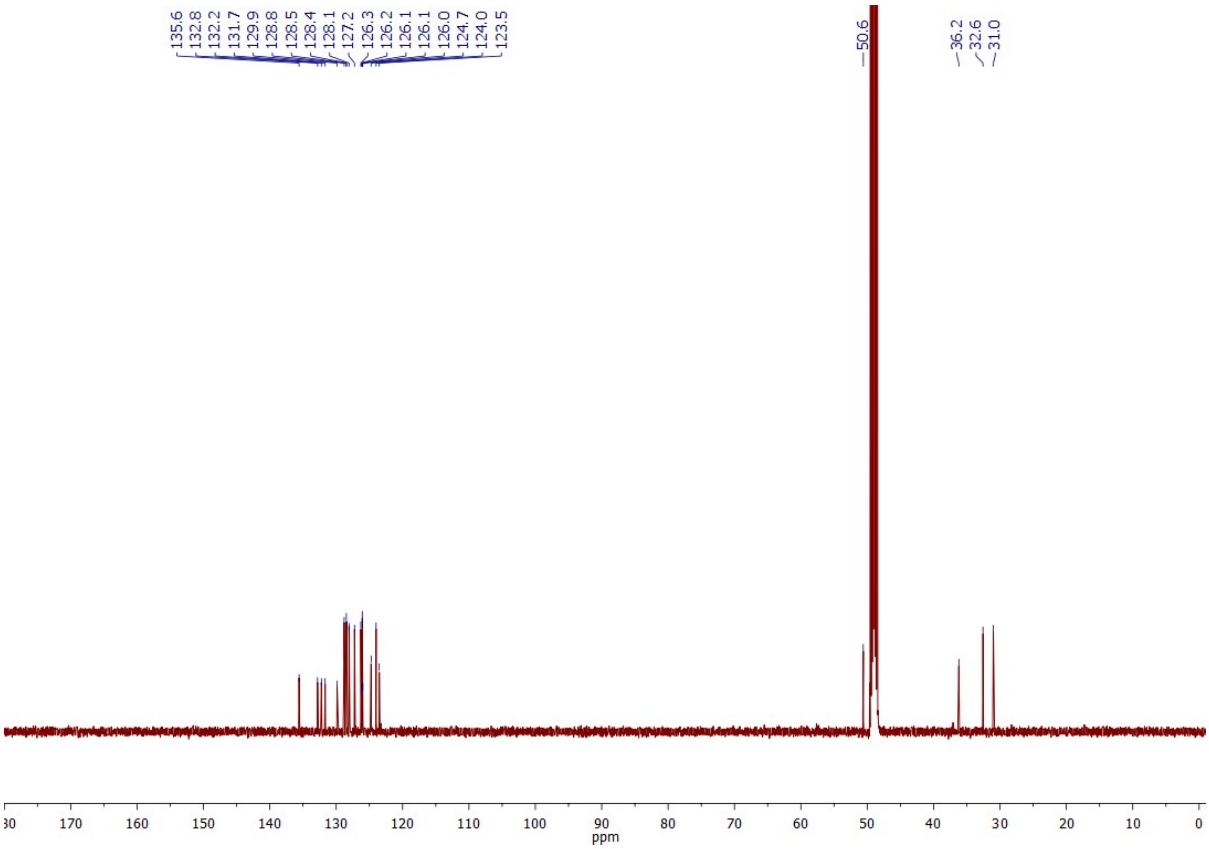

N-(3-(1-Pyrenyl)propyl)pyridinium bromide (PRD_3)

^{1}H-NMR (400 MHz, MeOD-d_4)

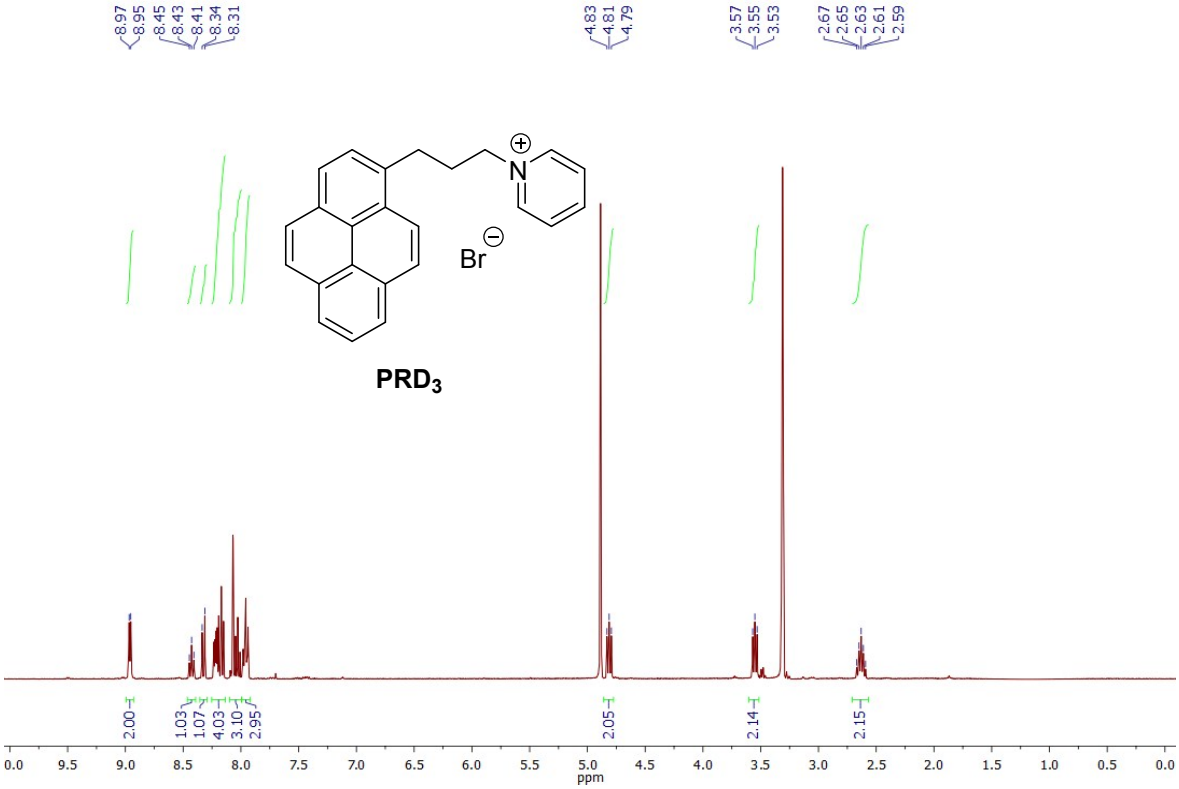

^{13}C-NMR (125 MHz, MeOD-d_4)

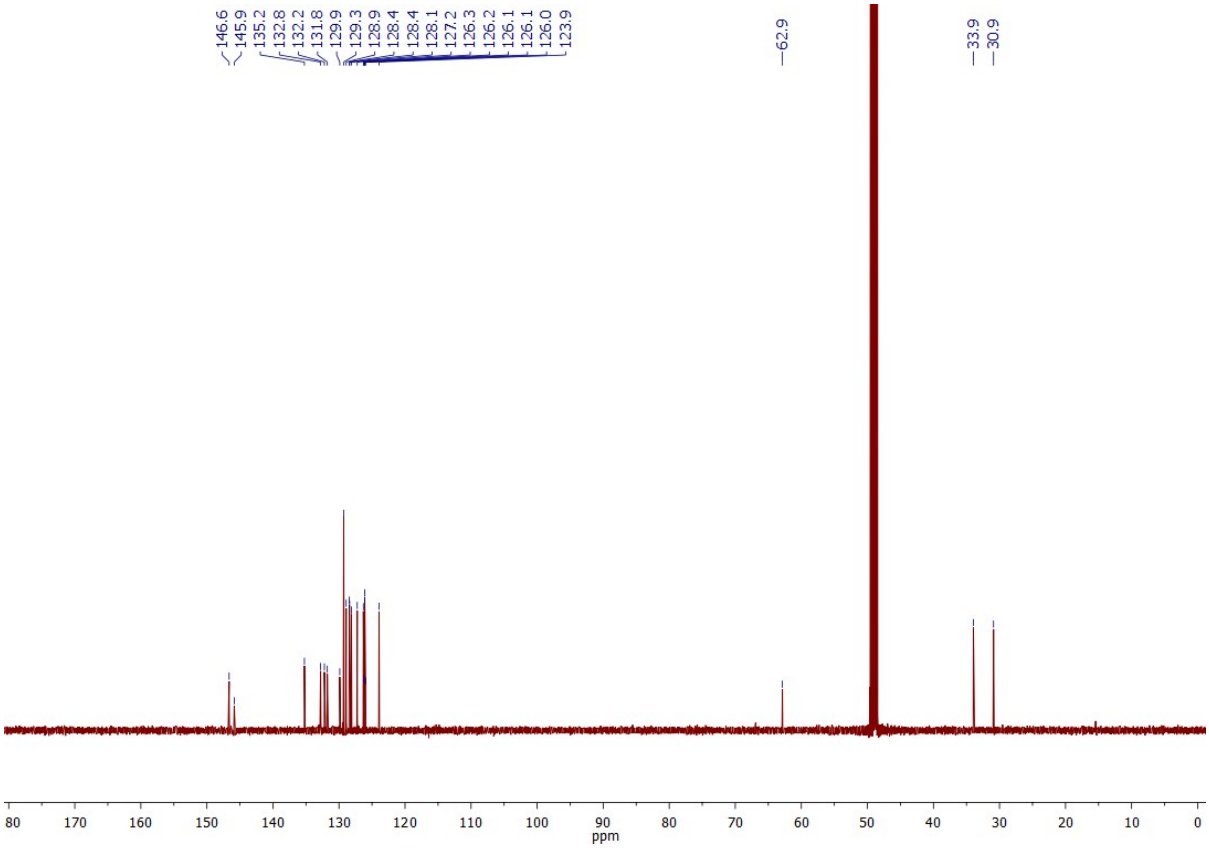

4-(1-Pyrenyl)-1-butanol (S8)

^{1}H-NMR (400 MHz, $CDCl_3$)

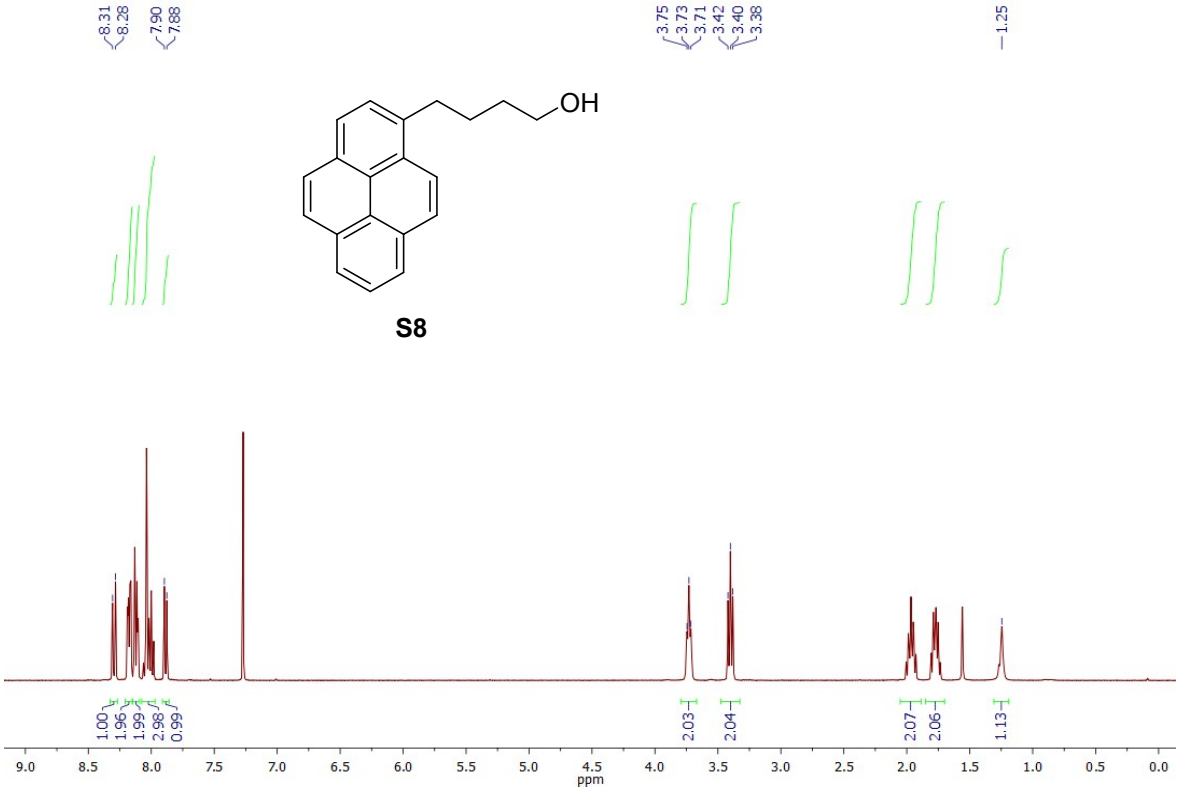

^{13}C-NMR (125 MHz, $CDCl_3$)

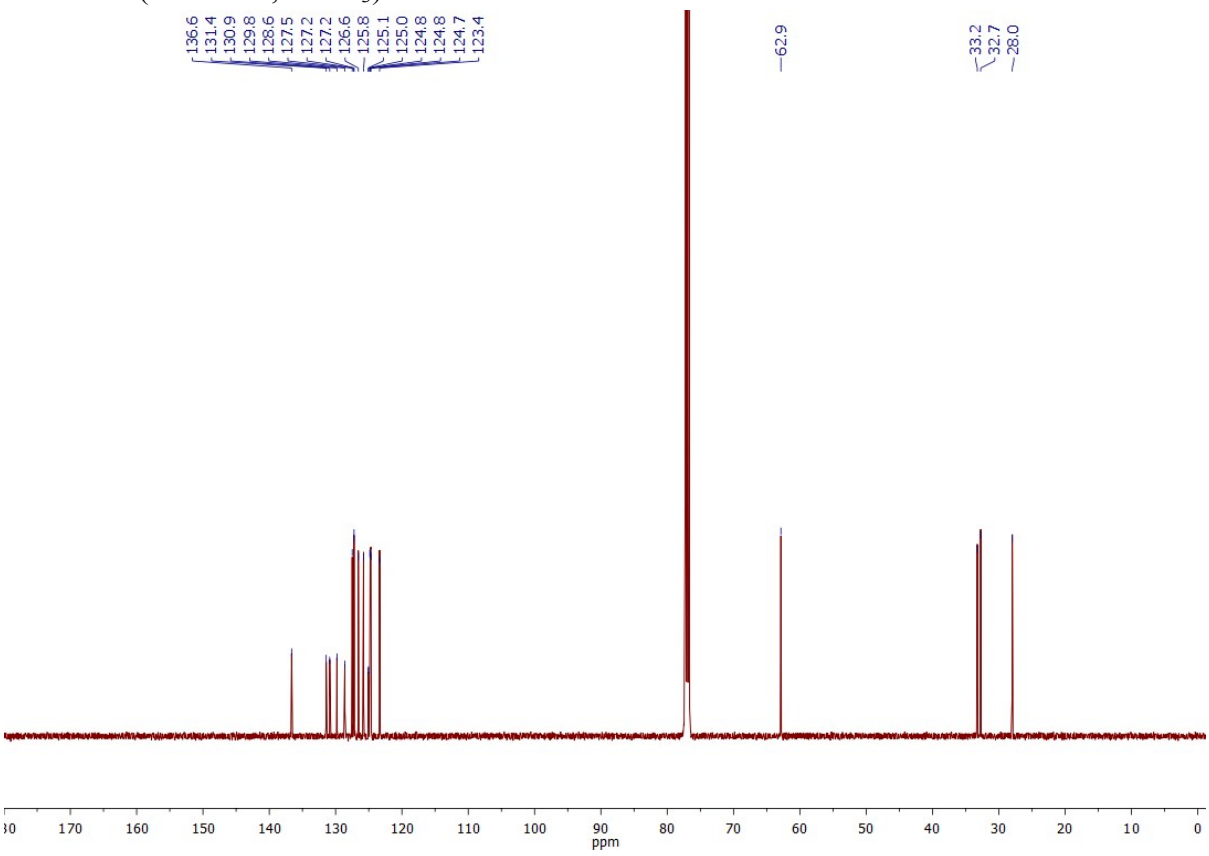

1-(4-Bromobutyl)pyrene (S9)

^{1}H-NMR (400 MHz, $CDCl_3$)

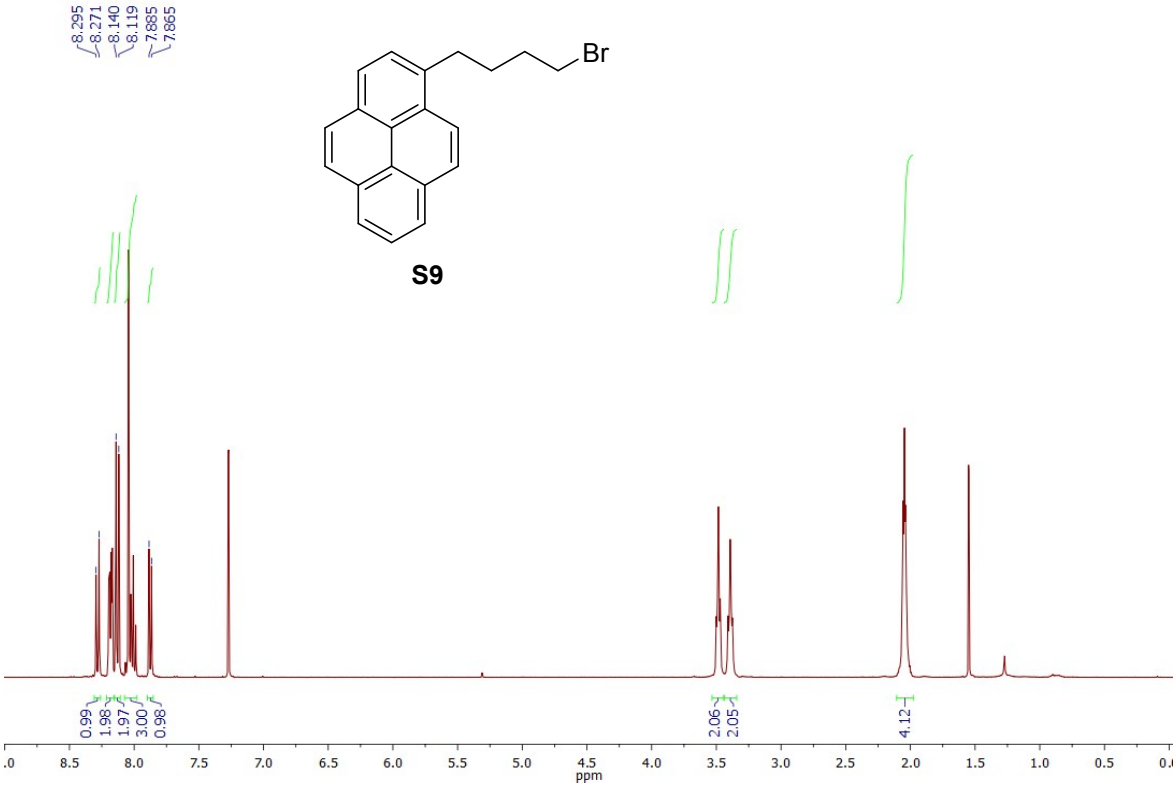

^{13}C-NMR (125 MHz, $CDCl_3$)

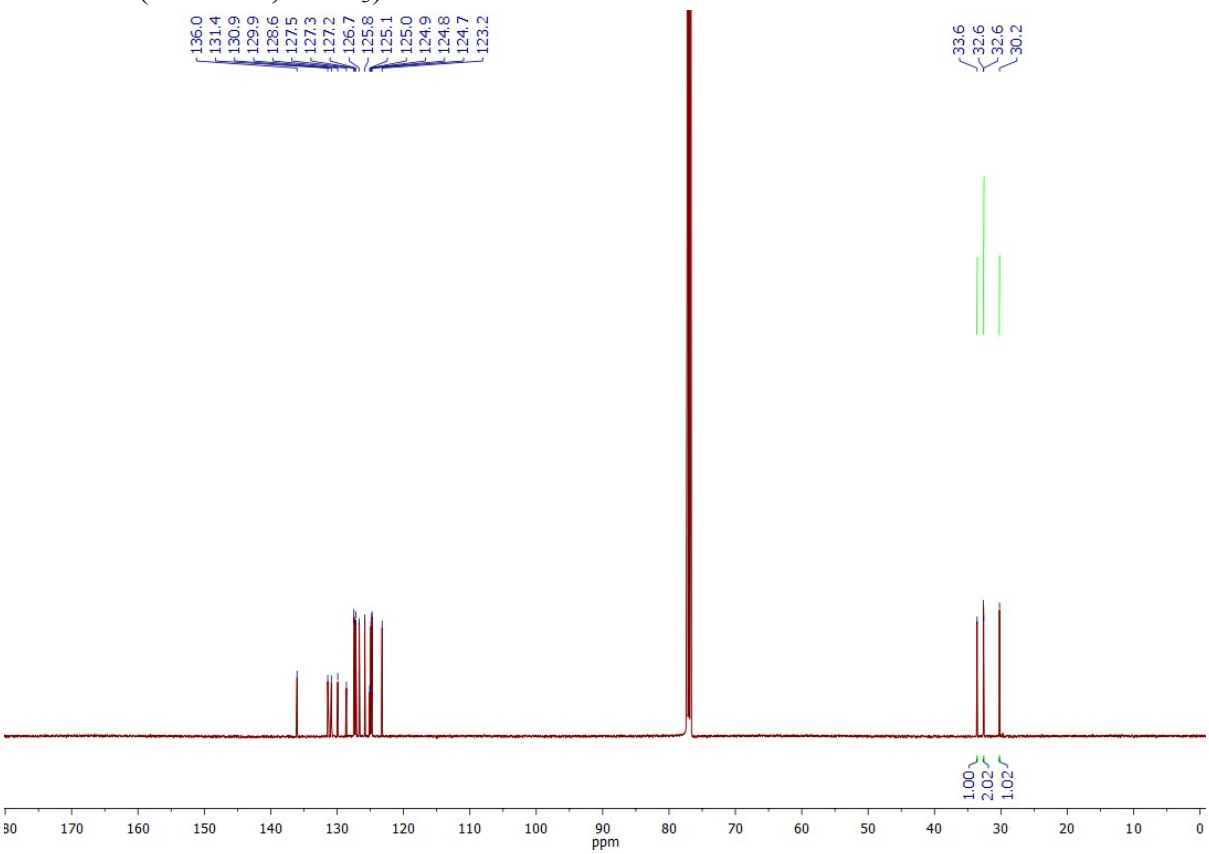

***N*-(4-(1-Pyrenyl)butyl)-*N*,*N*,*N*-trimethyl ammonium bromide (TMA_4)**

^{1}H-NMR (400 MHz, MeOD-d_4)

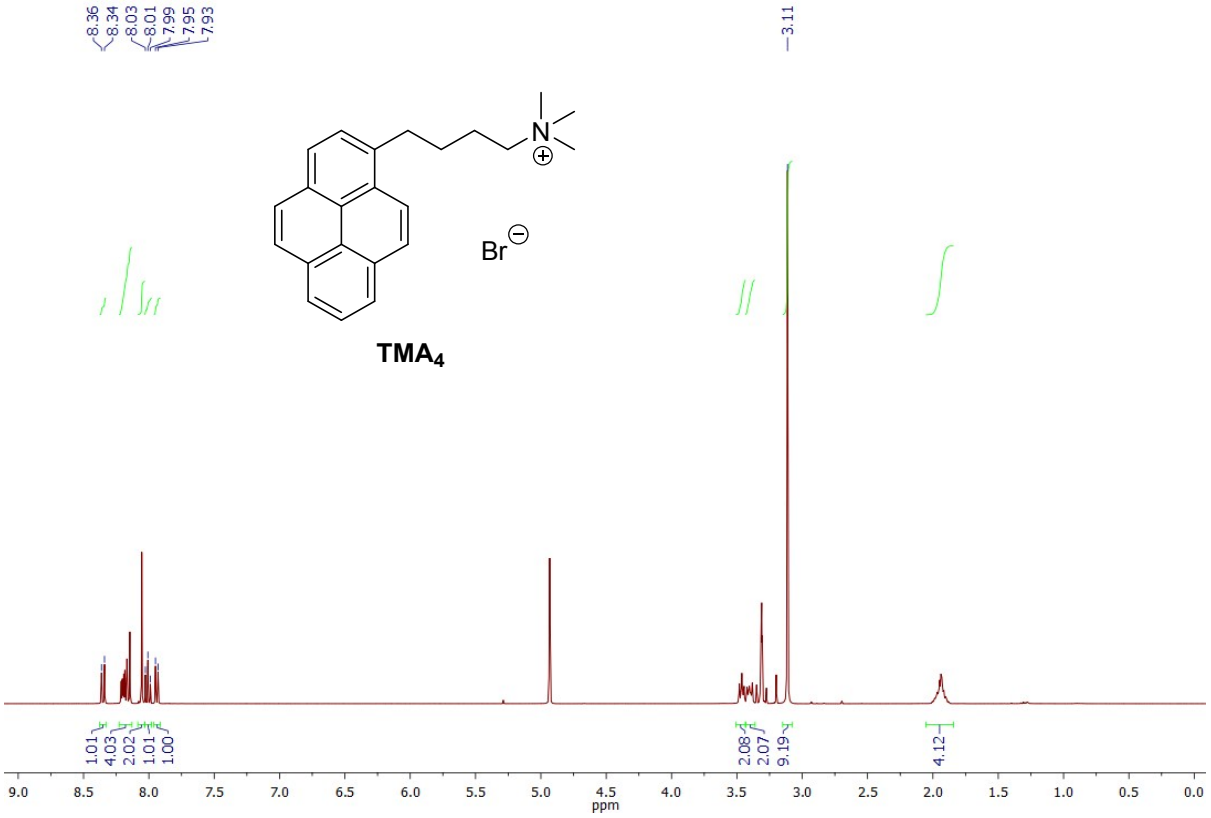

^{13}C-NMR (125 MHz, MeOD-d_4)

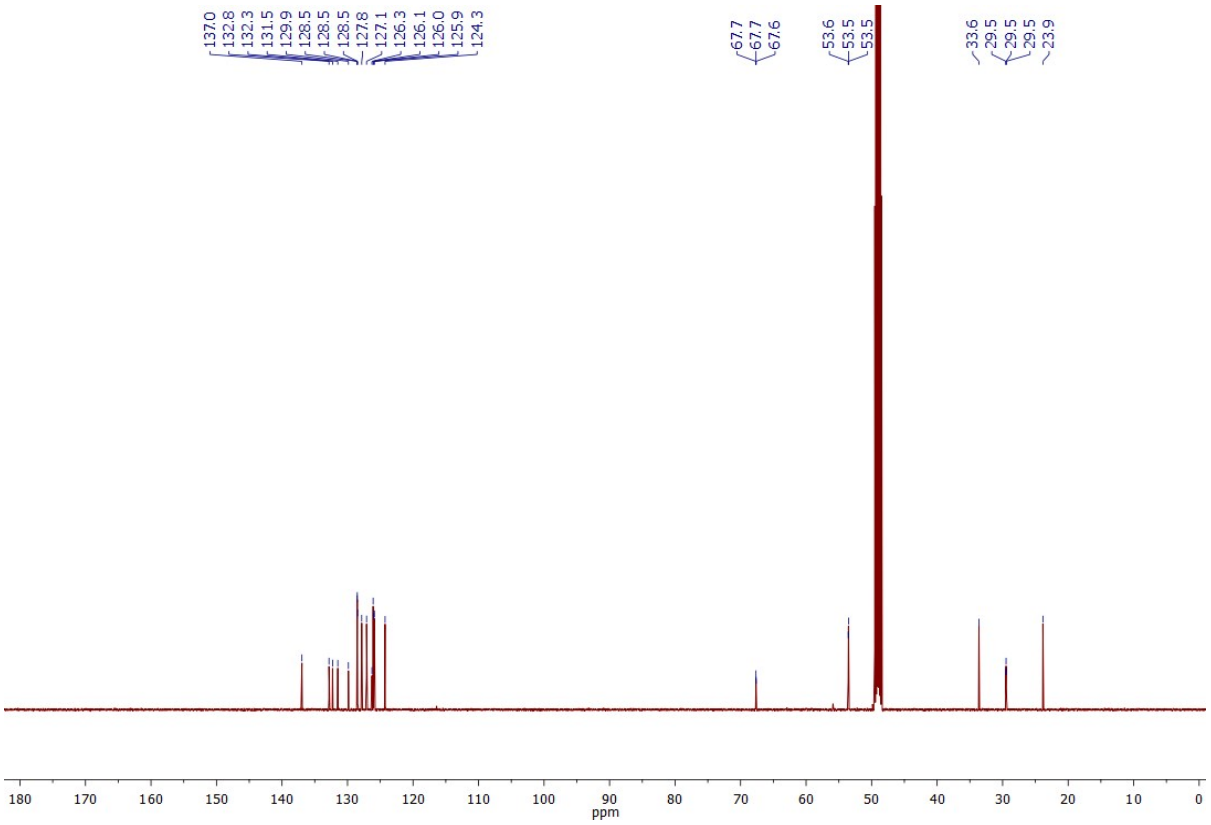

1-Methyl-3-(4-(1-Pyrenyl)butyl)imidazolium bromide (IMI_4)

^{1}H-NMR (400 MHz, MeOD-d_4)

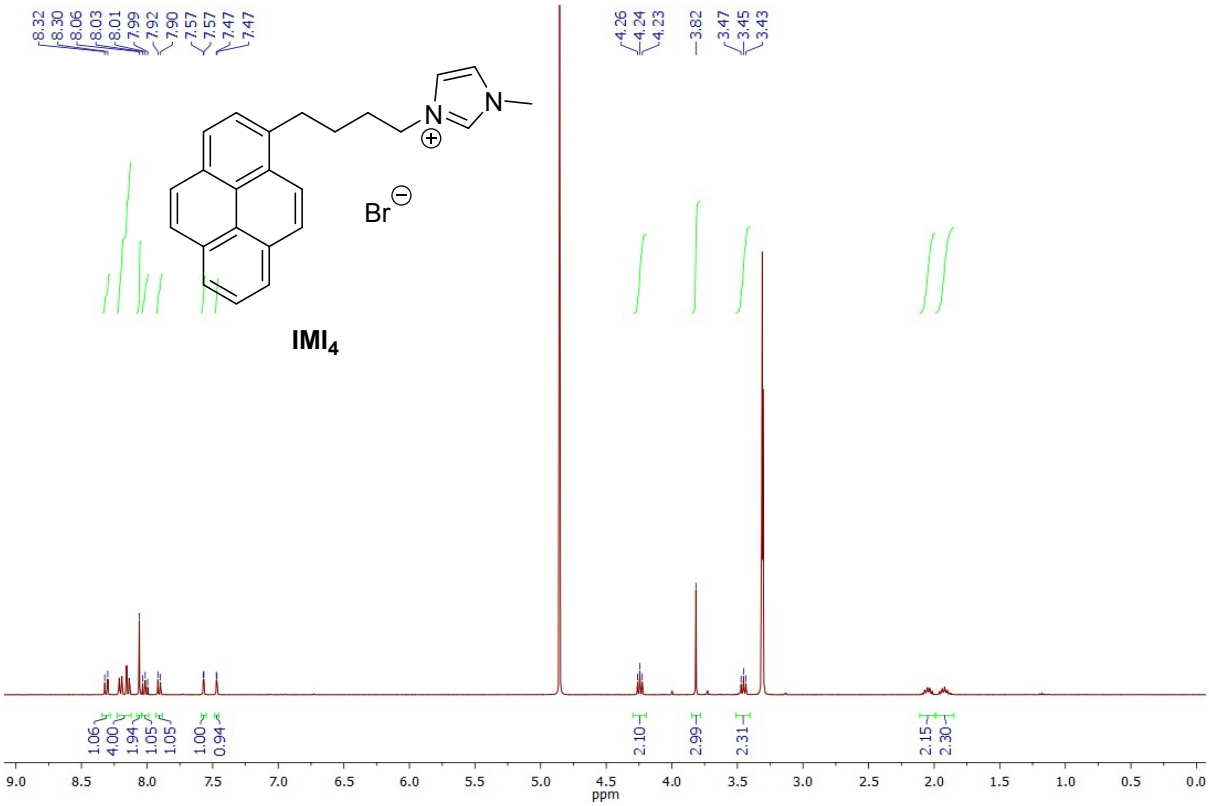

^{13}C-NMR (125 MHz, MeOD-d_4)

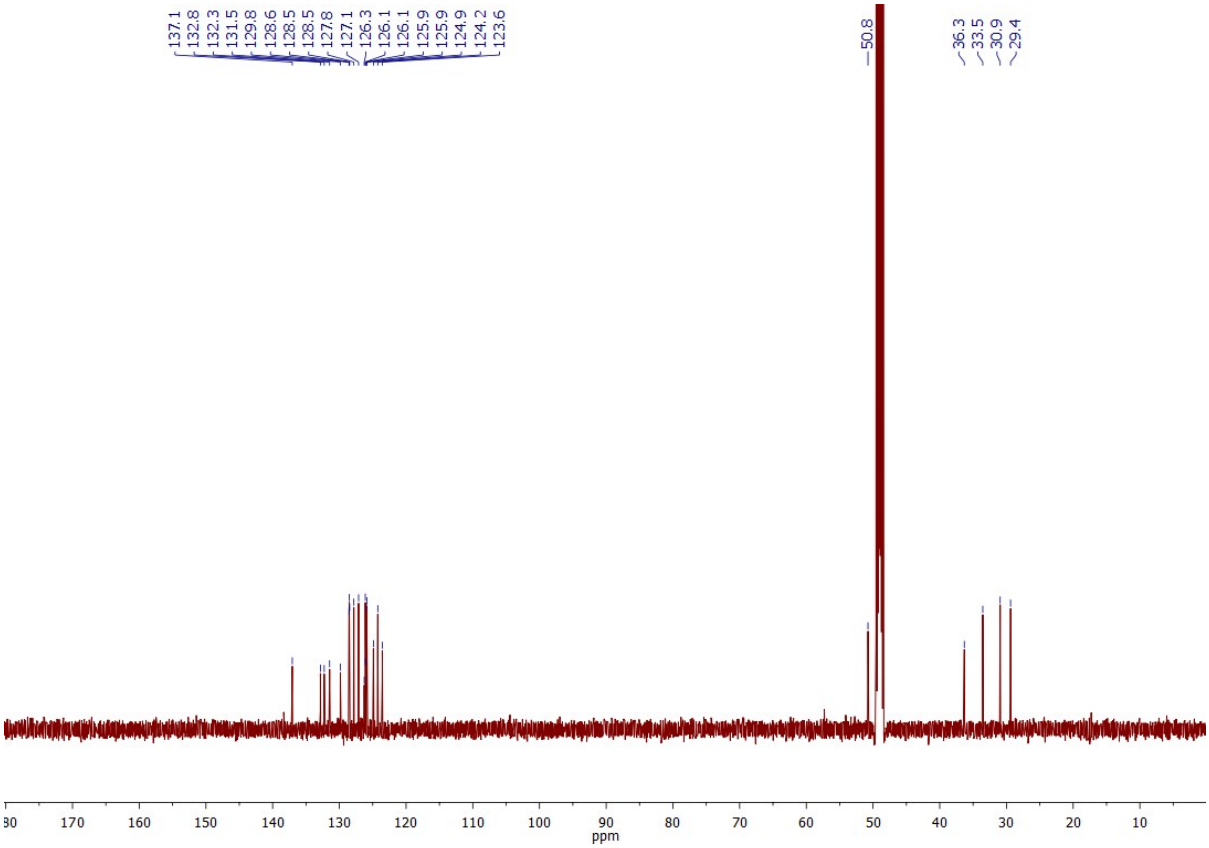

N-(4-(1-Pyrenyl)butyl)pyridinium bromide (PRD_4)

^{1}H-NMR (400 MHz, MeOD-d_4)

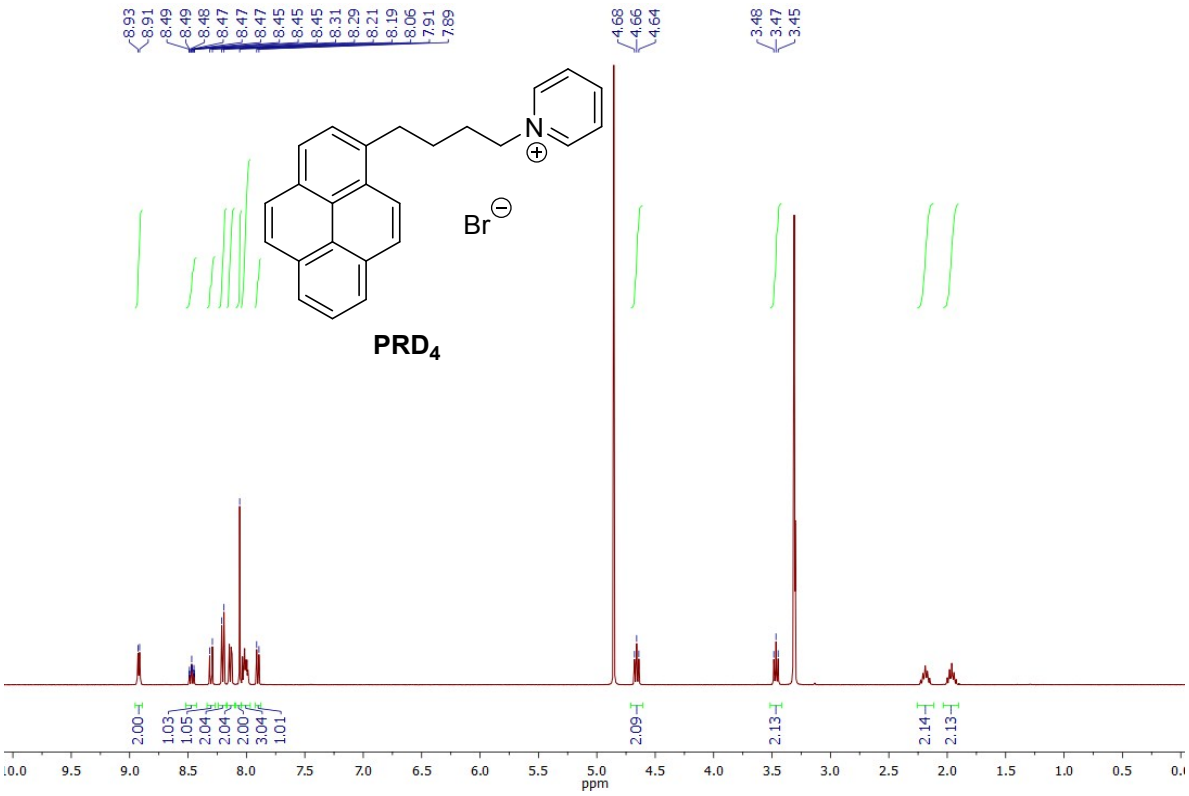

^{13}C-NMR (125 MHz, MeOD-d_4)

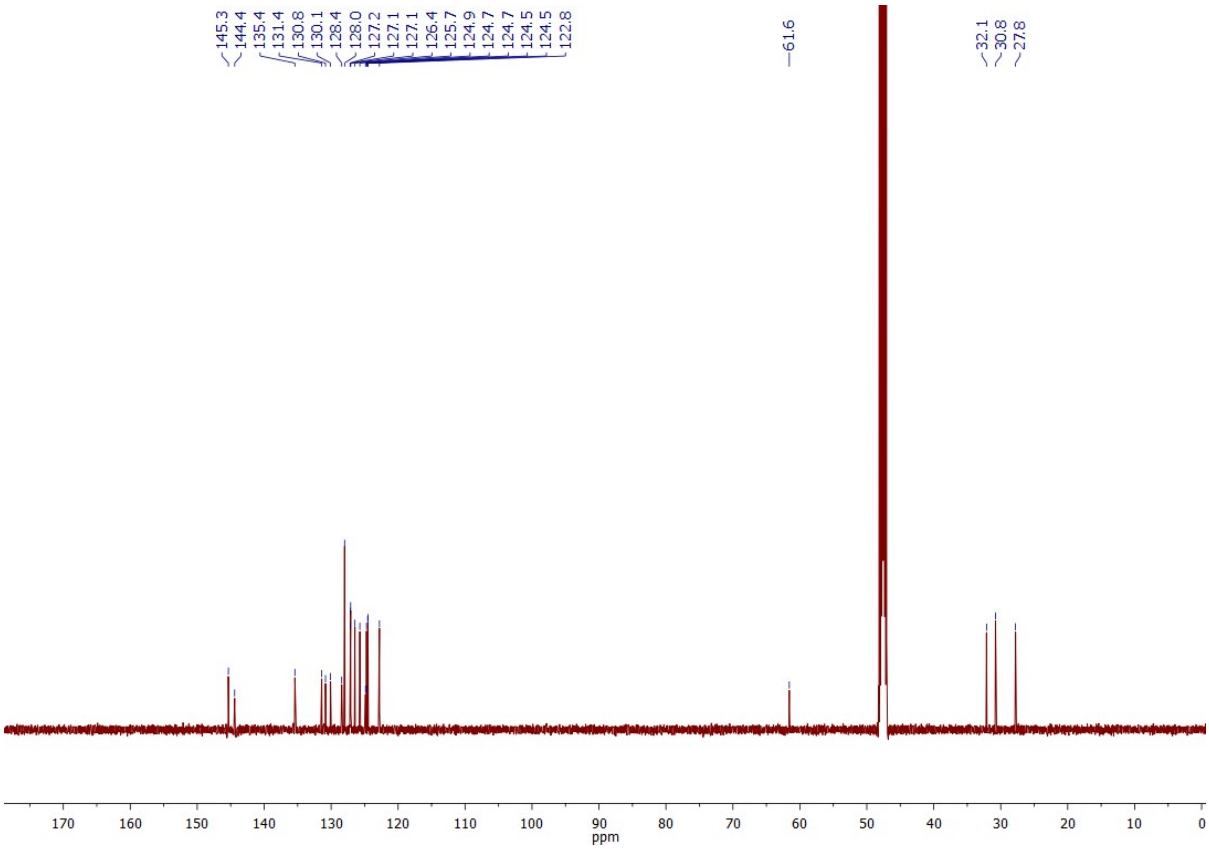

S2. MD Simulation Results

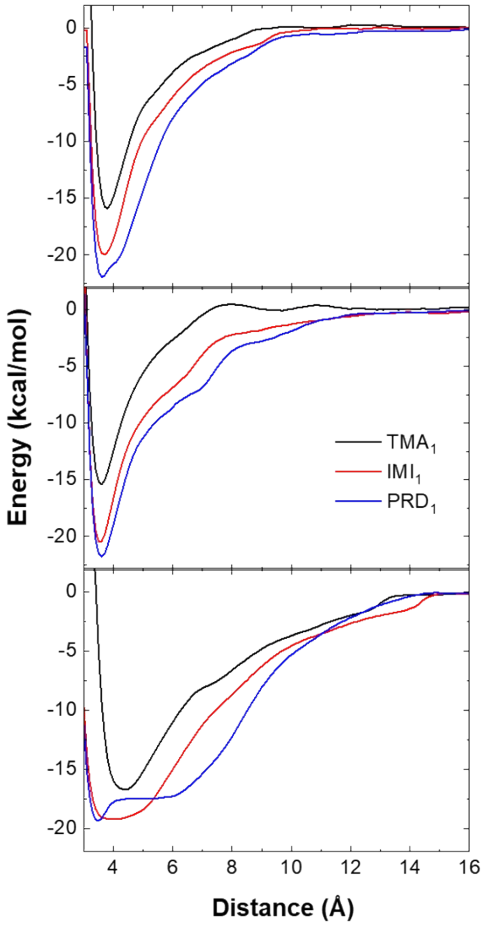

Figure S2 PMF profiles of cationic pyrene molecules with n = 1 for (top) the center of mass (COM), (middle) pyrene base (PYR) and (bottom) functional group (FUN).

The effect of different functional groups on the stabilization of cationic pyrene molecules in the system is shown in Figure S2, showing the PMF profiles obtained for cationic pyrene molecules with a single carbon chain length (n = 1). All the PMF profiles of **IMI_1** and **PRD_1** show lower free energy of interaction than that of **TMA_1**. The PMF profiles of PYR for all the three cationic pyrene molecules show the minima at ~3.5 Å, indicating the π – π interaction between the pyrene base and the graphene surface. However, **TMA_1** shows higher free energy minimum compared to **IMI_1** and **PRD_1** showing that the pyrene base of **IMI_1** and **PRD_1** is more strongly adsorbed on the graphene surface. Also, the position of minimum of **TMA_1** of the PMF profile for the functional group is slightly shifted to larger value, ~4.4 Å, compared to ~3.9 Å of **IMI_1** and **PRD_1**, showing that the **TMA** functional group tends to be more stable in water whereas **IMI** and **PRD** are more stable close to the graphene surface.

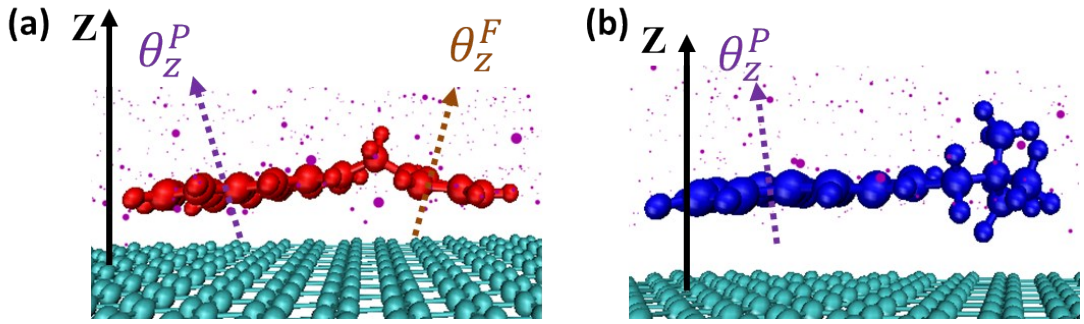

Figure S3 Representation of tilt angle for pyrene base (θ_z^P) and for **PRD** functional group (θ_z^F) shown in MD snapshot of (a) **PRD$_1$** and (b) **TMA$_1$**.

θ_z^P = Angle between the vector perpendicular to the pyrene unit and the 'z' axis

θ_z^F = Angle between the vector perpendicular to the functional unit and the 'z' axis

Angle/Unit	θ_z^P (°)	θ_z^F (°)
PRD$_1$	173.7 ± 3.3	169.8 ± 7.2
PRD$_2$	165.5 ± 20.6	155.7 ± 15.3
PRD$_3$	153.7 ± 28.6	153.3 ± 16.7
PRD$_4$	175.7 ± 2.2	169.2 ± 7.4
TMA$_1$	175.1 ± 2.7	--
TMA$_2$	175.8 ± 2.5	--
TMA$_3$	175.8 ± 2.3	--
TMA$_4$	175.3 ± 2.7	--

Table S1 Calculated tilt angles for cationic pyrene molecules with **PRD** and **TMA** functional groups from MD simulation.

A tilt angle, an angle between the vector perpendicular to the pyrene base and the vector perpendicular to the graphene surface, is calculated for pyrene base and **PRD** functional groups. As shown in Table S1, compared to the tilt angle or **PRD$_1$**, **PRD$_4$** and all **TMA** pyrenes, the **PRD$_2$** and **PRD$_3$** shows lower tilt angle value, further away from 180°, showing that they are less parallel to the graphene surface. It is the same for the case of functional group: **PRD$_2$** and **PRD$_3$** shows less tilt angle than **PRD$_1$** and **PRD$_4$**. These calculated tilt angle shows that in case of **PRD$_2$** and **PRD$_3$**, the conformation of the molecules are energetically frustrated to be adsorbed on the surface of graphene in parallel, and thus less energetically stable.

S3. Dispersion Stability

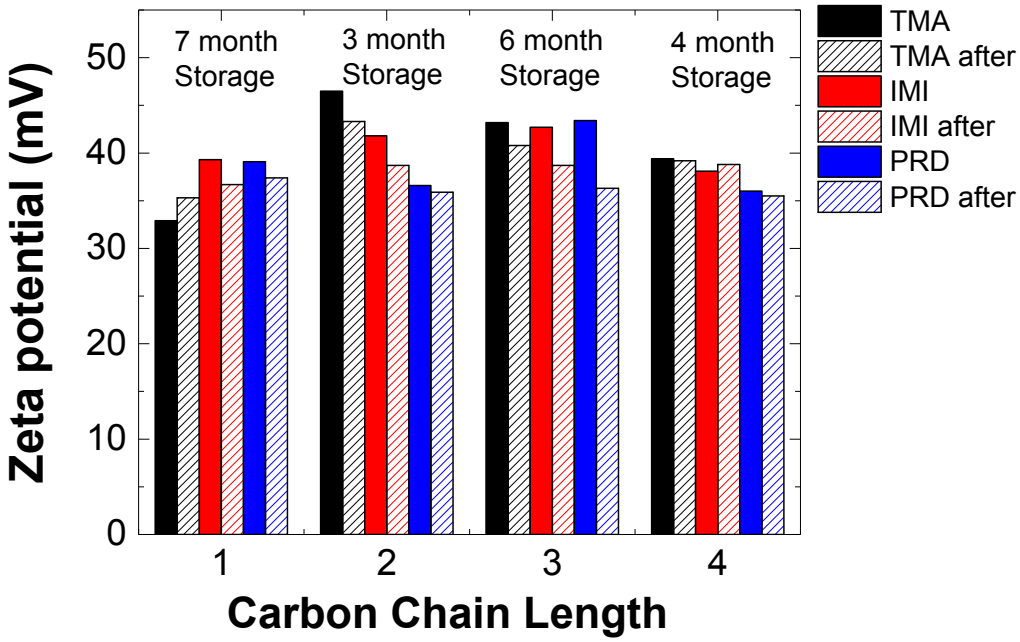

Figure S4 Comparison of zeta potential of the graphene dispersions after several months storage.

The colloidal stability of the produced graphene dispersions was studied by measuring zeta potential at fresh state and after several months' storage. As shown in Figure S4, no significant changes in the zeta potential was observed, demonstrating the excellent stability of the graphene dispersions produced in this study.

S4. AFM Analysis

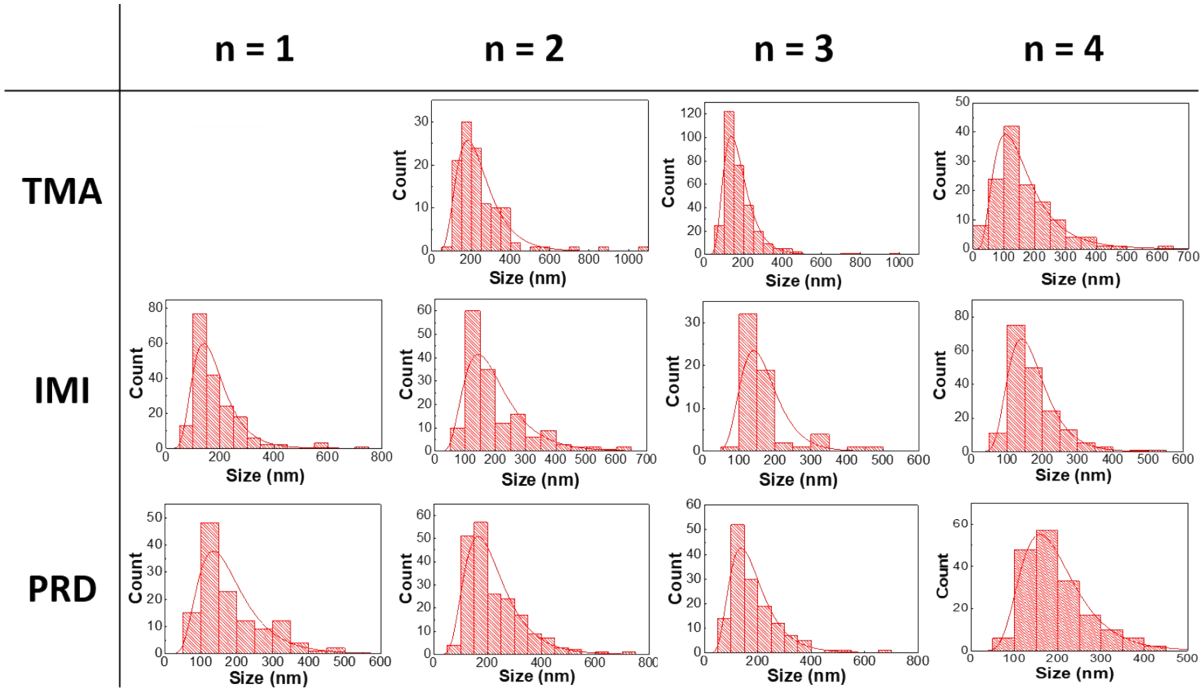

Figure S5 Histograms of AFM statistical analysis of the lateral size of graphene flakes for each graphene dispersion.

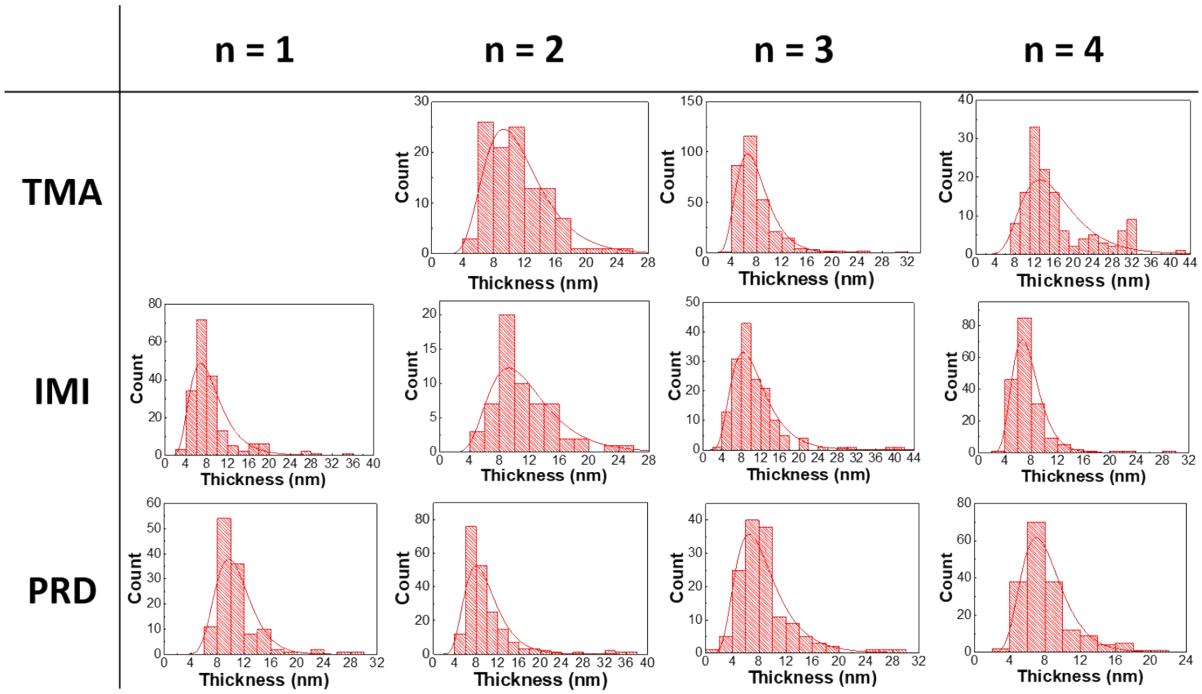

Figure S6 Histograms of AFM statistical analysis of the thickness of graphene flakes for each graphene dispersion.

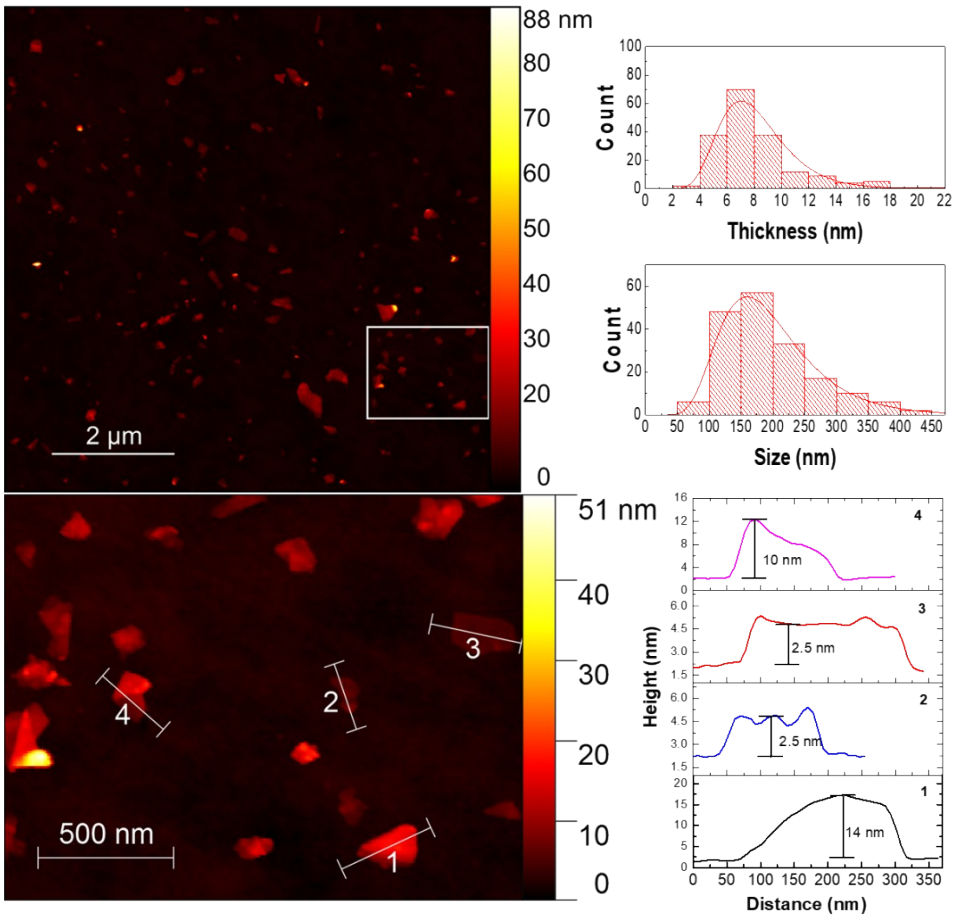

Figure S7 (top) A typical AFM image of individual graphene flakes deposited on silicon substrate and thickness and size distribution of individual flakes (bottom) zoom-in image of the rectangular-marked region in the top image and cross-section analysis of several flakes (sample PRD_4).

AFM is used to characterize the lateral size and thickness distribution of the exfoliated graphene nanosheets. For statistical analysis, AFM images of large area (typically between 25 and 100 μm^2 size) with more than two hundreds of individual flakes were used, as shown in Figure S7, top. Aggregated nanosheets are excluded from the statistics. The AFM sample is prepared by drop casting dilute (conc. = ~5 μg/ml) graphene dispersion on clean silicon wafer. The obtained histogram of lateral size and thickness distribution for each graphene dispersion prepared with cationic pyrene molecules are shown in Figure S5 and S6, respectively. Due to the strong aggregation of the graphene flakes deposited on silicon wafer, statistical analysis of $\mathbf{TMA_1}$ sample could not be obtained. The distribution histograms show log-normal distribution with expected lateral size range of 50 - 400 nm and a thickness range of 2 – 10 nm. It should be noted that the measured thickness of graphene by AFM does not directly reflect the theoretical thickness of single-layer graphene, which is known to be ~0.34 nm, due to the instrumental offset caused by capillary forces or adhesion.[1,2] Especially in case of LPE graphene, due to the remaining solvent molecules or exfoliating agents on the surface of graphene, most studies observed higher height measurement, typically between 1 and 2 nm for single-layer graphene.[3–6]

S5. Raman Analysis

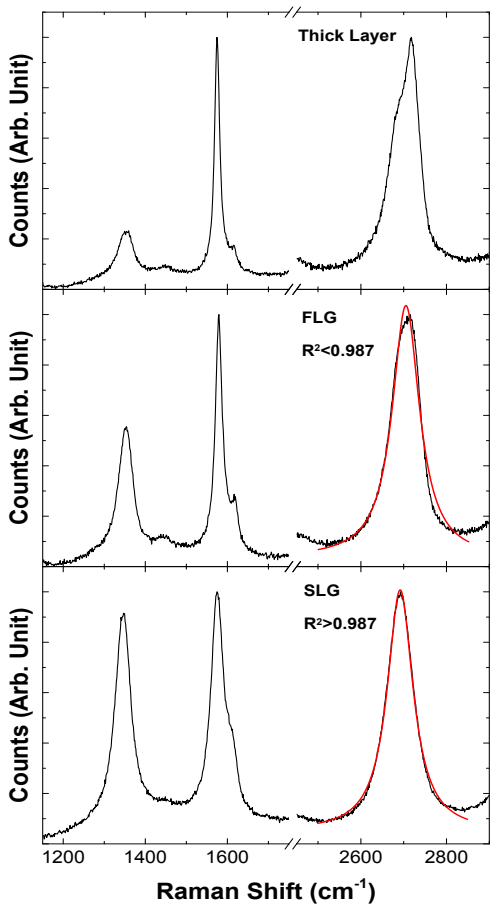

Figure S8 Representative Raman spectra for graphene flakes for qualitative Raman analysis for thickness distribution.

Raman spectroscopy is a widely used technique for the characterization of graphene,[7–9] and previously we used simple qualitative protocol for analysing LPE graphene using two parameters: the shape of the 2D peak for determination of thickness distribution and intensity (as height) ratio between D and G peak, I(D)/I(G) for probing the defect concentration.[10–14] As shown in the Figure S8, 2D peak is fitted with a Lorentzian lineshape to distinguish between single-layer graphene (SLG), few-layer sheets (FLG, re-stacked or retaining AB stacking) and graphitic thick-layered material (> ~7 layers with AB stacking). By evaluating the coefficient of determination, R^2, the thickness of each flakes were determined, allowing to derive qualitative information on the thickness distribution. The second parameter, I(D)/I(G), is used to get information on the amount of defects. It should be noted that LPE graphene always shows a D peak, which is activated by the edges of the flakes that break the translation symmetry of the crystal. Also, general increase of the intensity ratio is observed with decreasing thickness because decrease in thickness occurs with decreasing in size during sonication. Here in this study, all the dispersions showed the percentage of SLG between 20 - 40% (Table S2), the typical range observed for well-dispersed LPE graphene dispersion. The defect concentration of graphene nanosheets characterised by I(D)/I(G) showed no noticeable deviation for any of the dispersions, showing that chemical functionalisation of graphene surface did not occur during the sonication.

	n = 1	**n = 2**	**n = 3**	**n = 4**
TMA_n	SLG = 24.3% FLG = 75.7%	SLG = 30% FLG = 70%	SLG = 27.5% FLG = 70.0% Thick = 2.5%	SLG = 40.0% FLG = 60.0%
IMI_n	SLG = 25% FLG = 70% Thick = 5%	SLG = 22.5% FLG = 77.5%	SLG = 30.0% FLG = 70.0%	SLG = 40.0% FLG = 60.0%
PRD_n	SLG = 37.5% FLG = 62.5%	SLG = 40% FLG = 60%	SLG = 45.2% FLG = 52.4% Thick = 2.4%	SLG = 42.5% FLG = 55.0% Thick = 2.5%

Table S2 Qualitative thickness distribution analysis by Raman measurement of graphene flakes for each dispersions

S6. TEM images

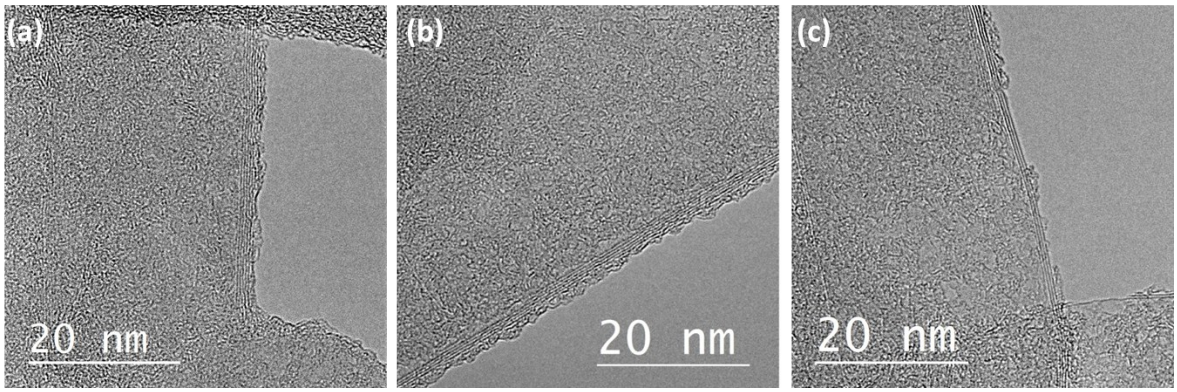

Figure S9 Representative HRTEM image of (a) **IMI_1**, (b) **PRD_1** and (c) **TMA_4** showing multilayer graphene.

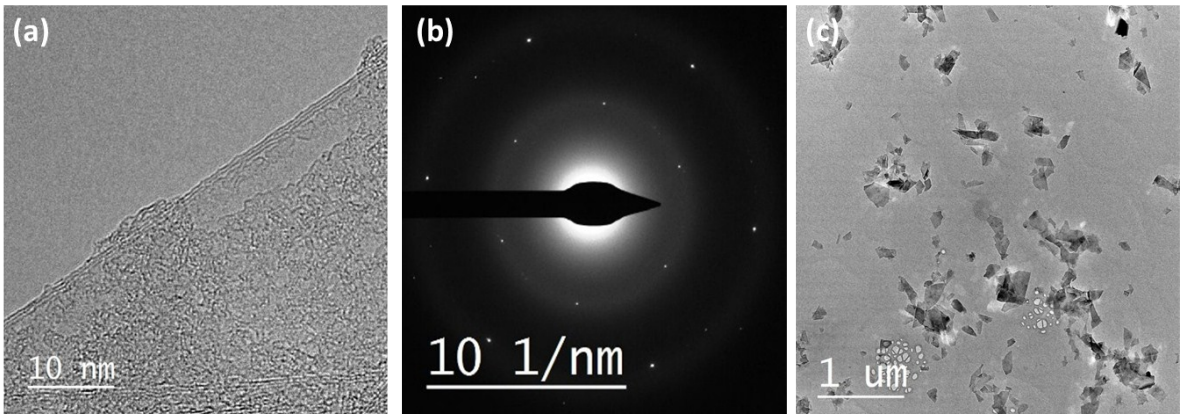

Figure S10 (a) HRTEM image, (b) electron diffraction patter of graphene flake in (a) and (c) Low-resolution image of graphene flakes for sample **TMA_4**.

TEM is often used technique to measure the lateral size and thickness of graphene flakes. The number of layers were counted at the edge of the graphene flakes (Figure s9). For statistical measurement, more than 100 flakes for each samples were measured.

S7. Uptake and biocompatibility of Gr *in vitro*

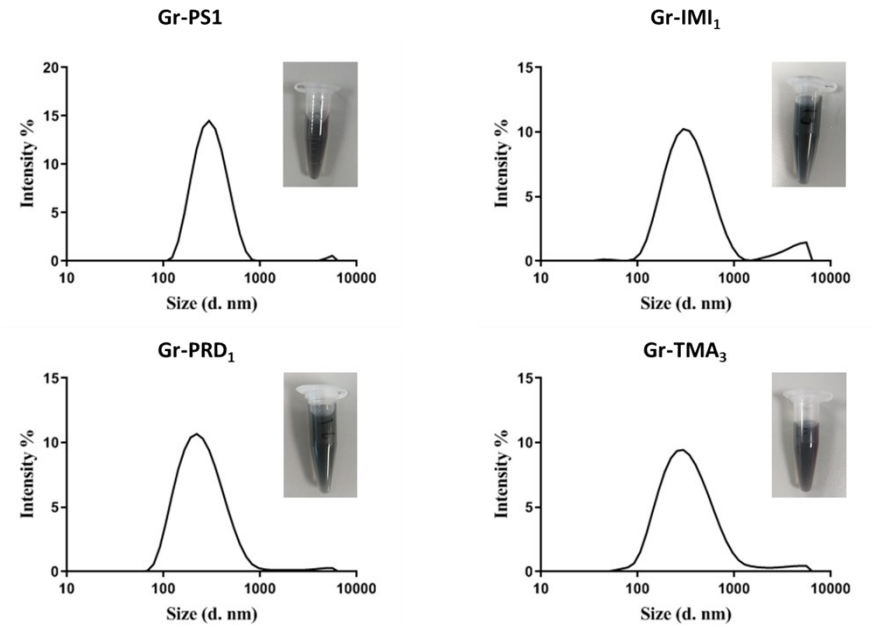

Figure S11. Characterization of Gr in cell culture medium. Four types of Gr were dispersed in cell culture medium (RPMI) supplemented with 10% FBS at 50 µg/mL and incubated for 24h at 37°C and 5% CO_2 (same conditions were used to expose the cells to Gr). After 24h of incubation, pictures were taken (insets) indicating excellent stability of Gr in cell culture medium. Subsequently, Gr were centrifuged, washed and dispersed in water to perform DLS measurements. The size distribution of the four types of Gr by intensity is shown in the graphs.

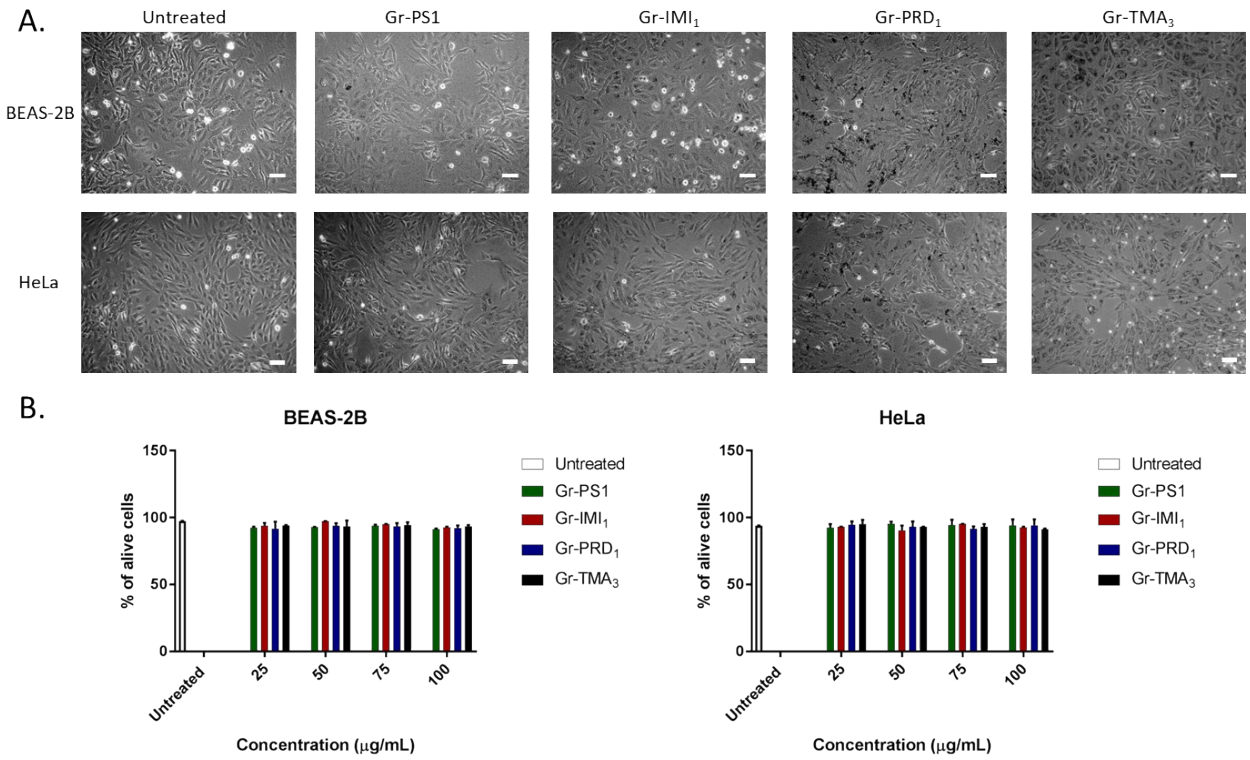

Figure S12. Cytotoxicity of Gr in BEAS-2B and HeLa cells. (A) BEAS-2B and HeLa cells were exposed to 100 µg/mL of Gr-PS1, Gr-IMI_1, Gr-PRD_1 or Gr-TMA_3 for 24h. After the treatment, cells were observed for morphological changes and loss of viability using optical microscopy. Scale bar is 50 µm. (B) BEAS-2B and HeLa cells were exposed to indicated concentrations of Gr for 24h. Cell viability was quantified by flow cytometry, using PI/Annexin V staining. Percentage of the cells in lower left (LL) quadrant of bivariate plots (alive cells) are shown in the graphs, data are represented as mean ± SD (n = 3, error bars indicating variations inside each set of triplicates).

To assess cytotoxicity of Gr, two complementary approaches were used: optical microscopy and flow cytometry. Optical microscopy was used to observe the morphology of the cells and healthiness of untreated and monolayers treated with four different types of graphene flakes. PI/AV staining was used to quantify the percentage of alive and dead cells as well as to differentiate types of cell death induced by the treatment

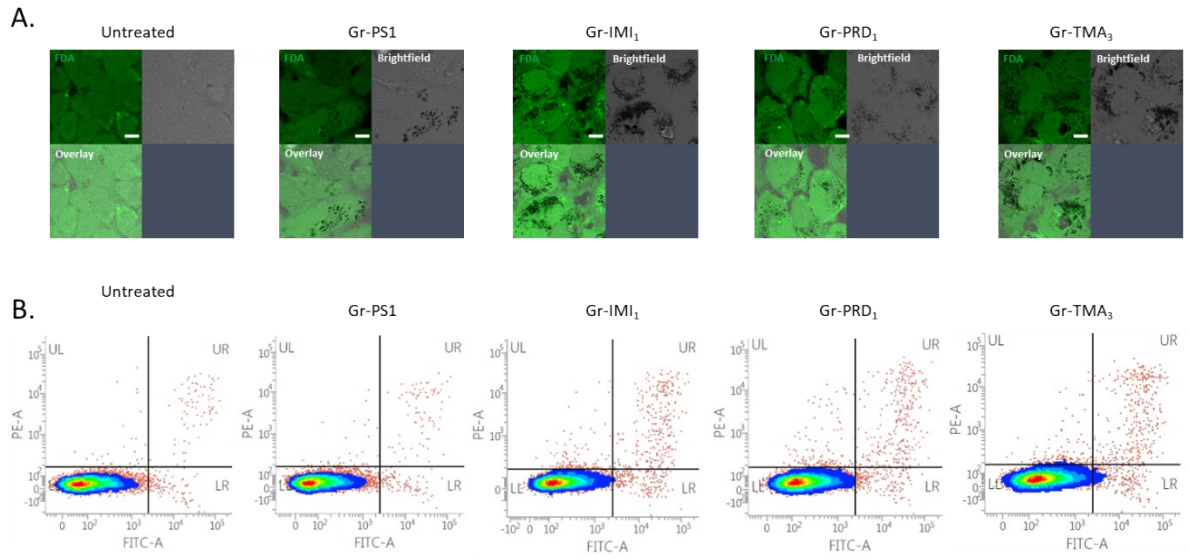

Figure S13. Uptake and cytotoxicity of Gr in HeLa cells. (A) HeLa cells were exposed to 50 µg/mL of Gr-PS1, Gr-IMI1, Gr-PRD1 or Gr-TMA3 for 24h. After the treatment, cells were stained using Fluorescein Diacetate (FDA) dye and the uptake of the flakes was estimated using confocal microscopy, by exploiting fluorescence quenching of the FDA dye due to the presence of the flakes inside the cells. Staining of the cells: FDA – green. Scale bar is 50 µm. (B) Assessment of the cytotoxicity of Gr by flow cytometry using Propidium Iodide/Annexin V staining. In the bivariate plots, live cells are represented in the lower left (LL) quadrant, early apoptotic in the lower right (LR), late apoptotic and/or necrotic cells are shown in upper right (UR) and necrotic cells are in the upper left (UL) quadrant.

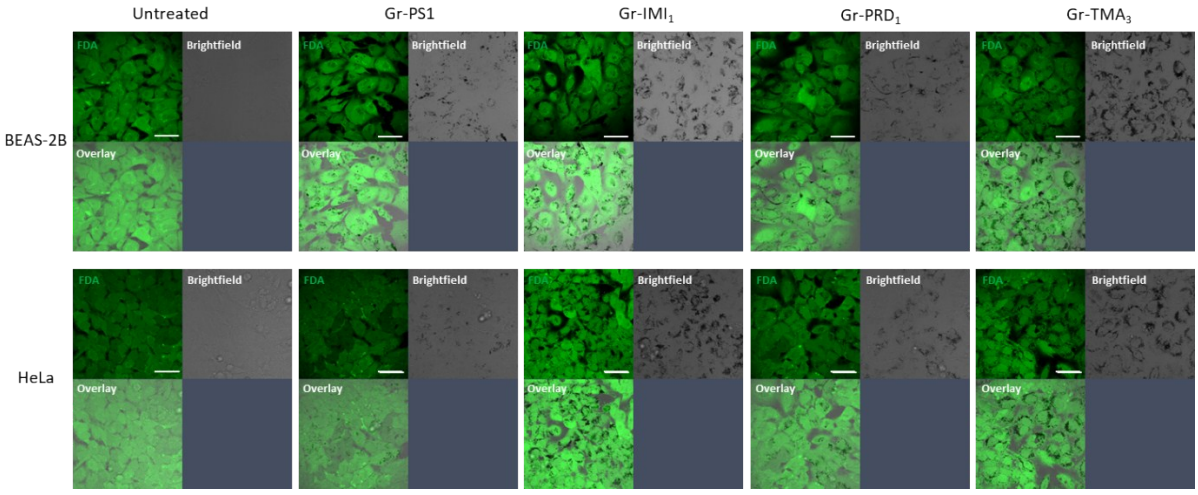

Figure S14. Uptake of Gr in BEAS-2B and HeLa cells. BEAS-2B (top panel) and HeLa (bottom panel) cells were exposed to 50 µg/mL Gr-PS1, Gr-IMI$_1$, Gr-PRD$_1$ or Gr-TMA$_3$ for 24h. After the treatment, cells were stained using Fluorescein Diacetate (FDA) dye and the uptake of the flakes was estimated using confocal microscopy. Staining of the cells: FDA – green. Scale bar is 50 µm.

We used confocal microscopy to follow the uptake of graphene flakes by the cells. Figure S14 shows images at lower magnification images compared to those shown in Figure 4A and Figure S13A, for better illustration of graphene flakes uptake by a higher number of cells.

	As prepared in Water		**After Cell Culture Medium Incubation**		
	Hydrodynamic size (nm)	**PDI**	**Hydrodynamic size (nm)**	**PDI**	**Zeta potential (mV)**
GF-PS1	200	0.25	290	0.22	-29
GF-IMI_1	210	0.31	310	0.31	-22
GF-PRD_1	180	0.25	220	0.22	-21
GF-TMA_3	210	0.26	280	0.26	-17

Table S3. Hydrodynamic size, polydispersity index, and zeta potential of graphene dispersions used in biological studies, as prepared in water and after mixing with cell culture medium

.

References

1. Gupta, A., Chen, G., Joshi, P., S. Tadigadapa & Eklund, and P. C. Raman Scattering from High-Frequency Phonons in Supported n -Graphene Layer Films. *Nano Lett.* **6**, 2667–2673 (2006).
2. Nemes-Incze, P., Osváth, Z., Kamarás, K. & Biró, L. P. Anomalies in thickness measurements of graphene and few layer graphite crystals by tapping mode atomic force microscopy. *Carbon N. Y.* **46**, 1435–1442 (2008).
3. Yang, H. *et al.* A simple method for graphene production based on exfoliation of graphite in water using 1-pyrenesulfonic acid sodium salt. *Carbon.* **53**, 357–365 (2013).
4. Paton, K. R. *et al.* Scalable production of large quantities of defect-free few-layer graphene by shear exfoliation in liquids. *Nat. Mater.* **13**, 624–630 (2014).
5. Narayan, R., Lim, J., Jeon, T., Li, D. J. & Kim, S. O. Perylene tetracarboxylate surfactant assisted liquid phase exfoliation of graphite into graphene nanosheets with facile re-dispersibility in aqueous/organic polar solvents. *Carbon.* **119**, 555–568 (2017).
6. Backes, C. *et al.* Production of highly monolayer enriched dispersions of liquid-exfoliated nanosheets by liquid cascade centrifugation. *ACS Nano* **10**, 1589–1601 (2016).
7. Ferrari, A. C. & Basko, D. M. Raman spectroscopy as a versatile tool for studying the properties of graphene. 1–13 (2013). doi:10.1038/nnano.2013.46
8. Jorio, A., Saito, R., Dresselhaus, G. & Dresselhaus, M. S. *Raman Spectroscopy in Graphene Related Systems*. *Raman Spectroscopy in Graphene Related Systems* (2011). doi:10.1002/9783527632695
9. Casiraghi, C. Raman spectroscopy of graphene. in *Spectroscopic Properties of Inorganic and Organometallic Compounds: Techniques, Materials and Applications, Volume 43* 29–56 (2012). doi:10.1039/9781849734899-00029
10. Conti, S. *et al.* Perchlorination of Coronene Enhances its Propensity for Self-Assembly on Graphene. *ChemPhysChem* **17**, 352–357 (2016).
11. Haar, S. *et al.* Enhancing the Liquid-Phase Exfoliation of Graphene in Organic Solvents upon Addition of n-Octylbenzene. *Sci. Rep.* **5**, 16684 (2015).
12. Shin, Y. *et al.* Synthesis and characterization of composite membranes made of graphene and polymers of intrinsic microporosity. *Carbon N. Y.* **102**, 357–366 (2016).
13. Schlierf, A. *et al.* Nanoscale insight into the exfoliation mechanism of graphene with organic dyes: effect of charge, dipole and molecular structure. *Nanoscale* **5**, 4205 (2013).
14. Ciesielski, A. *et al.* Harnessing the Liquid-Phase Exfoliation of Graphene Using Aliphatic Compounds: A Supramolecular Approach. *Angew. Chemie Int. Ed.* **53**, 10355–10361 (2014).